AD_____

Award Number: DAMD17-98-1-8525

TITLE: Adjuvant Action of Hepatocyte Growth Factor in Vitamin D Therapy of Androgen-Unresponsive Prostate Cancer

PRINCIPAL INVESTIGATOR: Bernard A. Roos, M.D.

CONTRACTING ORGANIZATION: University of Miami School of Medicine
Miami, Florida 33136

REPORT DATE: December 2001

TYPE OF REPORT: Final

PREPARED FOR: U.S. Army Medical Research and Materiel Command
Fort Detrick, Maryland 21702-5012

REPORT DOCUMENTATION PAGE

Form Approved
OMB No. 074-0188

1. AGENCY USE ONLY (Leave blank)	2. REPORT DATE	3. REPORT TYPE AND DATES COVERED
	December 2001	Final (1 Aug 98 - 30 Nov 01)

4. TITLE AND SUBTITLE
Adjuvant Action of Hepatocyte Growth Factor in Vitamin D Therapy of Androgen-Unresponsive Prostate Cancer

5. FUNDING NUMBERS
DAMD17-98-1-8525

6. AUTHOR(S)
Bernard A. Roos, M.D.

7. PERFORMING ORGANIZATION NAME(S) AND ADDRESS(ES)
University of Miami School of Medicine
Miami, Florida 33136

E-Mail: broos@med.miami.edu

8. PERFORMING ORGANIZATION REPORT NUMBER

9. SPONSORING / MONITORING AGENCY NAME(S) AND ADDRESS(ES)
U.S. Army Medical Research and Materiel Command
Fort Detrick, Maryland 21702-5012

10. SPONSORING / MONITORING AGENCY REPORT NUMBER

11. SUPPLEMENTARY NOTES

12a. DISTRIBUTION / AVAILABILITY STATEMENT
Approved for Public Release; Distribution Unlimited

12b. DISTRIBUTION CODE

13. ABSTRACT *(Maximum 200 Words)*

This research is aimed at discovering new therapies for advanced prostate cancer and developing in preclinical models a treatment for androgen-independent prostate cancer that bolsters vitamin D's antitumor actions. We are examining separate and combined growth-regulatory actions of growth factors and hormones with vitamin D. While we are focused on paradoxical growth-inhibitory actions of hepatocyte growth factor (HGF), we are also seeking agents that act similarly with vitamin D. We concentrated initially on developing information and model systems for characterizing androgen modulation of HGF's actions and interactions with vitamin D vis-à-vis growth inhibition and cell-cycle regulation in sublines transformed with stable androgen-receptor activity. In seeking agents similar to HGF, we discovered 2-methoxyestradiol, a normal estrogen metabolite that also exerts late cell-cycle inhibitory actions. This compound inhibits tumor progression in a transgenic mouse model of androgen-independent prostate cancer without toxic side effects. Because it is naturally occurring, readily synthesized, and reported to lack the angiogenic and other pleomorphic effects that characterize HGF activity in normal tissues, 2-methoxyestradiol could provide a cancer-cell-specific adjuvant to vitamin D therapy in prostate cancer.

14. SUBJECT TERMS
Prostate Cancer

15. NUMBER OF PAGES
84

16. PRICE CODE

17. SECURITY CLASSIFICATION OF REPORT	18. SECURITY CLASSIFICATION OF THIS PAGE	19. SECURITY CLASSIFICATION OF ABSTRACT	20. LIMITATION OF ABSTRACT
Unclassified	Unclassified	Unclassified	Unlimited

TABLE OF CONTENTS

FINAL REPORT - December 2001

DAMD17-98-1-8525
Adjuvant action of hepatocyte growth factor in vitamin D therapy of androgen-unresponsive prostate cancer

Bernard A. Roos, P.I.

[Total Pages: 84 pp]

Annual Report: **"Adjuvant action of hepatocyte growth factor in vitamin D therapy of androgen-unresponsive prostate cancer," Bernard A. Roos, M.D., PI (DAMD17-98-1-8525)**

INTRODUCTION

No effective therapy exists for prostate cancer that has advanced after palliation with androgen deprivation. Such advanced cancer no longer is responsive to withdrawal of testosterone, the normal primary growth regulator in the prostate. Vitamin D slows the growth of normal prostate epithelium and has some growth-inhibitory action in prostate cancer that has advanced to a testosterone-unresponsive state. However, the vitamin D doses required to slow cancer cause to toxic side effects, notably high blood calcium. The purpose of this research is to discover new therapies applicable for advanced prostate cancer and to develop in preclinical models a treatment for androgen-independent prostate cancer that incorporates and bolsters the antitumor actions of vitamin D. The scope of our research encompasses the separate and combined growth-regulatory effects of certain growth factors and hormones with vitamin D. While the research centers on paradoxical growth-inhibitory actions of hepatocyte growth factor (HGF) through MET (product of the c-met oncogene), its receptor, in human advanced prostate cancer cell lines, we are also seeking related growth factors and hormonal agents that may also paradoxically inhibit prostate cancer cells and bolster the antitumor activity of vitamin D.

BODY

Two specific aims were originally proposed:

Aim 1. Characterize androgen modulation of HGF's actions and interactions with vitamin D in regard to growth inhibition and cell-cycle regulation in ALVA-31 clones with inducible androgen-receptor activity and identify which, if any, androgenic modulating influences are mediated by HGF/MET-dependent signaling events.

Aim 2. Demonstrate in vivo that HGF and a novel HGF agonist (monoclonal antibody directed against MET's extracellular domain), alone or in combination with vitamin D, inhibit xenografted tumors derived from native ALVA-31 cells and ascertain whether androgenic influences on HGF and vitamin D actions seem in vitro can be demonstrated in xenografts of ALVA-31 clones with inducible androgen-receptor activity.

We have discovered that a growth factor (hepatocyte growth factor, HGF), which influences development and maintenance of all tissues and usually stimulates cell growth, paradoxically inhibits cultured prostate cancer cells that lost control by testosterone (Ref. 1; appended). In testing androgen-insensitive human prostate cancer cell lines, all but one of these lines showed inhibition by HGF. (Ref. 1; appended). Moreover, in the ALVA-31 cell line, when we combined HGF with vitamin D, which by itself had only a weak anti-tumor effect, cell growth was almost totally inhibited (see Fig. 5 in Ref 1; appended). We are engaged in a series of tissue culture and molecular biology experiments to understand why most androgen-independent prostate cancer cells can be inhibited by HGF. The experiments to date suggest that this activity involved inhibition of later cell-cycle events (see Fig. 6 in Ref. 1; appended).

To elucidate the mechanism of HGF inhibition of androgen-insensitive prostate cancer cells, we have pursued more detailed studies in the ALVA-31 cell line. The cell-cycle control mechanisms involved differ from the usual G1/S slowing involved in growth control by hormones and growth factors. Instead of the expected G1 accumulation, marked growth inhibition of androgen-unresponsive cells is associated with a higher fraction of cells in later cell-cycle phases (Fig. 6 in Ref. 1; appended), suggesting that cell-cycle slowing by an HGF-vitamin D combination involves some preferential inhibition of progression through later phases. In support of this idea, we find that combined treatment markedly reduces cyclin B, which regulates entry into cell division via activation of maturation promoting factor (MPF, or $p34^{cdc2}$).

HGF's switch from stimulus in normal prostate to inhibitor in androgen-unresponsive cells suggests that androgen-receptor (AR) and androgen action can influence HGF action. We have documented expression and activation of the HGF receptor (MET) in androgen-responsive and -unresponsive prostate cells (Fig. 2 in Ref. 1; appended). We believe that the cell line differences in HGF responsiveness reflect both altered MET expression and altered regulation of intracellular targets of MET activation and/or alteration of MET's signal transduction cascade.

We initially sought to produce suitable (AR-inducible) ALVA-31 sublines that would provide a model system to elucidate why HGF in combination with vitamin D markedly inhibited androgen-unresponsive cells and to begin to establish the theoretical and practical framework for enhancing vitamin D biotherapy of advanced prostate cancer with HGF and HGF agonists. However, we experienced several problems regarding generation of ALVA-31 clones that stably express the human AR. For selection of ALVA-31 stable transformants after successfully introducing the AR into the cells we used limiting dilutions (1:10, 1:15, 1:20) to clone the cells. Androgen-receptor binding assays (using radio tracer-labeled, nonmetabolizeable R1881 androgen) of whole cells was performed to determine the clone(s) with the highest binding capacity. These newly produced AR-containing sublines provide a good opportunity to identify which, if any, androgen-modulating influences are mediated by HGF-MET-dependent signaling events.

In seeking agents that might mimic the actions of HGF, we discovered that 2-methoxyestradiol, a normal estrogen metabolite, exerts late cell-cycle inhibitory actions similar to HGF in all human prostate cancer cell lines. Because this metabolite is naturally occurring, readily synthesized, and reported to lack the angiogenic and other pleomorphic effects that characterize HGF activity in normal tissues, 2-methoxyestradiol could well provide a cancer-cell-specific adjuvant to bolster vitamin D therapy of prostate cancer. Accordingly, we have incorporated the studies of 2-methoxyestradiol into our studies of HGF and its interactions with vitamin D. We have found growth inhibition (Fig. 1 in Ref. 2; appended) and inhibitory effects on later cell-cycle events (Fig. 2 in Ref. 2; appended). Specifically, through cell-cycle distribution analysis (via flow cytometry) we determined that 2-methoxyestradiol caused a marked shift from G1 to G2/M, confirming a cell-cycle arrest. This cell-cycle distribution was reversible after one but not after 2 days treatment with 2-methoxyestradiol. Both biochemical and morphological assays support a role for apoptosis in 2-methoxyestradiol's dose-dependent growth inhibition of prostate cancer cells (Figs. 3-5 in Ref. 2; appended).

To assess the ability of 2-methoxyestradiol to inhibit prostate cancer cell growth in vivo, we used the Gγ/T-15 transgenic mouse model of androgen-independent prostate cancer that we previously developed (Perez-Stable, et al., 1996, Perez-Stable, et al., 1997). These mice contain the human fetal Gγ globin promoter linked to the SV40 T antigen oncogene and result in the development of an aggressive highly metastatic form of prostate cancer originating from normal prostate epithelial cells. Because of the reversibility of 2-methoxyestradiol's effects, slow-release tablets were used. Overall, we found that primary prostate tumors from 2-methoxyestradiol (75 mg/kg body weight)-treated mice were significantly smaller (38% reduction of wet weight) compared to placebo-treated mice (Fig. 6

in Ref. 2; appended). However, the total wet weight of lymph node metastases was not significantly different between 2-methoxyestradiol-treated and placebo-treated mice. Despite this result, histological analysis of small size-matched lymph node metastatic lesions consistently showed greater focal areas of necrosis in 2-methoxyestradiol-treated compared to placebo-treated mice (Fig. 7 in Ref. 2; appended).

Mice without palpable prostate tumors that received the 60-day slow-release 2-methoxyestradiol or placebo tablets developed prostate tumors with the same frequency (3 of 4), suggesting a lack of chemoprevention by 2-methoxyestradiol. During the time of 2-methoxyestradiol treatment (21 to 60 days), no toxic side effects were noted – i.e., there were no significant differences in body weight, behavior, or histology of multiple tissues including bone marrow and duodenum. These results demonstrating the powerful antitumor activity of 2-methoxyestradiol and lack of toxic side effects on quiescent normal cells would support further studies investigating the molecular mechanisms of 2-methoxyestradiol's anti-prostate tumor activity and possible clinical use.

KEY RESEARCH ACCOMPLISHMENTS

- Discovery of HGF's paradoxical growth inhibition as a common, but not universal, feature of human androgen-insensitive prostate cancer lines.
- Discovery of synergism (in vitro) between vitamin D and HGF growth inhibition in human androgen-insensitive prostate cancer cell lines.
- Discovery that the synergistic growth inhibitory actions are directed at late cell-cycle events.
- Discovery that 2-methoxyestradiol, a normal estrogen metabolite, exerts late cell-cycle inhibitory actions similar to HGF in human prostate cancer cell lines.
- Discovery that 2-methoxyestradiol induces apoptosis in prostate cancer cell lines.
- Discovery that 2-methoxyestradiol inhibits prostate tumor progression in the Gγ/T-15 transgenic mouse model of androgen-independent prostate cancer without toxic side effects.

REPORTABLE OUTCOMES

Manuscripts

1. Qadan LR, Perez-Stable CM, Schwall RH, Burnstein KL, Ostenson RC, Howard GA, Roos BA: Hepatocyte growth factor and vitamin D cooperatively inhibit androgen-unresponsive prostate cancer cell lines. *Endocrinology* 141:2567–2573, 2000
2. Qadan LR, Perez-Stable CM, Anderson C, D'Ippolito G, Herron A, Howard GA, Roos BA: 2-Methoxyestradiol induces G2/M arrest and apoptosis in prostate cancer. *Biochem Biophys Res Commun* 285:1259–1266, 2001
3. Yang ES, Maiorino CA, Roos BA, Knight SR, Burnstein KL: Vitamin D-mediated growth inhibition of an androgen-ablated LNCaP cell line model of human prostate cancer. *Mol Cell Endocrinol* 186:69–79, 2002
4. Perez-Stable CM, Schwartz GG, Farinas A, Finegold M, Binderup L, Howard GA, Roos BAS: Transgenic mouse model of androgen-independent prostate cancer Gγ/T-15: target cells of carcinogenesis and the effect of the vitamin D analogue EB 1089. *Cancer Epidemiol Biomarkers Prev*, under review, 2002

Abstracts

1. Qadan LR, Schwall R, Howard GA, Roos BA: 1,25 Dihydroxyvitamin D transformation of prostate carcinoma from epithelial to stromal morphology is mediated by an autocrine mechanism involving hepatocyte growth factor (HGF) and its receptor c-Met. Program and Abstracts, 10th Intl Congress of Endocrinology, p 723, 1996
2. Qadan LR, Schwall R, Howard GA, Roos BA: Hepatocyte growth factor sensitizes prostate cancer cells to antiproliferative action of vitamin D. Program and Abstracts, 79th Annual Meeting, The Endocrine Society, p 535, 1997
3. Perez-Stable CM, Qadan LR, Schwartz GG, Finegold MJ, Farinas A, Anderson C, Herron AJ, Howard GA, Roos BA: The Gγ/T-15 transgenic mouse model of advanced prostate cancer: testing the effects of the estrogen metabolite 2-methoxyestradiol and the vitamin D_3 analog EB 1089. Conference on Modeling Human Prostate Cancer in Mice, The Jackson Laboratory, Bar Harbor, ME, 2001

Cell line development

Development of androgen receptor–expression ALVA-31 sublines

CONCLUSIONS

Our original idea that loss of androgen receptor activity signals a new scheme of cell-cycle regulation continues to gain support. The development of AR-ALVA cells helps to support that concept. Most exciting to the larger issue of prostate cancer therapy is our discovery of a natural estrogen metabolite that selectively inhibits late cell-cycle events. We incorporated this finding into our experimental strategy to develop adjuvant therapy that will bolster the antitumor activity of vitamin D. With our findings on the anti-tumor activity of 2-methoxyestradiol in a transgenic mouse model of prostate cancer, qur original concern that clinical application of HGF's late cell-cycle inhibitory actions might prove difficult to apply clinically has become less critical. The discovery of a novel agent that affects tumor cells but not normal cells provides us with a good opportunity to develop a clinical application from our basic studies of later cell-cycle events. These results demonstrating the powerful antitumor activity of 2-methoxyestradiol and lack of toxic side effects on quiescent normal cells would support further studies investigating clinical use in humans.

REFERENCES

1. Qadan LR, Perez-Stable CM, Schwall RH, Burnstein KL, Ostenson RC, Howard GA, Roos BA: Hepatocyte growth factor and vitamin D cooperatively inhibit androgen-unresponsive prostate cancer cell lines. *Endocrinology* 141:2567-2573, 2000
2. Qadan LR, Perez-Stable CM, Anderson C, D'Ippolito G, Herron A, Howard GA, Roos BA: 2-Methoxyestradiol induces G2/M arrest and apoptosis in prostate cancer. *Biochem Biophys Res Commun* 285:1259-1266, 2001
3. Perez-Stable C, Altman NH, Brown J, Harbison M, Cray C, Roos BA: Prostate, adrenocortical, and brown adipose tumors in fetal globin/T antigen transgenic mice. *Lab Invest* 74:363–373, 1996

4. Perez-Stable C, Altman NH, Mehta PP, Deftos LJ, Roos BA: Prostate cancer progression, metastasis, and gene expression in transgenic mice. *Cancer Res* 57:900–906, 1997

APPENDICES

Manuscripts

Qadan LR, Perez-Stable CM, Schwall RH, Burnstein KL, Ostenson RC, Howard GA, Roos BA: Hepatocyte growth factor and vitamin D cooperatively inhibit androgen-unresponsive prostate cancer cell lines. *Endocrinology* 141:2567–2573, 2000

Qadan LR, Perez-Stable CM, Anderson C, D'Ippolito G, Herron A, Howard GA, Roos BA: 2-Methoxyestradiol induces G2/M arrest and apoptosis in prostate cancer. *Biochem Biophys Res Commun* 285:1259–1266, 2001

Yang ES, Maiorino CA, Roos BA, Knight SR, Burnstein KL: Vitamin D-mediated growth inhibition of an androgen-ablated LNCaP cell line model of human prostate cancer. *Mol Cell Endocrinol* 186:69–79, 2002

Perez-Stable CM, Schwartz GG, Farinas A, Finegold M, Binderup L, Howard GA, Roos BAS: Transgenic mouse model of androgen-independent prostate cancer Gγ/T-15: target cells of carcinogenesis and the effect of the vitamin D analogue EB 1089. *Cancer Epidemiol Biomarkers Prev*, under review, 2002

Abstracts

Qadan LR, Schwall R, Howard GA, Roos BA: 1,25 Dihydroxyvitamin D transformation of prostate carcinoma from epithelial to stromal morphology is mediated by an autocrine mechanism involving hepatocyte growth factor (HGF) and its receptor c-Met. Program and Abstracts, 10th Intl Congress of Endocrinology, p 723, 1996

Qadan LR, Schwall R, Howard GA, Roos BA: Hepatocyte growth factor sensitizes prostate cancer cells to antiproliferative action of vitamin D. Program and Abstracts, 79th Annual Meeting, The Endocrine Society, p 535, 1997

Perez-Stable CM, Qadan LR, Schwartz GG, Finegold MJ, Farinas A, Anderson C, Herron AJ, Howard GA, Roos BA: The Gγ/T-15 transgenic mouse model of advanced prostate cancer: testing the effects of the estrogen metabolite 2-methoxyestradiol and the vitamin D_3 analog EB 1089. Conference on Modeling Human Prostate Cancer in Mice, The Jackson Laboratory, Bar Harbor, ME, 2001

0013-7227/00/$03.00/0
Endocrinology

Vol. 141, No. 7
Printed in U.S.A.

Hepatocyte Growth Factor and Vitamin D Cooperatively Inhibit Androgen-Unresponsive Prostate Cancer Cell Lines*

LAILA R. QADAN, CARLOS M. PEREZ-STABLE, RALPH H. SCHWALL, KERRY L. BURNSTEIN, RICHARD C. OSTENSON, GUY A. HOWARD, AND BERNARD A. ROOS

Geriatric Research, Education, and Clinical Center and Research Service, Veterans Affairs Medical Center (L.R.Q., C.M.P.-S., K.L.B., G.A.H., B.A.R.); and Departments of Medicine (L.R.Q., C.M.P.-S., G.A.H., B.A.R.), Molecular and Cellular Pharmacology (K.L.B.), Biochemistry and Molecular Biology (G.A.H.), and Neurology (B.A.R.), and Sylvester Comprehensive Cancer Center (L.R.Q., C.M.P.-S., K.L.B., G.A.H., B.A.R.), University of Miami School of Medicine, Miami, Florida 33101; Genentech, Inc. (R.H.S.), South San Francisco, California 94080; and Good Samaritan Cancercare and Research Center (R.C.O.), Puyallup, Washington 98371

ABSTRACT

Expression of MET, the receptor for hepatocyte growth factor (HGF), has been associated with androgen-insensitive prostate cancer. In this study we evaluated MET activation by HGF and HGF action in prostate cancer cell lines. HGF causes phosphorylation (activation) of the MET receptor in three androgen-unresponsive cell lines (DU 145, PC-3, and ALVA-31) together with morphological change. Although HGF is known to stimulate the growth of normal epithelial cells, including those from prostate, we found that HGF inhibited ALVA-31 and DU 145 (hormone-refractory) cell lines. Moreover, HGF and vitamin D additively inhibited growth in each androgen-unresponsive cell line, with the greatest growth inhibition in ALVA-31 cells. Further studies in ALVA-31 cells revealed distinct cooperative actions of HGF and vitamin D. In contrast to the accumulation of cells in G_1 seen during vitamin D inhibition of androgen-responsive cells (LNCaP), growth inhibition of the androgen-unresponsive ALVA-31 cell line with the HGF and vitamin D combination decreased, rather than increased, the fraction of cells in G_1, with a corresponding increase in the later cell cycle phases. This cell cycle redistribution suggests that in androgen-unresponsive prostate cancer cells, HGF and vitamin D act together to slow cell cycle progression via control at sites beyond the G_1/S checkpoint, the major regulatory locus of growth control in androgen-sensitive prostate cells. (*Endocrinology* **141:** 2567–2573, 2000)

PROSPECTS for prostate cancer biotherapy were brightened by the observations that prostate cancer cells express vitamin D receptors and that 1,25-dihydroxycholecalciferol [1,25-$(OH)_2$D] and its active analogs (for simplicity, hereafter referred to as vitamin D) dramatically inhibit growth and promote differentiation of normal and neoplastic androgen-sensitive prostate epithelial cells (1–3). Unfortunately, only modest growth inhibition by vitamin D and its analogs has been achieved in androgen-refractory aggressive prostate cancer cell lines *in vitro* (4, 5) and *in vivo*, as assessed in xenograft models (6). The mechanism for this diminished inhibition remains obscure. Neither vitamin D receptor abundance nor transcriptional activity completely explains the different responses (7).

Hepatocyte growth factor (HGF; also known as scatter factor) is a mesenchymal protein with mitogenic, motogenic, and morphogenic effects on nonneoplastic as well as neoplastic epithelial cell types (8, 9). HGF's pleiotropic effects are mediated via its receptor (MET), the transmembrane tyrosine kinase encoded by the *MET* protooncogene (10). Unlike vitamin D, which usually slows growth, HGF stimulates the proliferation of most normal and neoplastic cells (9). However, *in vitro* studies have shown that some carcinomas, such as hepatoma, melanoma, and breast carcinoma, are paradoxically inhibited by HGF (11–13). In normal prostate, HGF is produced by stromal cells nearest to the basal epithelial cells, which have more HGF receptor and less androgen receptor compared with luminal prostate epithelium (14–16). During prostate growth the basal cells respond to a series of induced stromal growth factors, including HGF, which regenerate differentiated luminal secretory epithelium with high sensitivity to and dependence on androgen (14, 17–19). MET is increased early in epithelial neoplasia, including prostatic intraepithelial neoplasia (15, 20), and remains highly expressed in virulent carcinomas and derived cell lines (15, 20, 21).

The prominence of MET expression in prostate carcinoma in concert with our previous finding of HGF and vitamin D synergistic action in increasing alkaline phosphatase activity in cartilage (22) prompted our investigation of HGF's action in prostate cancer and HGF's possible interactions with vitamin D. We surveyed HGF's effects on cell morphology and growth of the androgen-sensitive LNCaP cells and on three androgen-refractory cell lines (DU 145, PC-3, and ALVA-31). Based on that

Received December 29, 1999.

Address all correspondence and requests for reprints to: Bernard A. Roos, M.D., University of Miami School of Medicine, P.O. Box 016960 (D-503), Miami, Florida 33101. E-mail: broos@med.miami.edu.

* This work was supported in part by the VA Research Service, a Department of Defense grant (DAMD-17–98-1–8525, to B.A.R.), a NCI Center for Psycho-Oncology grant (1P50CA84944, to B.A.R.), and the American Institute for Cancer Research and the American Cancer Society, Florida Division (grants to K.L.B.).

survey, we pursued more detailed characterization of the separate and combined effects of HGF and vitamin D in ALVA-31, the cell line our initial survey found to be most inhibited by the growth factor-vitamin D combination. We observed that a significant inhibition was obtained by combining low doses of the agents, amounts that by themselves had no growth effect. Similarly, the HGF-vitamin D combination, but neither agent alone, decreased the fraction of cells in G_1 and increased the fraction in later cell cycle phases. These results support slowing of cell cycle events by cooperative actions of vitamin D and HGF at loci beyond the G_1/S contact point.

Materials and Methods

Reagents

1,25-$(OH)_2$D was purchased from Calbiochem (La Jolla, CA). Recombinant heterodimeric human HGF was generated and purified as previously reported (23). Ribonuclease A (RNase A) from bovine pancreas was purchased from Roche Molecular Biochemicals (Indianapolis, IN) and propidium iodide was obtained from Sigma (St. Louis, MO). Biotin-conjugated antiphosphotyrosine antibody was obtained from Upstate Biotechnology, Inc. (Lake Placid, NY), horseradish peroxidase-streptavidin was purchased from Zymed Laboratories, Inc. (San Francisco, CA), and tetramethylbenzidine peroxidase solution was obtained from Kirkegaard & Perry Laboratories (Gaithersburg, MD). Maxisorp 96-well plates were purchased from VWR Scientific (Atlanta, GA).

Cell culture

Human prostate carcinoma cell lines (24) (DU 145; ATCC HTB81), LNCaP (25) (ATCC CRL 1740), and PC-3 (26) (ATCC CRL 1435) were obtained from the American Type Culture Collection (Manassas, VA). ALVA-31 cells were obtained as previously described (27). All cells were cultured in RPMI 1640 medium (Life Technologies, Inc., Grand Island, NY) supplemented with 7.5% FBS (HyClone Laboratories, Inc., Logan, UT), 100 IU/ml penicillin, and 100 μg/ml streptomycin at 37 C in a humidified atmosphere of 5% CO_2 in air.

Androgen receptor expression

Because it had previously been reported that ALVA-31 cells express the androgen receptor (27), we assessed the expression of this receptor using the RNase protection technique (28). Human androgen receptor messenger RNA (mRNA) levels were measured with a ^{32}P-labeled T7 polymerase-synthesized antisense RNA probe from *Stu*I-digested *Hin*dIII-*Eco*RI/Bluescript-KS. Human glyceraldehyde-3-phosphate dehydrogenase mRNA was measured with a ^{32}P-labeled T7 polymerase-synthesized antisense RNA probe from *Sty*I-digested pTRIPLEscript-glyceraldehyde-3-phosphate dehydrogenase (Ambion, Inc., Austin, TX). Forty micrograms of total RNA were hybridized at 37 C for 16 h and digested with RNase mixture (Ambion, Inc.) for 30 min at 37 C. RNase digestion products were separated by electrophoresis on polyacrylamide-urea gels and analyzed by autoradiography. Androgen receptor mRNA was present in LNCaP (positive control), absent in DU 145 (negative control), and absent in PC-3 and ALVA-31 cells.

Isolation of human MET RNA by RT-PCR

Total RNA was isolated from PC-3 human prostate cancer cells by the LiCl-urea method (29) and treated with deoxyribonuclease (RNase-free). RT-PCR was performed for MET using the oligonucleotide primers 5′-GGTTGCTGATTTTGGTCATGC-3′ (forward, residues 3905–3925 bp) and 5′-TTCGGGTTGTAGGAGTCTTCT-3′ (reverse, residues 4146–4166 bp) (30). After the RT reaction, PCR was carried out in a DNA thermal cycler (Perkin-Elmer Corp./Cetus, Palo Alto, CA) under the following conditions: 1-min denaturing at 94 C, 1-min annealing at 55 C, 2-min extension at 72 C for 35 cycles, and 7-min extension at 72 C. The expected 261-bp PCR fragment was cloned into *Eco*RV-digested Bluescript-KS (treated with *Taq* polymerase), and the correct sequence was confirmed by DNA sequencing to give plasmid hMET/BS.

RNase protection analysis

RNA was isolated from the human prostate cancer cell lines LNCaP, PC-3, DU 145, and ALVA-31 by the LiCl-urea method (29). Human MET mRNA levels were measured with ^{32}P-labeled T7 polymerase-synthesized antisense RNA probe from *Hin*dIII-digested hMET/BS. Human cyclophilin mRNA was measured with a ^{32}P-labeled T3 polymerase-synthesized antisense RNA probe from pTRI-cyclophilin (Ambion, Inc.). Ten micrograms of total RNA were simultaneously hybridized with the MET and cyclophilin probes at 37 C for 16 h and digested with RNase mixture (Ambion, Inc.) for 30 min at 37 C. RNase digestion products were analyzed by electrophoresis on polyacrylamide-urea gels and autoradiography. The protected RNA fragments are 261 nucleotides (MET) and 103 nucleotides (cyclophilin).

Western blot analysis

Total protein lysates from LNCaP, PC-3, DU 145, and ALVA-31 cells were prepared as previously described (31) except without boiling. After separation of 10 μg protein by SDS-PAGE, proteins were transferred by electrophoresis to Immobilon-P membrane (Millipore Corp., Bedford, MA) and incubated in 5% nonfat dry milk, PBS, and 0.05% Tween-20 for 1 h. Rabbit polyclonal antibodies specific for human MET (1/1000 dilution; h-MET C-12, Santa Cruz Biotechnology, Inc., Santa Cruz, CA) were diluted in 5% nonfat dry milk, PBS, and 0.05% Tween-20 and incubated overnight at 4 C. Membranes were washed in PBS and 0.05% Tween-20 (three times, 10 min each time) and incubated with horseradish peroxidase-conjugated secondary antibody (antirabbit; 1/1000 dilution; Roche Molecular Biochemicals, Indianapolis, IN) for 1 h, washed in PBS and 0.05% Tween-20, and analyzed by exposure to x-ray film (X-Omat, Eastman Kodak Co., Rochester, NY) using enhanced chemiluminescence (ECL, Amersham Pharmacia Biotech, Arlington Heights, IL).

MET activation (P-Tyr) measurement by KIRA (kinase receptor activation) assay

Cells were plated in 10-cm dishes with RPMI medium supplemented with 7.5% FBS. After incubation overnight at 37 C, semiconfluent cultures were washed three times with PBS, then treated for 10 min with HGF at 10 ng/ml diluted in serum-free RPMI 1640 with 1 mg/ml BSA. Cells were rinsed and lysed in 1 ml PBS, 0.2% Triton X-100, 10 μg/ml aprotinin, 5 mM sodium fluoride, 2 mM orthovanadate, and 0.2 mM phenylmethylsulfonylfluoride for 30 min at room temperature. The lysate was cleared by centrifugation, and the supernatant was collected; the protein was quantified by the bicinchoninic acid protein assay (Pierce Chemical Co., Rockford, IL). One hundred-microliter aliquots were transferred in duplicate to a Maxisorp 96-well plate that had been coated with 5 μg/ml protein A-purified rabbit IgG antibody against MET-extracellular domain (anti-MET/ECD IgG) (32). Cell lysates were incubated for 2 h at room temperature. The bound P-Tyr was detected after another 2-h incubation with biotin-conjugated antiphosphotyrosine antibody, followed by horseradish peroxidase-streptavidin and development with tetramethylbenzidine peroxidase solution (32). The reaction was stopped with 1 M phosphoric acid, and MET activation (*i.e.* phosphorylated tyrosine) was determined based on optical density at 450–690 nm in an automatic plate reader.

Assay of cell proliferation

Cell proliferation was assessed by cell counting. To test the separate and combined antiproliferative effects of 1,25-$(OH)_2$D and HGF, cells were seeded at a density of 5000 cells/6-cm dish. After incubation for 24 h, medium was replaced with fresh medium containing vehicle (ethanol, final concentration of 0.01%), 1,25-$(OH)_2$D (to a final concentration of 1, 10, or 100 nM), HGF (added in medium to a final concentration of 1, 10, or 20 ng/ml), or a combination of HGF and 1,25-$(OH)_2$D. After 3 days, the medium was changed and replenished, and on the sixth day, cells were harvested by trypsinization and counted with a Neubauer hemocytometer (Hausser Scientific, Hursham, PA). Cell numbers of each experiment were derived from the mean value of triplicate wells in an experiment. Nearly all (>98%) cells under all treatment conditions excluded trypan blue.

Analysis of cell cycle effects

Cell cycle distribution and changes with HGF and 1,25-$(OH)_2$D were estimated for ALVA-31 cells by analytical flow cytometry (33). To accumulate sufficient cells for cell cycle analyses, cells were seeded at 30,000 cells/10-cm dish (twice the density used for proliferation studies). They were treated 24 h later with ethanol (0.01%), HGF (10 ng/ml), 1,25-$(OH)_2$D (10 nM), or a combination of HGF (10 ng/ml) and 1,25-$(OH)_2$D (10 nM). After 6 days of treatment, cells were trypsinized and washed twice with ice-cold PBS containing 0.1% glucose, then fixed by dropwise addition of 70% ethanol. After at least 12 h of ethanol fixation, DNA was stained with propidium iodide (50 μg/ml) for 30 min. RNase (100 U/ml) was included in the staining solution to degrade double stranded RNA. Analyses were performed with a FACScan unit (Becton Dickinson and Co., San Jose, CA). Excitation was at 488 nm, with emission measured at 630 nm. Distribution of cells with respect to their DNA content was analyzed for 5000 cells for each test condition. The relative proportions of cells in various cell cycle phases were estimated by compartment analysis of DNA fluorescence using cell cycle analysis software from the manufacturer to set cut-offs for G_1, S, and G_2/M (33).

Statistical analysis

Statistical analysis was performed by ANOVA. For single comparisons of the difference between means, unpaired Student's t test was applied. Significance levels are indicated in the figure legends.

Results

MET (mRNA and protein) in LNCaP, PC-3, DU 145, and ALVA-31 cells

MET mRNA was previously shown by Northern blot analysis to be present in PC-3 and DU 145 cells, but not in LNCaP cells (34). We used the RNase protection technique to determine whether MET was also present in ALVA-31 cells. We found the MET mRNA in ALVA-31 cells comparable to that found in PC-3 and DU 145 cells, but there was no detectable MET in LNCaP cells (Fig. 1). Similarly, MET protein was not detectable in LNCaP by Western blot, whereas it was present in equivalent amounts in the other cell lines (Fig. 1).

Phosphorylation of MET tyrosine

With the double antibody technique we analyzed whether the addition of HGF to the prostate cancer cell lines resulted in the activation of MET. Tyrosine phosphorylation of MET was readily detectable in all androgen-unresponsive cell lines (DU 145, PC-3, and ALVA-31), but not in LNCaP cells. This finding indicates activation of the MET receptor in the three cell lines in response to HGF treatment (Fig. 2).

Initial survey of HGF effects on growth in prostate cancer cell cultures

We conducted initial experiments to assess the growth effects of adding HGF (10 ng/ml) and vitamin D (10 nM) alone and in combination (Table 1). After 6 days of treatment with HGF alone, no growth inhibition was noted in LNCaP or PC-3, but ALVA-31 and DU 145 were inhibited 49% and 35%, respectively (Table 1). Vitamin D alone markedly inhibited LNCaP (71% decrease from control), with much smaller effects on PC-3 (8% decrease) and ALVA-31 (42% decrease) and no significant effect on DU 145 (9% increase). Although the addition of HGF together with vitamin D did not further inhibit LNCaP, HGF addition did further inhibit each of the androgen-unresponsive cell lines: PC-3 showed

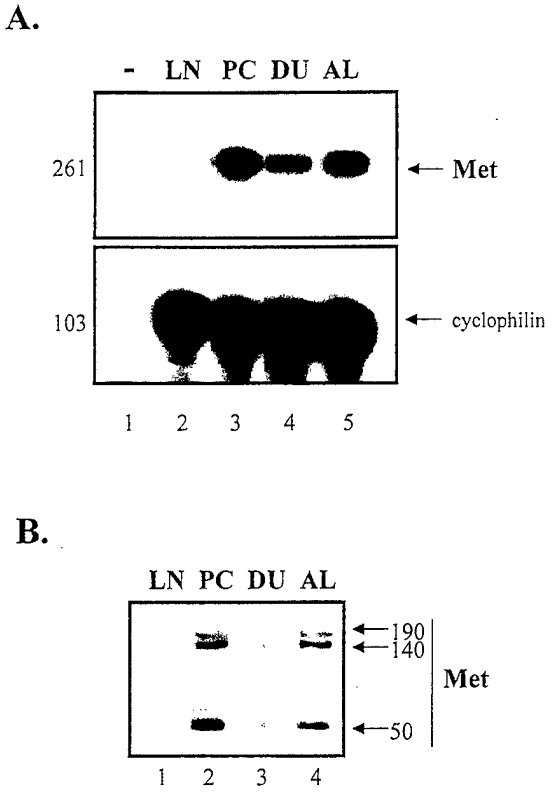

FIG. 1. Expression of MET RNA and protein in androgen-independent, but not in androgen-responsive, human prostate cell lines. A, RNase protection analysis of human MET expression showing high levels in PC-3 (PC; lane 3), DU 145 (DU; lane 4), and ALVA-31 (AL; lane 5) and no expression in LNCaP (LN; lane 2). The sizes of the protected fragments are 261 nucleotides (MET) and 103 nucleotides (cyclophilin). Lane 1 is a no RNA negative control. B, Ten micrograms of total protein were analyzed by Western blot using a polyclonal antibody that recognizes human MET. Expression of the 190-kDa precursor, the proteolytically processed 140-kDa β-chain, and the 50-kDa α-chain was detected in PC-3 (PC; lane 2), DU 145 (DU; lane 3), and ALVA-31 (AL; lane 4), but not in LNCaP (LN; lane 1). Relatively equal amounts of protein were loaded, based on Coomassie blue staining of membranes.

a 15% decrease with the combination *vs.* an 8% decrease with vitamin D alone, DU 145 showed a 35% decrease with the combination *vs.* no inhibition with vitamin D alone, and ALVA-31 manifested a 78% decrease with the combination *vs.* 42% with vitamin D alone. Because combining HGF with vitamin D caused as great an inhibition in the androgen-unresponsive ALVA-31 cells as the marked inhibition seen with vitamin D treatment of the androgen-sensitive LNCaP cells, we selected ALVA-31 for further study.

1,25-$(OH)_2$D and HGF exert separate, cooperative, and reversible antiproliferative effects on ALVA-31 cells

Vitamin D (1,25-$(OH)_2$D) at concentrations of 1, 10, and 100 nM decreased cell number by 14% (P = NS), 45%, and 67%, respectively. HGF at 1, 10, and 20 ng/ml decreased cell number by 10% (P = NS), 59%, and 61%, respectively (Fig. 3). Inhibition with the HGF-vitamin D combination was significantly more potent than with either agent alone at all concentrations, with the maximal effect (>85% decrease) of the combination always significantly greater than that

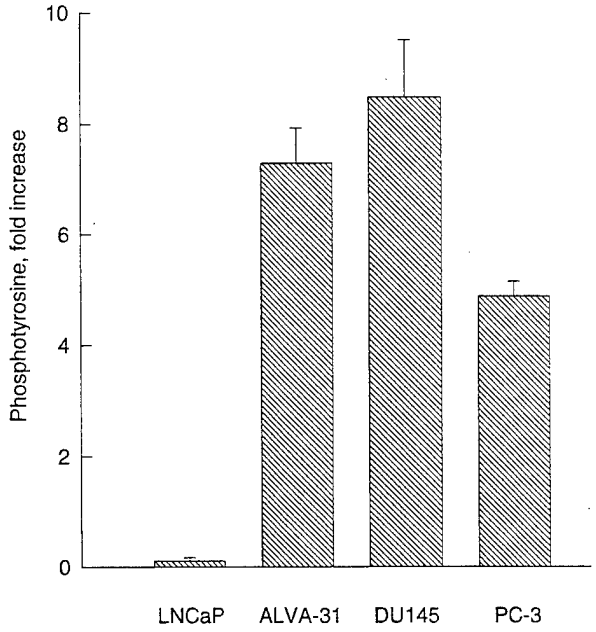

FIG. 2. MET activation measurement using the KIRA assay. After HGF treatment, phosphorylated tyrosine was determined in the three androgen-independent cell lines based on OD at 450–690 nm. Treated cells were compared with controls. The results are expressed as the fold increase compared with LNCaP as a negative control (because it lacks the MET receptor).

TABLE 1. Survey of separate and combined growth inhibitory (percent decrease from control/vehicle only) effects of HGF and vitamin D in four prostate cancer cell lines

	% of control		
	HGF (10 ng/ml)	Vitamin D (10 nM)	Combination
LNCaP	110 ± 12	29 ± 11[a]	26 ± 5[a]
PC-3	102 ± 8	92 ± 6	85 ± 9[a]
ALVA-31	51 ± 11[a]	58 ± 5[a]	22 ± 8[a,b]
DU 145	65 ± 13[a]	109 ± 10	68 ± 13[a,b]

Cultures were plated at an initial density of 200–400 cells/cm^2 and treated for 6 days as indicated in *Materials and Methods*. Values are the mean percentages of control ± SD from four experiments.

[a] Significant difference from control, $P < 0.05$.

[b] Significant difference between combination-treated and vitamin D-treated cells.

achieved by either agent alone. Although no significant inhibition occurred with 1 nM vitamin D or 1 ng/ml HGF, combining the two agents at these low concentrations produced a significant inhibition (35% decrease). Ten-fold higher concentrations of HGF or vitamin D were needed to achieve comparable inhibition with only one agent (Fig. 3).

In contrast to the irreversible antiproliferative effects of vitamin D in androgen-sensitive cells (2), the antiproliferative effect of the vitamin D-HGF combination is reversible in ALVA-31. After treatment for 3 days with the combination of 10 ng/ml HGF and 10 nM vitamin D, cultures were divided into two groups, continuing the combined treatment in one group and withdrawing treatment in the other. Cell cultures were monitored daily by microscopy, and after 3 more days of treatment, cells were counted. Treatment withdrawal doubled cell number compared with cultures treated continuously.

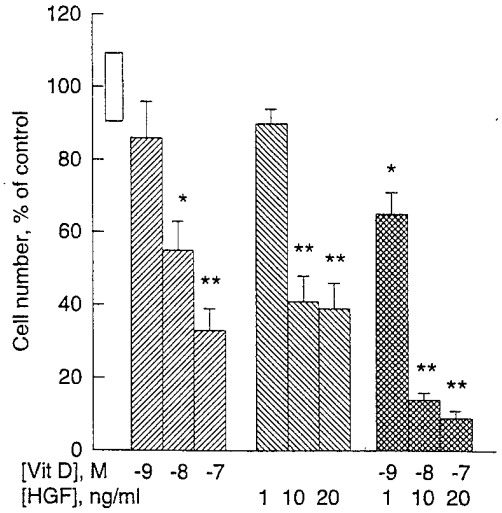

FIG. 3. Additive growth inhibitory effects of HGF and vitamin D on ALVA-31 cells. A dose response of ALVA-31 cell proliferation was obtained for separate and combined treatment with HGF and vitamin D [1,25-$(OH)_2$D]. Cultures were prepared and treated as indicated for 6 days, as described in *Materials and Methods*. *Bars* indicate the mean and SE for four to six experiments (triplicate dishes for each condition in each experiment). *, $P < 0.005$; **, $P < 0.001$ (*vs.* control, by Student's *t* test). The mean values for cells treated with HGF and vitamin D at 10 ng and 10^{-8} M or 20 ng and 10^{-7} M are significantly different from those of cells treated with vitamin D or HGF alone ($P < 0.005$, by ANOVA; controls averaged 2.3 ± 0.4 × 10^5 cells/dish).

HGF-vitamin D combination treatment alters cell cycle distribution

Cells grown in 10 nM vitamin D or in 10 ng/ml HGF did not show significant changes in cell cycle distribution. However, with the HGF-vitamin D combination, the percentage of cells in G_1 decreased from 60 ± 3% to 50 ± 2.5%, and the fraction of cells in later cell cycle phases ($S/G_2/M$) increased from 39 ± 3.2% to 48 ± 1% (Fig. 4). Cell cycle analysis performed at 2, 3, and 6 days of treatment failed to show any lower DNA mass fluorescence peaks, which argues against DNA fragmentation and apoptosis. The generalized increase in later cell cycle phases suggests that the growth inhibitory effects involved cell cycle slowing at points beyond the G_1/S checkpoint.

Discussion

Our results indicate that HGF can inhibit the growth of some androgen-independent prostate cancer cell lines. Such inhibition by HGF has been reported for only a few cancers (11, 13, 35). Growth inhibition and antitumorigenic effects have been reported in hepatoma both *in vitro* and *in vivo* (11, 12, 36, 37). Because HGF stimulates normal hepatocytes and is a potent inhibitor of hepatoma cells (36), it is likely that the intracellular signaling in response to HGF stimulation is different in normal and malignant cells. These findings in hepatoma could well pertain to prostate, because HGF stimulates normal prostate epithelium cells and inhibits androgen-unresponsive prostate cancer.

Inhibition of prostate cancer cells with HGF seems paradoxical in view of its classical role as a paracrine growth stimulator (9) as well as previous investigations that suggested an adverse role for HGF in prostate carcinoma based

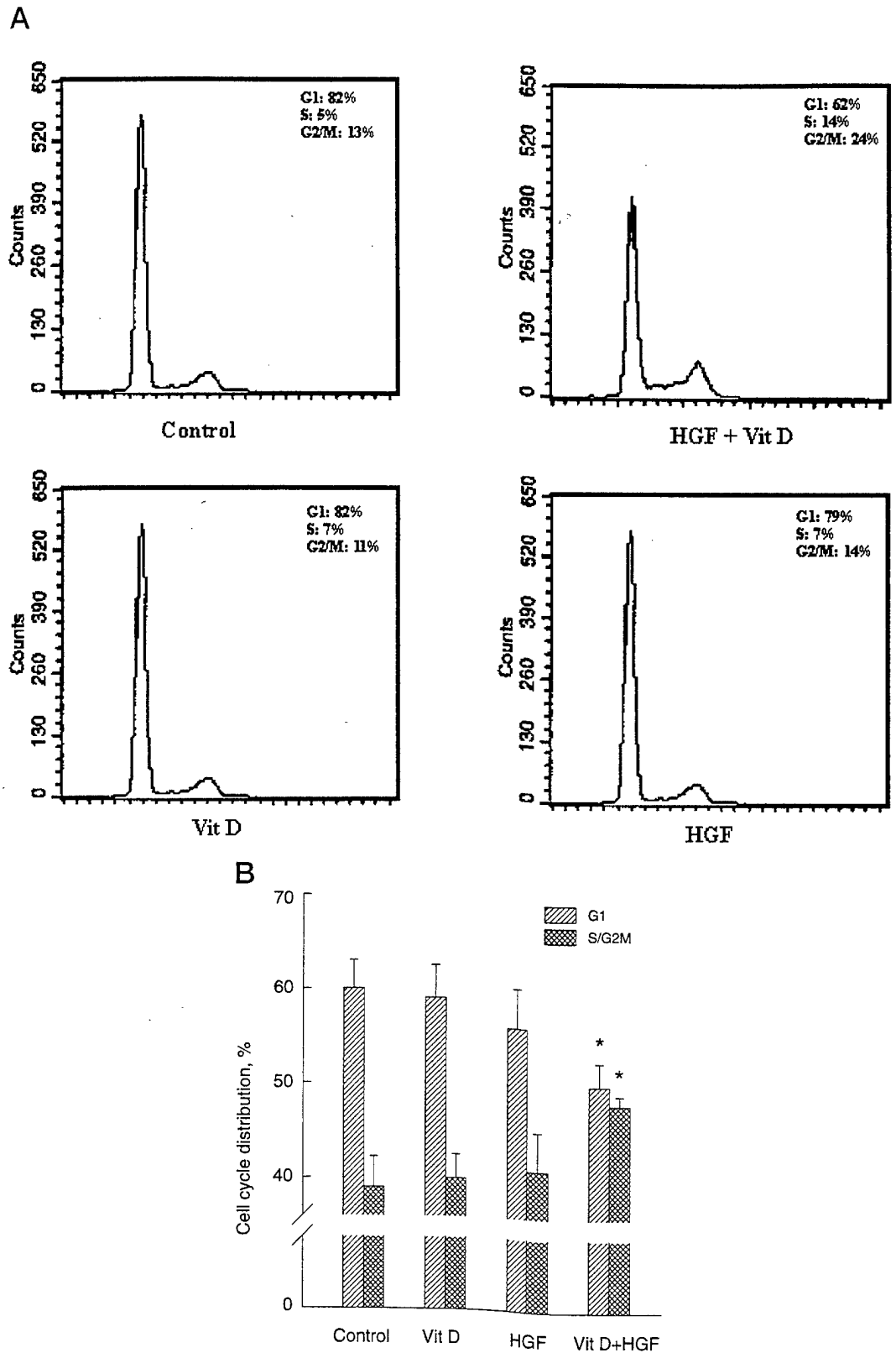

FIG. 4. Cell cycle phase distribution changes during treatment of ALVA-31 cells with the combination of vitamin D [1,25-$(OH)_2$D] and HGF. Cultures were prepared and treated with vehicle (ethanol), HGF (10 ng/ml), 1,25-$(OH)_2$D (10 nM), or their combination, as described in *Materials and Methods*. After 6 days of treatment, cells were harvested and fixed in ethanol for subsequent staining with propidium iodide and cell cycle analyses as described in *Materials and Methods*. A, Representative FACS profiles for control, vitamin D, HGF, and combination-treated cells. B, For each condition, the cell cycle distribution between G_1 and later cell cycle phases (S, G_2, and M combined) in four separate experiments. *Bars* indicate the mean and SE. *, Significantly different from control at $P < 0.05$.

on several findings (14, 15). First, MET expression appears to correlate with prostate tumor invasion and spread (15). Second, growth stimulation by HGF was reported in nonneoplastic rat prostate cells (14) and in one androgen-refractory (DU 145) human prostate cancer cell line (34). Third, increased invasion potential in the Matrigel invasion chamber assay was stimulated by HGF (38). Although we observed growth inhibition at higher plating densities, the greater effects on growth were seen at lower plating densities. However, the difference in cell density is unlikely to explain the finding of growth stimulation (34) or lack of inhibition (38) by HGF in DU 145 cells. The most likely reason for the difference from our results was the lack of serum in their experiments (34, 38). Therefore, we compared the effect of HGF on DU 145 cells grown under full serum and serum-free conditions. Despite an HGF-induced growth inhibition in the presence of serum, we found that HGF had no significant effect on the growth of DU 145 cells in serum-free medium (unpublished data). A similar discrepancy of growth effects in the presence and absence of serum has been reported for LNCaP cells with vitamin D treatment (4).

The lack of mitogenic, motogenic, and morphogenic responses of LNCaP cells to HGF was not surprising in view of the absence of MET RNA transcript and protein by RNase protection and Western blot, respectively. Although all three androgen-independent cell lines (ALVA-31, DU 145, and PC-3) showed equivalent MET activation (tyrosine phosphorylation) with HGF, PC-3 lacked the antimitogenic and morphogenic responses. A similar lack of proliferative and invasive response of PC-3 to HGF was reported by Nishimura *et al.* (38). Because signals given to epithelial cells by HGF are mediated through the MET receptor tyrosine kinase, the lack of response by PC-3 despite the receptor's activation points to a defect(s) in the downstream signaling pathway, which might be true for other malignant cell types.

We selected ALVA-31 cells for studies of the HGF and vitamin D interaction because they show clear-cut growth inhibition with either agent alone. The cooperative interaction of HGF with vitamin D was revealed by the significant inhibition resulting from the combination of low doses of these agents, which by themselves exerted no effect on growth. In addition, although neither HGF nor vitamin D alone significantly altered cell cycle distribution, their combination did, with an accumulation of cells in $S/G_2/M$ phases. These results are consistent with earlier reports that despite significant antiproliferative effects on androgen-refractory cells, vitamin D alone did not alter cell cycle distribution (39). Our finding that the HGF-vitamin D combination treatment decreased the fraction of cells in G_1 and increased the fraction in later cell cycle phases (S, G_2, and M), in concert with the marked growth inhibition, suggests that the slowed cell cycle progression with these factors involves cooperative, but distinct, actions at loci beyond the G_1/S checkpoint. Down-regulation of cyclin B and/or cyclin-dependent kinase-1, which regulate late cell cycle events, is a plausible mechanism at which future work will be directed. Slowing of cell cycle progression through these later phases was previously noted in T47D breast cancer cells by vitamin D, an agent considered to exert its inhibition via G_1/S slowing (40). In our experiments, cell loss through apoptotic mechanisms seems unlikely, given the large inhibition observed and the lack of any evidence for apoptosis during serial microscopy or from flow cytometric analyses (33). Furthermore, despite the lower cell number under treatment conditions, the number of cells present at the end of the experiment still represents a 10-fold increase over the number of cells initially plated. The reversibility of the antiproliferative effect with treatment withdrawal also argues strongly against apoptosis.

Androgen-responsive prostate epithelial cells, such as LNCaP, are markedly and irreversibly inhibited by vitamin D, with decreased G_1/S transit that results in accumulation of cells in the G_1 phase of the cell cycle, suggesting G_1/S arrest (39, 41). The development of vitamin D resistance in androgen-unresponsive prostate cancer cells could signal their diminished ability for G_1/S checkpoint regulation. Although decreasing vitamin D receptor expression during tumor progression to androgen unresponsiveness could explain some of the apparent vitamin D resistance (42), neither vitamin D receptor loss nor diminished transcriptional activity fully accounts for this difference, because the androgen-unresponsive ALVA-31 cells have higher vitamin D receptor number and activity than the androgen-responsive LNCaP cells (7). Each androgen-unresponsive cell line has well-documented mutations (43, 44) involving Rb, p53, p21, and/or other antioncogenes critical to G_1/S checkpoint control by vitamin D and other hormones (44–46). Such mutations may provide a reason for why vitamin D is less effective in inhibiting G_1/S transit in androgen-unresponsive cell lines (39, 47, 48). Another reason is the loss of androgen modulation of cell cycle control. Restoring androgen receptor activity has been shown to reinstitute G_1/S checkpoint control (49). Although no one regulatory or genetic alteration is likely to disrupt G_1/S control, cumulative changes may result in loss of cell cycle control.

In conclusion, although most of the previous work on vitamin D and HGF-mediated growth inhibition involved effects on early cell cycle events, our results suggest that in androgen-insensitive prostate cancer cells, HGF and vitamin D can use distinct mechanisms to slow cell cycle progression at loci beyond the G_1/S checkpoint. Prostate neoplasia is associated with increased MET (HGF receptor) immunostaining (15). Such heightened MET expression together with the paradoxical inhibition by HGF we observed *in vitro* might offer an opportunity to slow the progression of disease that has advanced in the face of androgen deprivation. Similarly, other pleiotropic growth factors might be used to inhibit aggressive prostate cancers (which lost control of G_1/S) if they gain or retain their ability to inhibit later in the cell cycle. A combination of such agents with diverse, albeit minor, cooperative inhibitory actions at these later cell cycle loci might ultimately serve as an important adjuvant to vitamin D and other therapeutic agents in advanced prostate cancer. Notwithstanding the novel potential benefits our *in vitro* results imply, any clinical use of HGF in advanced prostate cancer will have to address problems attached to mode, duration, and cost of HGF administration (50) as well as potential adverse effects related to angiogenesis. The prospects for HGF as adjunct to vitamin D therapy are currently being addressed in preclinical xenograft studies.

Acknowledgments

We appreciate the technical assistance of Ling Chang, Mary Ann Hart, Blanca N. Rodriguez, Kelly Tabor, and David Vazquez. Drs. Balakrishna Lokeshwar and Parmender Mehta made important contributions to the inception of this work. We are grateful to James Phillips for FACS analyses and to Drs. Paul Braunschweiger and Gary Schwartz for their comments and suggestions.

References

1. **Skowronski RJ, Peehl DM, Feldman D** 1993 Vitamin D and prostate cancer: 1,25-dihydroxyvitamin D_3 receptors and actions in human prostate cancer cell lines. Endocrinology 132:1952–1960
2. **Peehl DM, Skowronski RJ, Leung GK, Wong ST, Stamey TA, Feldman D** 1994 Antiproliferative effects of 1,25-dihydroxyvitamin D_3 on primary culture of human prostatic cells. Cancer Res 54:805–810
3. **Konety BR, Schwartz GG, Acierno Jr JS, Becich MJ, Getzenberg RH** 1996 The role of vitamin D in normal prostate growth and differentiation. Cell Growth Differ 7:1563–1570
4. **Miller GJ, Stapleton GE, Hedlund TE, Moffatt KA** 1995 Vitamin D receptor expression, 24-hydroxylase activity, and inhibition of growth by 1α,25-dihydroxyvitamin D_3 in seven human prostatic carcinoma cell lines. Clin Cancer Res 1:997–1003
5. **Schwartz GG, Oeler TA, Uskokovic MR, Bahnson RR** 1994 Human prostate cancer cells: inhibition of proliferation by vitamin D analogs. Anticancer Res 14:1077–1082
6. **Schwartz GG, Hill CC, Oeler TA, Becich MJ, Bahnson RR** 1995 1,25-Dihydroxy-16-ene-23-yne-vitamin D_3 and prostate cancer cell proliferation *in vivo*. Urology 46:365–369
7. **Zhuang SH, Schwartz GG, Cameron D, Burnstein KL** 1997 Vitamin D receptor content and transcriptional activity do not fully predict antiproliferative effects of vitamin D in human prostate cancer cell lines. Mol Cell Endocrinol 126:83–90
8. **Brinkmann V, Forouton H, Sachs M, Weidner KM, Birchmeier W** 1995 Hepatocyte growth factor/scatter factor induces a variety of tissue-specific morphogenic programs in epithelial cells. J Cell Biol 131:1573–1586
9. **Rosen EM, Goldberg ID** 1996 Scatter factor. In: Aggarwal BB, Gutterman JU (eds) Human Cytokines–Handbook for Basic and Clinical Research, vol. 2. Blackwell, Cambridge, pp 286–315
10. **Bottaro DP, Rubin JS, Faletto DL, Chan AM-L, Kmiecik TE, Vande Woude GF, Aaronson SA** 1995 Identification of the hepatocyte growth factor receptor as the *c-met* protooncogene product. Science 251:802–804
11. **Tajima H, Matsumoto K, Nakamura T** 1995 Hepatocyte growth factor has potent antiproliferative activity in various tumor cells lines. FEBS Lett 291:229–232
12. **Shiota G, Kawasaki H, Nakamura T, Schmidr EV** 1996 Inhibitory effect of hepatocyte growth factor on metastasis of hepatocellular carcinoma in transgenic mice. Res Commun Mol Pathol 91:33–39
13. **Ronen D, Altstock RT, Firon M, Mittelman L, Sobe T, Resau JH, Vande Woude GF, Trasfaty I** 1999 Met-HGF/SF mediates growth arrest and differentiation in T47D breast cancer cells. Cell Growth Differ 10:131–140
14. **Kasai S, Sugimura K, Matsumoto K, Nishi N, Kishimoto T, Nakamura T** 1996 Hepatocyte growth factor is a paracrine regulator of rat prostate epithelial growth. Biochem Biophys Res Commun 228:646–652
15. **Pisters LL, Troncoso P, Zhau HE, Li W, Von Eschenbach AC, Chung LWK** 1995 *c-met* proto-oncogene expression in benign and malignant human prostate tissues. J Urol 154:293–298
16. **Prins GS, Birch L** 1995 The developmental pattern of androgen receptor expression in rat prostate lobes is altered after neonatal exposure to estrogen. Endocrinology 136:1303–1314
17. **Katz AE, Benson MC, Wise GJ, Olsson CA, Bandyk MG, Sawczuk IS, Tomashefsky P, Buttyan R** 1989 Gene activity during the early phase of androgen-stimulated rat prostate regrowth. Cancer Res 49:5889–5894
18. **Davies P, Eaton CL** 1991 Regulation of prostate growth. J Endocrinol 131:5–17
19. **Nishi N, Oya H, Matsumoto K, Nakamura T, Miyanaka H, Wada F** 1996 Changes in gene expression of growth factors and their receptors during castration-induced involution and androgen-induced regrowth of rat prostates. Prostate 28:139–152
20. **Zhau HE, Pisters LL, Hall C, Zhao LS, Troncoso P, Pollack A, Chung LWK** 1994 Biomarkers associated with prostate cancer progression. J Cell Biochem [Suppl] 19:208–216
21. **Klein KA, Reiter RE, Redula J, Moradi H, Zhu X-L, Brothman AR, Lamb DJ, Marcelli M, Belldegrun A, Witte ON, Sawyers CL** 1997 Progression of metastatic human prostate cancer to androgen independence in immunodeficient SCID mice. Nature Med 3:402–408
22. **Grumbles RM, Howell DS, Wenger L, Altman RD, Howard GA, Roos BA** 1996 Hepatocyte growth factor and its actions in growth plate chondrocytes. Bone 19:255–261
23. **Zioncheck TF, Richardson L, Liu J, Chang L, King KL, Bennett GL, Fugedi P, Chamow SM, Schwall RH, Stack RJ** 1995 Sulfated oligosaccharides promote hepatocyte growth factor association and govern its mitogenic activity. J Biol Chem 270:16871–16878
24. **Stone KR, Mickey DD, Wunderli H, Mickey GH, Paulson DF** 1978 Isolation of a human prostate carcinoma cell line (DU 145). Int J Cancer 21:274–281
25. **Horoszewicz JS, Leong SS, Kawinski E, Karr JP, Rosenthal H, Chu TM, Mirand AE, Murphy GP** 1983 LNCaP model of human prostatic carcinoma. Cancer Res 43:1809–1818
26. **Kaighn ME, Narayan KS, Ohnuki Y, Lechner JF, Jones LW** 1979 Establishment and characterization of a human prostatic carcinoma cell line (PC-3). Invest Urol 17:16–23
27. **Loop SM, Rozanski TA, Ostenson RC** 1993 Human primary prostate tumor cell line, ALVA-31: a new model for studying the hormonal regulation of prostate tumor cell growth. Prostate 22:93–108
28. **Czerwiec FS, Liaw JJ, Liu S-B, Perez-Stable C, Grumbles R, Howard GA, Roos BA, Burnstein KL** 1997 Absence of androgen-mediated transcriptional effects in osteoblastic cells despite presence of androgen receptors. Bone 21:49–56
29. **Auffray C, Rougeon F** 1980 Purification of mouse immunoglobulin heavy chain messenger RNAs from total myeloma tumor DNA. Eur J Biochem 107:303–314
30. **Yamamoto S, Wakimoto H, Aoyagi M, Hirakawa K, Hamada H** 1997 Modulation of motility and proliferation of glioma cells by hepatocyte growth factor. Jpn J Cancer Res 88:564–577
31. **Perez-Stable C, Altman NH, Mehta PP, Deftos LJ, Roos BA** 1997 Prostate cancer progression, metastasis, and gene expression in transgenic mice. Cancer Res 57:900–906
32. **Li Q, Weng J, Mohan RR, Bennett GL, Schwall R, Wang ZF, Tabor K, Kim J, Hargrave S, Cuevas KH, Wilson SE** 1996 Hepatocyte growth factor and hepatocyte growth factor receptor in the lacrimal gland, tears, and cornea. Invest Ophthalmol Vis Sci 37:727–739
33. **Noguchi PD** 1991 Use of flow cytometry for DNA analysis. In: Coligan JE, Kruisbeek AM, Margulies DH, Shevach EM, Strober W (eds) Current Protocols in Immunology. Wiley & Sons, New York, pp 5.7–5.7.6
34. **Humphrey PA, Zhu X, Zarnegar R, Swanson PE, Ratliff TL, Vollmer RT, Day ML** 1995 Hepatocyte growth factor and its receptor (c-MET) in prostatic carcinoma. Am J Pathol 147:386–396
35. **Liu ML, Mars WM, Michalopoulos GK** 1995 Hepatocyte growth factor inhibits cell proliferation *in vivo* of rat hepatocellular carcinomas induced by diethylnitrosamine. Carcinogenesis 16:841–843
36. **Shima N, Itagaki Y, Nagao M, Yasuda H, Morinaga T, Higashio K** 1995 A fibroblast-derived tumor cytotoxic factor/F-TCF (hepatocyte growth factor/HGF) has multiple functions *in vitro*. Cell Biol Int Rep 15:397–408
37. **Santoni-Rugiu E, Preisegger KH, Kiss A, Audolfsson T, Shiota G, Schmidt EV, Thorgeirsson SS** 1996 Inhibition of neoplastic development in the liver by hepatocyte growth factor in a transgenic mouse model. Proc Natl Acad Sci USA 93:9577–9582
38. **Nishimura K, Kitamura M, Takada S, Nonomura N, Tsujimura A, Matsumiya K, Miki T, Matsumoto K, Okuyama A** 1998 Regulation of invasive potential of human prostate cancer cell lines by hepatocyte growth factor. Int J Urol 5:276–281
39. **Zhuang SH, Burnstein KL** 1998 Antiproliferative effect of 1α,25-dihydroxyvitamin D_3 in the human prostate cancer cell line LNCaP involves reduction of cyclin-dependent kinase 2 activity and persistent G1 accumulation. Endocrinology 139:1197–1207
40. **Eisman JA, Koga M, Sutherland RL, Barkla DH, Tutton PJM** 1989 1,25-Dihydroxyvitamin D_3 and the regulation of human cancer cell replication. Proc Soc Exp Biol Med 191:221–226
41. **Blutt SE, Allegretto EA, Pike JW, Weigel NL** 1997 1,25-Dihydroxyvitamin D_3 and 9-*cis*-retinoic acid act synergistically to inhibit the growth of LNCaP prostate cells and cause accumulation of cells in G_1. Endocrinology 138:1491–1497
42. **Zhao X-Y, Ly LH, Peehl DM, Feldman D** 1997 1α,25-Dihydroxyvitamin D_3 actions in LNCaP human prostate cancer cells are androgen-dependent. Endocrinology 138:3290–3298
43. **Bookstein R, Rio P, Madreperla SA, Hong F, Allred C, Grizzle WE, Lee WH** 1990 Promoter deletion and loss of retinoblastoma gene expression in human prostate carcinoma. Proc Natl Acad Sci USA 87:7762–7766
44. **Gotoh A, Kao C, Ko S-C, Hamada K, Liu T-J, Chung LWK** 1997 Cytotoxic effects of recombinant adenovirus p53 and cell cycle regulator genes ($p21^{WAF1/CIP1}$ and $p16^{CDKN4}$) in human prostate cancers. J Urol 158:636–641
45. **Elledge SJ** 1996 Cell cycle checkpoints: preventing an identity crisis. Science 274:1664–1672
46. **Sherr CJ** 1996 Cancer cell cycle. Science 274:1672–1677
47. **Weinberg RA** 1995 The retinoblastoma protein and cell cycle control. Cell 81:323–330
48. **Mashal RD, Lester S, Corless C, Richie JP, Chandra R, Propert KJ, Dutta A** 1996 Expression of cell cycle-regulated proteins in prostate cancer. Cancer Res 56:4159–4163
49. **Heisler LE, Evangelou A, Lew AM, Trachtenberg J, Elsholtz HP, Brown TJ** 1997 Androgen-dependent cell cycle arrest and apoptotic death in PC-3 prostatic cell cultures expressing a full-length human androgen receptor. Mol Cell Endocrinol 126:59–73
50. **Roos F, Ryan AM, Chamow SM, Bennett GL, Schwall RH** 1995 Induction of liver growth in normal mice by infusion of hepatocyte growth/scatter factor. Am J Physiol 31:G380–G386

Biochemical and Biophysical Research Communications **285,** 1259–1266 (2001)
doi:10.1006/bbrc.2001.5320, available online at http://www.idealibrary.com on IDEAL®

2-Methoxyestradiol Induces G2/M Arrest and Apoptosis in Prostate Cancer

Laila R. Qadan,*,†,‡,[1,2] Carlos M. Perez-Stable,*,†,‡,[1,3] Curtis Anderson,* Gianluca D'Ippolito,*,†,‡ Alan Herron,‡,§ Guy A. Howard,*,†,‡,¶ and Bernard A. Roos*,†,‡,‖,**

**Geriatric Research, Education, and Clinical Center and Research Service, VA Medical Center, Miami, Florida 33125; †Department of Medicine, ¶Department of Biochemistry and Molecular Biology, ‖Department of Neurology, and §Department of Pathology and ‡Sylvester Comprehensive Cancer Center, University of Miami School of Medicine, Miami, Florida 33101; and **Stein Gerontological Institute, Miami, Florida 33137*

Received June 2, 2001

Few therapeutic treatment options are available for patients suffering from metastatic androgen-independent prostate cancer. We investigated the ability of the estrogen metabolite 2-methoxyestradiol to inhibit the proliferation of a variety of human prostate cancer cell lines *in vitro* and to inhibit the growth of androgen-independent prostate cancer in a transgenic mouse model *in vivo*. Our results showed that 2-methoxyestradiol is a powerful growth inhibitor of LNCaP, DU 145, PC-3, and ALVA-31 prostate cancer cells. Cell flow cytometry of 2-methoxyestradiol-treated DU 145 cells showed a marked accumulation of cells in the G2/M phase of the cell cycle and an increase in the sub-G1 fraction (apoptotic). In addition, staining for annexin V, changes in nuclear morphology, and inhibition of caspase activity support a role for apoptosis. More importantly, we showed that 2-methoxyestradiol inhibits prostate tumor progression in the Gγ/T-15 transgenic mouse model of androgen-independent prostate cancer without toxic side effects. These results in cell culture and an animal model support investigations into the clinical use of 2-methoxyestradiol in patients with androgen-independent prostate cancer.

Key Words: **estrogens; flow cytometry; annexins; transgenic mice; necrosis.**

Prostate cancer advances through an androgen-dependent stage, which is responsive to palliation by androgen deprivation. In time, most prostate cancers return through an androgen-independent stage, which is marked by skeletal metastasis and results in a painful death (1). The lack of effective therapy for androgen-independent prostate cancer continues to spur new efforts to find therapeutic avenues for managing this prevalent male neoplasm. Our recent report of the cooperative action of 1,25-dihydroxyvitamin D_3 (1,25D) and hepatocyte growth factor (HGF) to inhibit androgen-independent human prostate cancer cell lines by inducing G2/M arrest supports the targeting of late cell-cycle stages for therapeutic intervention in androgen-insensitive disease (2). Stages beyond G1/S are also targeted by other chemotherapeutic agents, including vinblastine, docetaxel, and estramustine, which are currently being tested for managing metastatic prostate cancer (3). However, these agents often act via the disruption of microtubule function and are relatively nonspecific in slowing cell proliferation, including nontumor cells, and may therefore cause toxic side effects (4).

Previous studies showed that high doses of estrogen (diethylstilbestrol) inhibit the growth of advanced prostate cancer cells via an estrogen receptor-independent mechanism involving cell-cycle arrest and apoptosis; however, cardiovascular complications limit the usefulness of this therapy (5, 6). In our search for other chemotherapeutic agents that would induce G2/M cell-cycle arrest of androgen-independent prostate cancer cells without adversely affecting nontumor cells, we investigated 2-methoxyestradiol (2-ME), a prominent endogenous estradiol metabolite (7, 8). 2-ME inhibits growth in virtually all tumor cell lines tested *in vitro* and in xenograft models *in vivo* (7–23). As for diethylstilbestrol, the putative mechanisms of 2-ME's antitumor action are also estrogen receptor independent and include: (a) disruption of microtubule function (11), (b) slowing G2/M transit of the cell cycle (12, 15, 17, 21), (c) inducing apoptosis (14, 15, 18, 19, 21, 23), (d) inhibiting angiogenesis (10, 13, 22), (d)

[1] The first two authors contributed equally to this work.

[2] Present address: Kuwait University, Faculty of Medicine, P.O. Box 24923, Safat, Kuwait 13110.

[3] To whom correspondence may be addressed at VAMC, GRECC (11-GRC), 1201 NW 16 Street, Miami, FL 33125. Fax: (305) 324-3365. E-mail: cperez@med.miami.edu.

0006-291X/01 $35.00

stimulating expression of the p53 tumor suppressor gene (14–16, 18), and (e) inhibiting superoxide dismutase (23). Because 2-ME has negligible affinity for estrogen receptors (<0.1% compared to estradiol) (7, 8), its use *in vivo* should not engender estrogenic side effects such as those observed with diethylstilbestrol (5, 6).

2-ME's powerful antitumor activity and its favorable toxicity profile enhance its promise as an investigative drug for potential use in managing prostate cancer (24). Here we demonstrate for the first time that 2-ME is a powerful growth inhibitor of androgen-dependent and -independent human prostate cancer cell lines by mechanisms involving G2/M cell-cycle arrest and apoptosis. We also demonstrate that 2-ME therapy in our established transgenic mouse model of androgen-independent prostate cancer, Gγ/T-15 (25, 26), slows the growth of primary tumors and increases the areas of necrotic cells in metastatic lesions without any of the side effects common with other therapies. These results together with the recent designation of investigative new drug (IND at EntreMed, Inc., Rockville, MD) status for 2-ME treatment of men with prostate cancer provide the framework for examining 2-ME therapy in prostate cancer.

MATERIALS AND METHODS

Reagents. 2-ME, dimethyl sulfoxide (DMSO), and propidium iodide (PI) were purchased from Sigma (St. Louis, MO). The annexinV-FITC apoptosis kit, Z-VAD-FMK general caspase inhibitor, and Z-FA-FMK negative control were obtained from Trevigen (Gaithersburg, MD). For the *in vivo* experiments, 2-ME purchased from Steraloids (Newport, RI) was processed into slow-release tablets by Innovative Research of America (Sarasota, FL). Innovative Research also supplied placebo pellets.

Cell culture. The human prostate carcinoma cell lines LNCaP (27), DU 145 (28), and PC-3 (29) were obtained from the American Type Culture Collection (Rockville, MD). ALVA-31 cells were provided by Dr. Richard Ostenson (30). All cells were cultured in RPMI-1640 medium (GIBCO, Grand Island, NY) supplemented with 5% fetal bovine serum (Hyclone, Logan, UT), 100 IU/ml penicillin, 100 μg/ml streptomycin, and 0.25 μg/ml amphotericin (Gibco BRL) at 37°C in a humidified atmosphere of 5% CO_2 in air.

Cell growth assay. Prostate cancer cells were seeded in 6-well plates at 1–2 × 10^4 cells per well for DU 145, PC-3, and ALVA-31 and at 5 × 10^4 cells per well for LNCaP. The next day, fresh medium containing 2-ME (0.1–5 μM) or 0.1% DMSO (vehicle) was added; medium was changed after 3 days. On day 6, cells were removed with trypsin-EDTA, and viable cells were counted with a Neubauer hemacytometer. Reversibility was assessed as described above, except that fresh medium not containing 2-ME was replenished after 1, 2, and 3 days of 2-ME treatment. Cell counts were normalized against the vehicle control; the data are expressed as a percentage of control (mean ± standard deviation) from three or four independent experiments done in triplicate.

Analysis of cell-cycle distribution. The DU 145 human prostate cancer cell line was seeded at 1 × 10^5 cells per 6-cm dish; the next day fresh medium containing 2-ME (5 μM) or 0.1% DMSO was added. After 1–3 days, cells were removed with trypsin-EDTA, rinsed with ice-cold PBS containing 0.1% glucose, and fixed for at least 12 h after drop-wise addition of 70% ethanol; the DNA was then stained with PI (50 μg/ml) containing DNase-free RNase (100 units/ml) for 30 min. To determine reversibility of 2-ME-induced cell-cycle distribution, cells were grown in medium containing 2-ME for 1, 2, and 3 days; medium was replenished with fresh medium without 2-ME. Cell-cycle analyses were performed using a FACS Scan unit (Becton Dickinson, San Jose, CA) by excitation at 488 nm and emission at 630 nm. Cell-cycle distribution as measured by DNA content was analyzed for 5,000 cells for each growth condition. The relative proportions of cells in the G1, S, and G2/M cell-cycle phases were estimated by compartment analysis of DNA fluorescence using cell-cycle analysis software from the manufacturer (2). Low-molecular-weight DNA fluorescence was indicative of apoptotic cells. Two independent experiments were done in triplicate.

Analysis of apoptosis. To detect early stages of apoptosis, we seeded 4 × 10^4 DU 145 cells per 6-cm dish and the next day added fresh medium containing 1 or 5 μM 2-ME. After 3 days, cells were removed with trypsin-EDTA and washed with medium. Live (unfixed) cells were costained with annexin V-FITC and PI *in situ* according to the manufacturer's instructions (Trevigen). Random fields were counted for cells that stained positively with annexin V-FITC alone or with annexin V-FITC and PI using a Nikon Diaphot fluorescence microscope; then the number of stained cells was normalized to the total number of cells as counted by phase microscopy of that field. Results are expressed as percentage annexin-positive/PI-negative (early apoptotic) and annexin-positive/PI-positive (necrotic) of the total number of cells (mean ± SE). Two independent experiments were done in triplicate. Statistical differences between early apoptotic and necrotic cells in 2-ME and control dishes were determined by ANOVA.

To assess nuclear morphology (late stages of apoptosis), we seeded DU 145 cells at 1 × 10^5 cells per 6-cm dish and the next day added fresh medium containing 2-ME (5 μM) or 0.1% DMSO (control). After 1, 2, and 3 days, cells were washed twice with PBS, fixed for 20 min with freshly prepared 4% paraformaldehyde in PBS, and stained with 0.1% PI for 20 min at room temperature. Nuclear morphology typical of apoptotic cells was sought using a Nikon Diaphot fluorescence microscope.

Caspase inhibition. For further demonstration of a role for apoptosis in 2-ME inhibition, 2 × 10^4 DU 145 cells per dish were seeded in triplicate, and the next day fresh medium containing Z-VAD-FMK peptide (20 μM, general caspase inhibitor), Z-FA-FMK peptide (20 μM, negative control), or 0.1% DMSO vehicle was added. After 1 h, 2-ME (5 μM) was added to the dishes containing Z-VAD-FMK and Z-FA-FMK, and DMSO was added to the control dishes. After 3 days, the cells were removed by trypsin-EDTA and counted on a Neubauer hemacytometer; cell counts were determined and expressed as percentages of untreated vehicle control (without added peptide; mean ± standard deviation) from two independent experiments done in triplicate.

In vivo effect of 2-ME. We utilized the Gγ/T-15 transgenic mouse model of androgen-independent prostate cancer (25, 26) to assess the *in vivo* antitumor effect of 2-ME. Transgenic male mice (16–20 weeks old) with palpable prostate tumors were randomly divided into experimental and control groups. In our initial studies, we used an oral feeder to administer daily 2-ME (75 mg/kg) (n = 3) or olive oil vehicle control (Sigma, best quality) (n = 2). Subsequently, we subcutaneously implanted 21-day slow-release tablets containing 2-ME (75 mg/kg) or placebo (n = 6 for each group) in anesthetized mice with palpable prostate tumors (4 days after first detected). In addition, we similarly implanted 60-day slow-release tablets containing 2-ME (75 mg/kg) or placebo (n = 4 for each group) into 20-week-old mice without palpable prostate tumors. Three of four mice in each 60-day tablet group eventually developed prostate tumors. Prostate tumor growth was monitored by palpation three times per week and allowed to progress for 21 days in the presence of 2-ME or placebo treatment. Primary prostate tumors and visible lymph node metastases were excised and their wet weight determined. Statistical

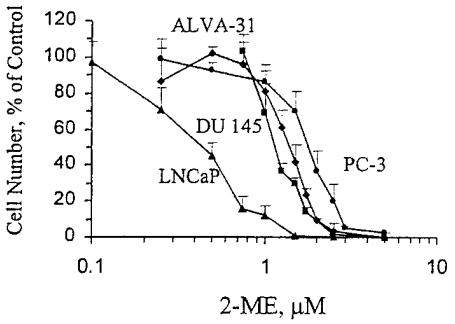

FIG. 1. 2-ME inhibits growth of human prostate cancer cell lines in a dose-dependent manner. Androgen-dependent LNCaP (▲) and androgen-independent DU 145 (■), ALVA-31 (◆), and PC-3 (●) human prostate cancer cell lines were treated with 2-ME (0.1–5 μM) or vehicle control, as described under Materials and Methods. Cell numbers were determined after 6 days of treatment; the data are expressed as a percentage of control (mean ± standard deviation) from three or four independent experiments done in triplicate.

differences between 2-ME (n = 12) and placebo (n = 11) primary and metastatic tumor weights were determined by Student's two-tailed t test. For histological analysis, primary and metastatic prostate tumors as well as liver, spleen, heart, lung, kidney, duodenum, and bone marrow were fixed in 10% buffered formalin, embedded in paraffin, sectioned at 5 μm, and stained with H&E. All animal studies were carried out with the approval of an Institutional Animal Care and Use Committee.

RESULTS

2-ME Inhibits Human Prostate Cancer Cell Growth in Vitro

Given that 2-ME has been shown to inhibit a wide variety of cancer cells (7–23), we first confirmed a similar response in androgen-dependent LNCaP and androgen-independent PC-3, DU 145, and ALVA-31 human prostate cancer cell lines. After 6 days, 2-ME was most effective at inhibiting prostate cancer cell growth between 1–5 μM, with the largest effects observed in the androgen-dependent LNCaP cell line (Fig. 1). Severe growth inhibition and cytotoxicity of androgen-independent PC-3, DU 145, and ALVA-31 were observed using 5 μM 2-ME. The half-maximal inhibitory concentrations (IC_{50}) were as follows: LNCaP, 0.5 μM; DU 145, 1.2 μM; ALVA-31, 1.5 μM; and PC-3, 1.8 μM. 2-ME mediated growth inhibition is also time dependent, because after 1 day but not after 2 days of 2-ME treatment, growth inhibition of prostate cancer cells was reversible (not shown).

G2/M Cell-Cycle Arrest and Apoptosis Induced by 2-ME: Flow Cytometry Analysis

One of the proposed mechanisms for 2-ME's antitumor effect is the disruption of microtubule function and blockade of progression through the G2 and M phases of the cell cycle (11, 12, 15, 17, 21). Accordingly, we performed flow cytometry analyses to assess cell-cycle distribution mediated by 2-ME treatment in the DU 145 human prostate cancer cell line. After only one day of 2-ME (5 μM) treatment, there was a marked shift from G1 to G2/M, confirming a late cell-cycle arrest (Fig. 2). This cell-cycle distribution was reversible after one (Fig. 2C) but not after 2 days of 2-ME (5 μM) treatment, which correlates with the time-dependent reversibility of cell growth inhibition (not shown). In addition, an apoptotic (sub-G1) peak was observed after 1 day of 2-ME (5 μM) treatment of DU 145 (Fig. 2B), which continues to increase after 2 days (not shown). Overall, these flow cytometry data suggest that 2-ME can inhibit the growth of prostate cancer cells *in vitro* by mechanisms involving G2/M cell-cycle arrest and apoptosis.

Biochemical and Morphological Parameters of Apoptosis

Because a proposed mechanism for 2-ME's antitumor effect is the induction of apoptosis (14, 15, 18, 19, 21, 23), we further analyzed in androgen-independent prostate cancer cells whether 2-ME can induce bio-

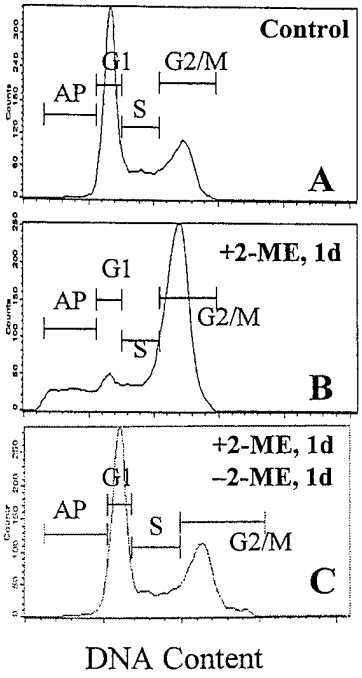

FIG. 2. 2-ME induces G2/M cell-cycle arrest and apoptosis in androgen-independent DU 145 prostate cancer cells. Cell-flow cytometry analysis measuring the number of cells (counts) in the different phases of the cell cycle (DNA content or PI staining) was done as described under Materials and Methods. Treatment of DU 145 cells for 1 day with 5 μM 2-ME (B) resulted in a marked increase of cells in the G2/M phase and sub-G1/apoptotic (AP) phase and a decrease in the G1 phase compared to vehicle control (A) treated cells. Removing 2-ME after 1 day of treatment and further growth for 1 day in medium not containing 2-ME showed reversibility of G2/M arrest (C). Two independent experiments were done in triplicate.

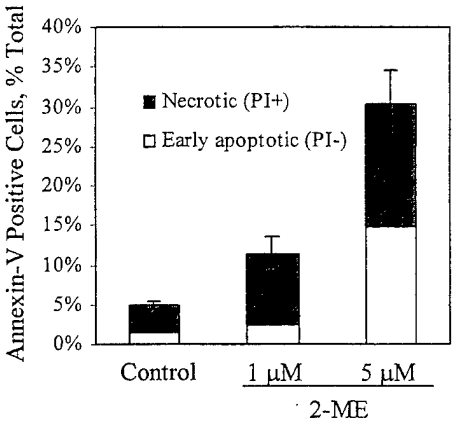

FIG. 3. 2-ME mediates a dose-dependent increase in apoptosis. DU 145 prostate cancer cells treated for 3 days with 2-ME (1 and 5 μM) or vehicle control were simultaneously stained *in situ* with annexin V-FITC antibodies and PI. Annexin membrane-stained cells and PI− or + nuclear stained cells were counted using a fluorescent microscope and expressed as a percentage of the total number of cells in the same field determined by phase microscope (mean ± SE). Results showed a dose-dependent increase ($P < 0.05$, ANOVA) in early apoptotic cells (annexin +/PI−) and necrotic cells (annexin +/PI +). Similar results were obtained in two independent experiments done in triplicate.

chemical and morphological markers of apoptosis. To assess the 2-ME induction of apoptosis in DU 145 cells, we used annexin V-FITC immunostaining, a marker for early apoptosis. To distinguish early apoptotic live cells from necrotic dead cells, we costained DU 145 cells *in situ* with annexin V-FITC and PI (excluded by live cells) after treatment with 2-ME (1 and 5 μM) or control (0.1% DMSO) (Fig. 3). We found a greater number of early apoptotic cells (annexin-positive/PI-negative) in 5 μM compared to 1 μM 2-ME-treated DU 145 cells, whereas necrotic cells (annexin-positive/PI-positive) increased in both 1 and 5 μM 2-ME-treated cells. Morphological changes associated with late apoptosis were observed in 2-ME-treated but not in control DU 145 cells, including condensed and fragmented chromatin (Fig. 4). These results further support a role for apoptosis in 2-ME's dose-dependent growth inhibition of prostate cancer cells.

Reduction of the 2-ME Effect by Caspase Inhibition

Because apoptosis proceeds by activation of caspases (31), we next assessed the extent of 2-ME's growth-inhibitory effects in DU 145 cells reduced by the broad-spectrum caspase inhibitor peptide, Z-VAD-FMK (Fig. 5). Compared to the negative control peptide Z-FA-FMK (does not inhibit caspase activity), Z-VAD-FMK significantly reduced the growth-inhibition effects of 2-ME in DU 145 cells (Fig. 5). However, 2-ME was still able to inhibit significantly DU 145 cell growth (33% of untreated vehicle control) in the presence of caspase inhibition.

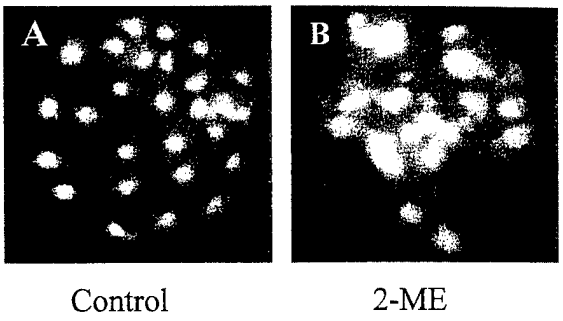

FIG. 4. 2-ME-treated DU 145 prostate cancer cells show nuclear morphology changes typical of late apoptosis. The fluorescent microscope analysis of PI-stained DU 145 cells after treatment with 5 μM 2-ME (B) or vehicle control (A) for 2 days depicts an area of 2-ME-treated DU 145 cells containing condensed and fragmented nuclei, typical of cells undergoing apoptosis (magnification ×200).

2-ME Can Inhibit Prostate Cancer in Vivo without Toxic Side Effects

To assess the ability of 2-ME to inhibit prostate cancer cell growth *in vivo,* we used the Gγ/T-15 transgenic mouse model of androgen-independent prostate cancer (25, 26). These mice contain the human fetal Gγ globin promoter linked to the SV40 T antigen oncogene and result in the development of an aggressive highly metastatic form of prostate cancer originating from normal prostate epithelial cells (25, 26; manuscript in preparation). Because of the reversibility of 2-ME's effects (see Fig. 2), slow-release tablets were used. Overall, we found that primary prostate tumors from

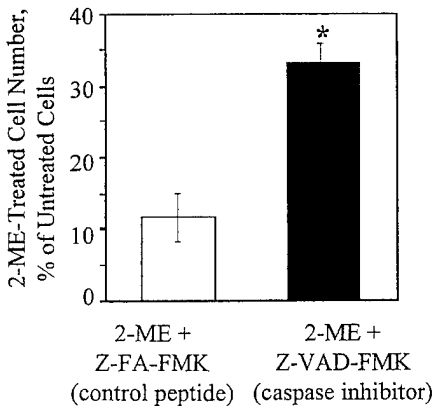

FIG. 5. 2-ME-mediated growth effects are partially overcome by general caspase inhibitor Z-VAD-FMK. DU 145 prostate cancer cells were incubated with the general caspase inhibitor Z-VAD-FMK or the negative control peptide Z-FA-FMK along with 5 μM 2-ME for 3 days; then cell counts were determined and expressed as percentages of untreated vehicle control (without added peptide; mean ± standard deviation). Inhibition of caspase activity (and presumably apoptosis) resulted in a partial recovery of cell growth with the addition of Z-VAD-FMK (33% of control) compared to the addition of Z-FA-FMK (11% of control). These differences were significant ($^*P = 0.001$, ANOVA). Similar results were obtained in two independent experiments done in triplicate.

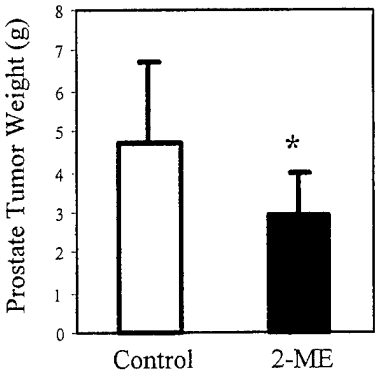

FIG. 6. 2-ME inhibits the growth of androgen-independent prostate cancer in Gγ/T-15 transgenic mice. Transgenic males (16–20 weeks) containing palpable prostate tumors were treated either orally (daily) or by subcutaneously transplanted slow-release tablets for 21 days with either 75 mg/kg 2-ME or placebo control (see Materials and Methods). Primary prostate tumors were removed and wet weight was determined (mean ± standard deviation). Transgenic mice treated with 2-ME (n = 12) contained smaller primary prostate tumors compared to control mice (n = 11) (*P = 0.02, two-tailed Student's t test).

2-ME (75 mg/kg)-treated mice were significantly smaller (38% reduction of wet weight) compared to placebo-treated mice (Fig. 6; P = 0.02) (see Materials and Methods). However, the total wet weight of lymph node metastases was not significantly different between 2-ME and placebo mice (not shown). Despite this result, histological analysis of small size-matched lymph-node metastasis lesions consistently showed greater focal areas of necrosis in 2-ME-compared to placebo-treated mice (Fig. 7). In addition, we observed increased intercellular spacing in 2-ME-treated lesions (likely from edema and typical of areas adjacent to necrotic areas), which possibly contributed to the softness of 2-ME-treated tumors compared to the firm placebo tumors. Because larger prostate tumor masses normally contain extensive areas of cellular necrosis, it was not possible to determine if 2-ME also induced greater areas of necrosis in primary prostate tumors.

Mice without palpable prostate tumors that received the 60-day slow-release 2-ME or placebo tablets developed prostate tumors with the same frequency (3 of 4), suggesting a lack of chemoprevention by 2-ME. During the time of 2-ME treatment (21 to 60 days), no toxic side effects were noted—i.e., there were no significant differences in body weight, behavior, or histology of multiple tissues including bone marrow and duodenum. Overall, these results suggest that 2-ME can significantly inhibit androgen-independent prostate cancer in the Gγ/T-15 transgenic mice without the toxic side effects associated with other therapies.

DISCUSSION

We previously demonstrated that the combination of 1,25D and HGF treatment of androgen-independent prostate cancer cells resulted in only modest G2/M cell-cycle arrest and growth inhibition (2). However, application of this combination in clinical studies must address potential problems arising from HGF's angiogenic and 1,25D's calcemic side effects (32, 33). In this report we show that the endogenous estrogen metabolite 2-ME provides more effective growth inhibition of androgen-independent prostate cancer cells than we observed with HGF and 1,25D. The mechanism whereby 2-ME blocks prostate cancer cell proliferation involves a marked G2/M arrest and induction of apoptosis *in vitro*. Finally, we show that continuous treatment with 2-ME has a significant antitumor effect in the Gγ/T-15 transgenic mouse model of androgen-independent prostate cancer without toxic side effects. These data encourage further study in the clinical use of 2-ME against androgen-independent prostate cancer, which currently has few treatment options.

2-ME inhibits the growth of all prostate cancer cell lines *in vitro*, including androgen-independent DU 145, PC-3, and ALVA-31 and particularly androgen-dependent LNCaP (Fig. 1). The IC_{50} doses for prostate

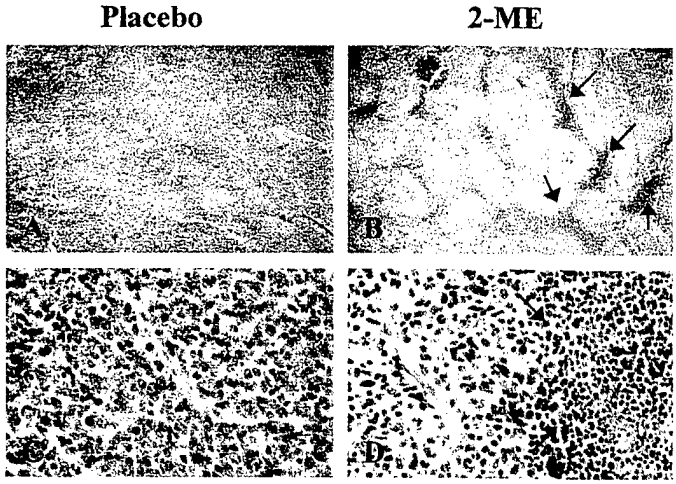

FIG. 7. Areas of cellular necrosis in metastatic lymph node lesions are increased by 2-ME. Small size-matched metastatic lesions from placebo-treated (A, C) and 2-ME-treated (B, D) mice were removed for histological analysis. (A) A light micrograph (H&E, ×40) of metastasis to lymph node from placebo-treated mouse shows homogenous architecture of tumor cells with little or no areas of necrosis. (B) A light micrograph (H&E, ×40) of metastasis to lymph node from 2-ME-treated mouse shows focal areas of necrosis (arrows indicating darker staining cells) surrounded by tumor cells (note lighter appearance of tumor cell areas compared to placebo). (C) Higher magnification (H&E, ×400) of metastatic lesion from placebo-treated mouse shows numerous mitotic tumor cells and cells with pyknotic nuclei (darker stain). (D) Higher magnification (H&E, ×400) of metastatic lesion from 2-ME-treated mouse reveals an area of necrosis (arrows) containing cells with pyknotic nuclei next to an area containing mitotic tumor cells. Note the increase in intercellular spacing in the tumor cell area (typical of areas adjacent to necrotic areas), resulting in the lighter appearance observed in B. Similar results were observed in analysis of other placebo (n = 3) and 2-ME (n = 3) metastatic lesions.

cancer cells (0.5–1.8 μM) are greater than for breast cancer cells (0.01–0.2 μM) but less than for lung, pancreatic, and hepatoma cancer cells (1.5–10 μM) (9, 13, 14, 19, 21). In addition, not all lung cancer cell lines are inhibited by 2-ME. For example, 2-ME growth inhibition of lung cancer cell lines depends on the expression of p53 tumor suppressor (14). In prostate cancer cells, the growth-inhibitory effect of 2-ME is p53 independent because DU 145 and PC-3 contain mutated p53 (34). These results suggest that similar to breast cancer cells, prostate cancer cells are very sensitive to the growth-inhibitory effects of 2-ME.

One of the postulated mechanisms for 2-ME's antitumor effect is the disruption of microtubules and the subsequent growth arrest of proliferating cells in the G2/M phase of the cell cycle (11, 12, 15, 17, 21). In agreement, we found a marked increase in DU 145 prostate cancer cells in the G2/M phase after 2-ME treatment (Fig. 2). In contrast, the effect of 2-ME on cell-cycle distribution is dissimilar for breast, lung, and pancreatic cancer cells (9, 14, 19). For example, in breast cancer cells, 2-ME treatment results in an accumulation in the G1 phase (9), whereas in pancreatic cancer cells the accumulation occurs in the S phase (19). In p53-positive lung cancer cells, 2-ME does not affect microtubule structure and has no effect on the cell cycle (14). In this case, the likely mechanism of growth inhibition is induction of p53-mediated apoptosis (14–16). In hepatoma cells, similar to prostate cancer cells, 2-ME growth inhibition results in accumulation in the G2/M phase (21). These results suggest that 2-ME utilizes diverse mechanisms, in addition to disruption of microtubules, to inhibit the growth of numerous cancer cell lines *in vitro*.

Using flow cytometry, annexin immunostaining, cell nucleus morphology, and caspase inhibition, we showed that 2-ME can induce apoptosis in DU 145 prostate cancer cells *in vitro*. It is apparent from the cell flow cytometry data that induction of apoptosis requires at least one day of treatment with 5 μM 2-ME, after which growth inhibition becomes irreversible (Fig. 2). Results obtained from annexin immunostaining suggest that treatment with a lower dose of 2-ME (1 μM) leads to cell growth inhibition and necrosis but without a considerable amount of apoptosis (Fig. 3). In addition, the caspase inhibitor Z-VAD-FMK results in a partial block of 2-ME's growth inhibition of DU 145 prostate cancer cells (Fig. 5). These results suggest that G2/M arrest and induction of apoptosis are distinct mechanisms utilized by 2-ME to inhibit prostate cancer cell growth *in vitro*. However, it is not clear if G2/M cell-cycle arrest is required before induction of apoptosis. We are currently investigating the molecular mechanisms of 2-ME-mediated G2/M arrest (for example, effect on cyclin B and cdc2 kinase; 35) and induction of apoptosis (for examples, mitochondrial cytochrome C release, caspase activation, and Bcl-2 family; 36) in prostate cancer cells.

2-ME appears to have a pleiotropic effect on prostate cancer cell growth and apoptosis because its activity is independent of the androgen and estrogen receptors, tumor suppressors (p53, Rb), and sensitivity to Fas (37–39). Our findings demonstrate the effectiveness of 2-ME in inhibiting the growth of proliferating prostate cancer cells *in vitro*. However, because more than 95% of androgen-independent prostate cancer cells are in a quiescent G0 state *in vivo* (40), it will be important to determine if 2-ME can induce cytotoxicity in nonproliferating prostate cancer cells. A major advantage for the clinical use of 2-ME is that it has little effect on normal cells *in vitro* and no toxic side effects *in vivo* (10, 13–15, 18–20). Therefore, 2-ME would be an ideal antitumor chemotherapeutic agent if it can target proliferating and nonproliferating prostate cancer without affecting normal tissues.

Finally, our results in Gγ/T-15 transgenic mice treated with 2-ME demonstrated significant but modest anti-prostate tumor activity without toxic side effects *in vivo* (Figs. 6 and 7). These findings contrast with the results of our studies in Gγ/T-15 with the 1,25D analog EB 1089, which produced minimal anti-prostate tumor activity and substantial toxic side effects including weight loss and hypercalcemia (manuscript in preparation). We do not yet know whether the anti-prostate tumor activity of 2-ME in Gγ/T-15 mice occurs by G2/M cell-cycle arrest and induction of apoptosis, similar to the *in vitro* results. Experiments involving short-term dosing of Gγ/T-15 mice with 2-ME followed by flow cytometry analysis of prostate tumors can help answer this question. It is also possible that higher doses of 2-ME (>75 mg/kg) are required for more effective growth inhibition of primary and metastatic prostate tumors.

Other studies demonstrating the antitumor effect of 2-ME *in vivo* have utilized cancer cell lines transplanted subcutaneously or intravenously into immunecompromised mice (10, 13, 16, 19, 20). These transplantable tumor models frequently respond to anticancer drugs or other therapies, but then show no activity in human trials (41, 42). Transgenic models of prostate cancer such as Gγ/T-15, TRAMP, and C(3)/T antigen (43) represent a more natural progression of tumor development, and results obtained from drug testing in these models may be more predictive of clinical outcome. However, it is too early to conclude that these mice will be better than transplantable models.

In conclusion, our results demonstrate that the anti-prostate tumor activity of 2-ME works through multiple mechanisms, including G2/M cell-cycle arrest and induction of apoptosis. This finding is significant, given that androgen-independent prostate cancer is an extremely heterogeneous disease and its growth response to androgen withdrawal is largely attributed to impair-

ment of cell-cycle regulation and apoptosis (44, 45). Chemotherapeutic agents like 2-ME hold great promise for the management of androgen-independent prostate cancer because of their powerful antitumor activity and lack of toxic side effects on quiescent normal cells. Further studies investigating the molecular mechanisms of 2-ME's anti-prostate tumor activity and possible clinical use in humans are clearly warranted.

ACKNOWLEDGMENTS

We appreciate the technical assistance of Alicia de las Pozas and Adan Farinas. We are grateful to James Phillips for FACS analyses and to Drs. Parmender Mehta, Herman Cheung, and Paul Braunschweiger for their comments and suggestions. This work was supported by a VA Merit Review Entry Program grant (98-69-01 to C.M.P.-S.), a Department of Defense grant (DAMD-17-98-1-8525 to B.A.R.), and the VA Medical Research Service. G.A.H. has a Senior Research Career Scientist award from the Department of Veterans Affairs.

REFERENCES

1. Isaacs, J. T. (1999) The biology of hormone refractory prostate cancer. Why does it develop? *Urol. Clin. North Am.* **26,** 263–273.
2. Qadan, L. R., Perez-Stable, C. M., Schwall, R. H., Burnstein, K. L., Ostenson, R. C., Howard, G. A., and Roos, B. A. (2000) Hepatocyte growth factor and vitamin D cooperatively inhibit androgen-unresponsive prostate cancer cell lines. *Endocrinology* **141,** 2567–2573.
3. Oh, W. K. (2000) Chemotherapy for patients with advanced prostate carcinoma. *Cancer* **88,** 3015–3021.
4. Pilat, M. J., Kamradt, J. M., and Pienta, K. J. (1999) Hormone resistance in prostate cancer. *Cancer Metastasis Rev.* **17,** 373–381.
5. deVoogt, H. J., Smith, P. H., Pavone-Macaluso, M., de Pauw, M., and Suciu, S. (1986) Cardiovascular side effects of diethylstilbesterol, cyproterone acetate, medroxyprogesterone acetate and estramustine phosphate used for the treatment of advanced prostate cancer: Results from European Organization for Research on Treatment of Cancer Trials 30761 and 30762. *J. Urol.* **135,** 303–307.
6. Robertson, C. N., Roberson, K. M., Padilla, G. M., O'Brien, E. T., Cook, J. M., Kim, C. S., and Fine, R. L. (1996) Induction of apoptosis by diethylstilbestrol in hormone-insensitive prostate cancer cells. *J. Natl. Cancer Inst.* **88,** 908–917.
7. Zhu, B. T., and Conney, A. H. (1998) Is 2-methoxyestradiol an endogenous estrogen metabolite that inhibits mammary carcinogenesis? *Cancer Res.* **58,** 2269–2277.
8. Pribluda, V. S., Gubish, E. R., LaValle, T. M., Treston, A., Swartz, G. M., and Green, S. J. (2000) 2-Methoxyestradiol: An endogenous antiangiogenic and antiproliferative drug candidate. *Cancer Metastasis Rev.* **19,** 173–179.
9. Lottering, M. L., Haag, M., and Seegers, J. C. (1992) Effects of 17 β-estradiol metabolites on cell cycle events in MCF-7 cells. *Cancer Res.* **52,** 5926–5932.
10. Fotsis, T., Zhang, Y., Pepper, M. S., Adlercreutz, H., Montesano, R., Nawroth, P. P., and Schweigerer, L. (1994) The endogenous estrogen metabolite 2-methoxyestradiol inhibits angiogenesis and suppresses tumor growth. *Nature* **368,** 237–239.
11. D'Amato, R. J., Lin, C. M., Flynn, E., Folkman, J., and Hamel, E. (1994) 2-Methoxyestradiol, an endogenous mammalian metabolite, inhibits tubulin polymerization by interacting at the colchicine site. *Proc. Natl. Acad. Sci. USA* **91,** 3964–3968.
12. Attalla, H., Makela, T. P., Adlercreutz, H., and Anderson, L. C. (1996) 2-Methoxyestradiol arrests cells in mitosis without depolymerizing tubulin. *Biochem. Biophys. Res. Commun.* **228,** 467–473.
13. Klauber, N., Parangi, S., Flynn, E., Hamel, E., and D'Amato, R. J. D. (1997) Inhibition of angiogenesis and breast cancer in mice by the microtubule inhibitors 2-methoxyestradiol and taxol. *Cancer Res.* **57,** 81–86.
14. Mukhopadhay, T., and Roth, J. (1997) Induction of apoptosis in human lung cancer cells after wild type p53 activation by methoxyestradiol. *Oncogene* **14,** 379–384.
15. Seegers, J. C., Lottering, M., Grobler, C. J. S., Papendrop, D. H., Habbersett, R. C., Shou, Y., and Lehnert, B. E. (1997) The mammalian metabolite, 2-methoxyestradiol, affects p53 levels and apoptosis induction in transformed cells but not in normal cells. *J. Steroid Biochem. Mol. Biol.* **62,** 253–267.
16. Kataoka, M., Schumacher, G., Cristiano, R. J., Atkinson, E. N., Roth, J. A., and Mukhopadhyay, T. (1998) An agent that increases tumor suppressor transgene product coupled with systemic transgene delivery inhibits growth of metastatic lung cancer in vivo. *Cancer Res.* **58,** 4761–4765.
17. Reiser, F., Bernas, M., Witte, M., and Witte, C. (1998) Inhibition of normal and experimental angiotumor endothelial cell proliferation and cell cycle progression by 2-methoxyestradiol. *Proc. Soc. Exp. Biol. Med.* **219,** 211–216.
18. Mukhopadhyay, T., and Roth, J. A. (1998) Superinduction of wild-type p53 protein after 2-methoxyestradiol treatment of Ad5p53-transduced cells induces tumor cell apoptosis. *Oncogene* **17,** 241–246.
19. Schumacher, G., Kataoka, M., Roth, J. A., and Mukhopadhyay, T. (1999) Potent antitumor activity of 2-methoxyestradiol in human pancreatic cancer cell lines. *Clin. Cancer Res.* **5,** 493–499.
20. Arbiser, J. L., Panigrathy, D., Klauber, N., Rupnick, M., Flynn, E., Udagawa, T., and D'Amato, R. J. (1999) The antiangiogenic agents TNP-470 and 2-methoxyestradiol inhibit the growth of angiosarcoma in mice. *J. Am. Acad. Dermatol.* **40,** 925–929.
21. Lin, H-L., Liu, T-Y., Chau, G-Y., Lui, W-Y., and Chi, C-W. (2000) Comparison of 2-methoxyestradiol-induced, docetaxel-induced, and paclitaxel-induced apoptosis in hepatoma cells and its correlation with reactive oxygen species. *Cancer* **89,** 983–994.
22. Banerjeei, S. K., Zoubine, M. N., Sarkar, D. K., Weston, A. P., Shah, J. H., and Campbell, D. R. (2000) 2-Methoxyestradiol blocks estrogen-induced rat pituitary tumor growth and tumor angiogenesis: Possible role of vascular endothelial growth factor. *Anticancer Res.* **20,** 2641–2645.
23. Huang, P., Feng, L., Oldham, E. A., Keating, M. J., and Punkett, W. (2000) Superoxide dismutase as a target for the selective killing of cancer cells. *Nature* **407,** 390–395.
24. D'Amato, R. J., and Folkman, M. J. (1999) Estrogenic compounds as anti-mitotic agents. U.S. Patent No. 5,892,069.
25. Perez-Stable, C., Altman, N. H., Brown, J., Harbison, M., Cray, C., and Roos, B. A. (1996) Prostate, adrenocortical, and brown adipose tumors in fetal globin/T antigen transgenic mice. *Lab. Invest.* **74,** 363–373.
26. Perez-Stable, C., Altman, N. H., Mehta, P. P., Deftos, L. J., and Roos, B. A. (1997) Prostate cancer progression, metastasis, and gene expression in transgenic mice. *Cancer Res.* **57,** 900–906.
27. Horoszewicz, J. S., Leong, S. S., Kawinski, E., Kerr, J. P., Rosenthal, H., Chu, T. M., Mirand, E. A., and Murphy, G. P. (1983) LNCaP model of human prostatic carcinoma. *Cancer Res.* **43,** 1809–1818.
28. Stone, K. R., Mickey, D. D., Wunderli, H., Mickey, G. H., and Paulson, D. F. (1978) Isolation of a human prostate carcinoma cell line (DU 145). *Int. J. Cancer* **21,** 274–281.

29. Kaighn, M. E., Narayan, K. S., Ohnuki, Y., Lechner, J. F., and Jones, L. W. (1979) Establishment and characterization of a human prostatic carcinoma cell line (PC-3). *Invest. Urol.* **17,** 16–23.
30. Loop, S. M., Rozansky, T. A., and Ostenson, R. C. (1993) Human primary tumor cell line ALVA-31: A new model for studying the hormonal regulation of tumor cell growth. *Prostate* **22,** 93–108.
31. Earnshaw, W. C., Martins, L. M., and Kaufmann, S. H. (1999) Mammalian caspases: Structure, activation, substrates, and functions during apoptosis. *Annu. Rev. Biochem.* **68,** 383–424.
32. Roos, F., Ryan, A. M., Chamow, S. M., Bennett, G. L., and Schwall, R. H. (1995) Induction of liver growth in normal mice by infusion of hepatocyte growth/scatter factor. *Am. J. Physiol.* **31,** G380–G386.
33. Miller, G. J. (1999) Vitamin D and prostate cancer: Biological interactions and clinical potentials. *Cancer Metastasis Rev.* **17,** 353–360.
34. Isaacs, W. B., Carter, B. S., and Ewing, C. M. (1991) Wild-type p53 suppresses growth of human prostate cancer cells containing mutant p53 alleles. *Cancer Res.* **51,** 4716–4720.
35. Zoubine, M. N., Weston, A. P., Johnson, D. C., Campbell, D. R., and Banerjee, S. K. (1999) 2-Methoxyestradiol-induced growth suppression and lethality in estrogen-responsive MCF-7 cells may be mediated by down regulation of p34cdc2 and cyclin B1 expression. *Int. J. Oncol.* **15,** 639–646.
36. Bruckheimer, E. M., and Kyprianou, N. (2000) Apoptosis in prostate carcinogenesis. A growth regulator and a therapeutic target. *Cell Tissue Res.* **301,** 153–162.
37. Webber, M. M., Bello, D., and Quader, S. (1997) Immortalized and tumorigenic adult human prostatic epithelial cell lines: Characteristics and applications. 3. Oncogenes, suppressor genes, and applications. *Prostate* **30,** 136–142.
38. Lau, K. M., LaSpina, M., Long, J., and Ho, S. M. (2000) Expression of estrogen receptor (ER)-alpha and ER-beta in normal and malignant prostatic epithelial cells: Regulation by methylation and involvement in growth regulation. *Cancer Res.* **60,** 3175–3182.
39. Rokhlin, O. W., Bishop, G. A., Hostager, B. S., Waldschmidt, T. J., Sidorenko, S. P., Pavloff, N., Kiefer, M. C., Umansky, S. R., Glover, R. A., and Cohen, M. B. (1997) Fas-mediated apoptosis in human prostatic carcinoma cell lines. *Cancer Res.* **57,** 1758–1768.
40. Berges, R. R., Vukanovic, J., Epstein, J. I., CarMichel, M., Cisek, L., Johnson, D. E., Veltri, R. W., Walsh, P. C., and Isaacs, J. T. (1995) Implication of cell kinetic changes during the progression of human prostatic cancer. *Clin. Cancer Res.* **1,** 473–480.
41. Rosenberg, M. P., and Bortner, D. (1999) Why transgenic and knockout animal models should be used (for drug efficacy studies in cancer). *Cancer Metastasis Rev.* **17,** 295–299.
42. Kerbel, R. S. (1999) What is the optimal rodent model for anti-tumor drug testing? *Cancer Metastasis Rev.* **17,** 301–304.
43. Sharma, P., and Schreiber-Agus, N. (1999) Mouse models of prostate cancer. *Oncogene* **18,** 5349–5355.
44. Bruckheimer, E. M., Gjertsen, B. T., and McDonnell, T. J. (1999) Implications of cell death regulation in the pathogenesis and treatment of prostate cancer. *Semin. Oncol.* **26,** 382–398.
45. Amanatullah, D. F., Reutens, A. T., Zafonte, B. T., Fu, M., Mani, S., and Pestell, R. G. (2000) Cell-cycle dysregulation and the molecular mechanisms of prostate cancer. *Front. Biosci.* **5,** D372–D390.

ELSEVIER

Molecular and Cellular Endocrinology 186 (2002) 69–79

MCE
Molecular and Cellular Endocrinology

www.elsevier.com/locate/mce

Vitamin D-mediated growth inhibition of an androgen-ablated LNCaP cell line model of human prostate cancer

Eddy S. Yang [a], Carol A. Maiorino [a], Bernard A. Roos [b,c], Selena R. Knight [a], Kerry L. Burnstein [a,c,*]

[a] *Department of Molecular and Cellular Pharmacology (R-189), University of Miami School of Medicine, PO Box 016189 (R-189), Miami, FL 33136, USA*

[b] *Department of Medicine, University of Miami School of Medicine, Miami, FL, USA*

[c] *Geriatric Research Education and Clinical Center (GRECC), Miami VA Medical Center, Miami, FL, USA*

Received 30 July 2001; accepted 14 September 2001

Abstract

1,25-$(OH)_2$ vitamin D_3 (1,25-$(OH)_2$ D), the active metabolite of vitamin D, exerts antiproliferative effects on a variety of tumor cells including prostate. This inhibition requires vitamin D receptors (VDRs) as well as downstream effects on the G1 to S phase checkpoint of the cell cycle. Recent data raise the possibility that androgen plays a role in the antiproliferative effects of 1,25-$(OH)_2$ D in prostate cancer cells; however, this hypothesis has been difficult to test rigorously as the majority of prostate cancer cell lines (unlike human prostate tumors) lack androgen receptors (ARs). We utilized two different models of androgen-independent prostate cancer that express functional ARs and VDRs to evaluate a possible role of androgen in 1,25-$(OH)_2$ D mediated growth inhibition. We stably introduced the AR cDNA into the human prostate cancer cell line ALVA 31, which expresses functional VDR but is relatively resistant to growth inhibition by 1,25-$(OH)_2$ D. Neither ALVA-AR nor the control cells, ALVA-NEO, exhibited substantial growth inhibition by 1,25-$(OH)_2$ D in the presence or absence of androgen. This observation suggests that the basis for the resistance of ALVA 31 to 1,25-$(OH)_2$ D-mediated growth inhibition is not the lack of AR. The second model was LNCaP-104R1, an AR-expressing androgen independent prostate cancer cell line derived from androgen dependent LNCaP. 1,25-$(OH)_2$ D inhibited the growth of LNCaP-104R1 cells in the absence of androgen and this effect was not blocked by the antiandrogen Casodex. As was observed in the parental LNCaP cells, this effect was correlated with G1 phase cell cycle accumulation and upregulation of the cyclin dependent kinase inhibitor (CKI) p27, as well as increased association of p27 with cyclin dependent kinase 2. These findings suggest that the antiproliferative effects of 1,25-$(OH)_2$ D do not require androgen-activated AR but do involve 1,25-$(OH)_2$ D induction of CKIs required for G1 cell cycle checkpoint control.

Keywords: Androgen receptor; Cyclin dependent kinase inhibitor; $p21^{WAF1/CIP1}$; $p27^{KIP1}$; Androgen independence; Vitamin D receptor

1. Introduction

1,25-Dihydroxyvitamin D_3 (1,25-$(OH)_2$ D), the active metabolite of vitamin D and a critical regulator of calcium and phosphate homeostasis, also exerts important effects on cellular proliferation and differentiation (reviewed in Bikle 1992, Feldman et al., 1997, Pols et al., 1990, and Walters, 1992). 1,25-$(OH)_2$ D activates the vitamin D receptor (VDR), a ligand-dependent transcription factor that binds *cis*-acting DNA sequences known as vitamin D response elements (VDREs) (reviewed in Glass (1994)). Several established human prostate cancer cell lines, as well as primary cultures of benign and cancerous prostatic tissue, express functional VDRs and are growth inhibited by 1,25-$(OH)_2$ D (Blutt et al., 1997a; Miller et al., 1992, 1995; Schwartz et al., 1994; Skowronski et al., 1993; Zhuang et al., 1997; Zhuang and Burnstein 1998). However, the antiproliferative effects of 1,25-$(OH)_2$ D in prostate cancer cells are extremely variable, ranging from no effect in some cells to profound growth inhibition in the LNCaP human prostate cancer cell line (Blutt et al., 1997a; Miller et al., 1992, 1995; Schwartz et al., 1994; Skowronski et al., 1993; Zhuang et al., 1997; Zhuang and Burnstein 1998).

* Corresponding author. Tel.: +1-305-243-5732; fax: +1-305-243-4555.

E-mail address: kburnste@miami.edu (K.L. Burnstein).

0303-7207/02/$ - see front matter
PII: S0303-7207(01)00671-2

Our previous studies established that inhibition of LNCaP growth by 1,25-$(OH)_2$ D correlates with accumulation of cells in the G1 phase of the cell cycle and hypophosphorylation of Rb, which is the major regulator of the G1 → S phase transition (Zhuang and Burnstein 1998). 1,25-$(OH)_2$ D treatment of LNCaP cells results in a profound decrease in cyclin-dependent kinase 2 (CDK2) activity, a transient increase in the levels of the cyclin dependent kinase inhibitor (CKI) $p21^{WAF1,CIP1}$ and decreased transcriptional activity of the E2F transcription factor family, which regulate the expression of genes necessary for transition into S phase (Zhuang and Burnstein 1998). In contrast, despite the presence of higher levels of transcriptionally active VDR compared to LNCaP cells, 1,25-$(OH)_2$ D had little effect on the growth of or cell cycle events in ALVA31 cells (Zhuang and Burnstein 1998).

Because LNCaP cells are highly sensitive to growth inhibition by 1,25-$(OH)_2$ D and express androgen receptor (AR) while ALVA31 and several other prostate cancer cell lines lack AR and are much less sensitive to growth inhibition by 1,25-$(OH)_2$ D, Zhao et al. (1997) proposed that the antiproliferative effects of 1,25-$(OH)_2$ D require androgen. It is well established that LNCaP cells cultured in media devoid of androgen (charcoal stripped serum, CSS) are not significantly growth inhibited by 1,25-$(OH)_2$ D (Miller et al., 1992) whereas LNCaP grown in 10% serum are inhibited (Blutt et al., 1997b; Zhao et al., 1997; Zhuang and Burnstein 1998). However, when cells (grown in CSS) were co-treated with 1,25-$(OH)_2$ D and low (growth promoting) concentrations of androgen, substantial growth inhibition was observed. Further, the antiandrogen Casodex abolished this growth inhibition (Zhao et al., 1997). However, since LNCaP cells cultured in CSS or Casodex exhibit significantly decreased proliferation rate (Esquenet et al., 1996; Zhao et al., 1997), it is difficult to establish a role for androgen in 1,25-$(OH)_2$ D's growth inhibitory effects in this model.

1,25-$(OH)_2$ D-mediated growth inhibition of two newer human prostate cancer cell lines, MDA PCa-2a and -2b, does not appear to involve androgen as addition of casodex has no effect (Zhao et al., 2000a). However, these cell lines, which were derived from the same bone metastasis, express mutated AR with very poor affinity for androgen (Zhao et al., 1999, 2000b). Thus, a potential role of androgen in 1,25-$(OH)_2$ D-mediated growth inhibition cannot be readily studied in these cell lines.

In this study, we tested the capacity of 1,25-$(OH)_2$ D to inhibit the growth of AR-expressing, androgen-independent prostate cancer cells. The two models of androgen independent prostate cancer examined were ALVA31 cells stably transfected with a human AR cDNA (ALVA-AR, generated in this study) and a derivative of LNCaP cells (LNCaP-104R1) that arose after passaging cells for 2 years in the absence of androgen (generously provided by Drs S. Liao and J. Konkontis, Kokontis et al., (1994)). Because neither of these models are dependent on androgen for proliferation and both express high affinity AR, these cell lines are appropriate for addressing a potential role of androgen and AR in 1,25-$(OH)_2$ D-mediated growth inhibition. Further, both cell lines exhibit characteristics of more aggressive, androgen independent prostate cancer including relatively low levels of the CKIs p21 and p27. Loss of p27 expression, in particular, correlates with prostate cancer recurrence, a more aggressive phenotype, and decreased patient prognosis and survival (Cheng et al., 2000; Cote et al., 1998; Fernandez et al., 1999; Guo et al., 1997; Tsihlias et al., 1998; Yang et al., 1998).

Heterologous expression of functional, wild type AR in ALVA31 cells did not, in the presence or absence of androgen, confer enhanced sensitivity to 1,25-$(OH)_2$ D-mediated growth inhibition. In contrast, the androgen independent LNCaP-104R1 cells were growth inhibited by 1,25-$(OH)_2$ D in the absence of androgen. This growth inhibition was accompanied by accumulation of cells in the G1 phase of the cell cycle, upregulation of the CKI p27, and increased association of p27 with CDK2. We also found in this study that 1,25-$(OH)_2$ D-mediated growth inhibition of the parental androgen dependent LNCaP cells is accompanied by upregulation of p27 and increased association of p27 with CDK2. Thus, a critical determinant of growth regulation by 1,25-$(OH)_2$ D is not the presence of AR, but appears to be the capacity of 1,25-$(OH)_2$ D to regulate CKIs, particularly p27, and thereby inhibit G1 to S progression.

2. Materials and methods

2.1. Materials

Cell culture media (RPMI-1640 and DMEM-H) were obtained from Gibco-BRL (Gaithersburg, MD), and fetal bovine sera (FBS) from Hyclone (Logan, UT). 1,25-$(OH)_2$ vitamin D_3 (1,25-$(OH)_2$ D) was purchased from BIOMOL Research Laboratories (Plymouth Meeting, PA). Dihydrotestosterone (DHT, 5α-androstan-17β-ol-3-one) was purchased from Steraloids, Inc. (Wilton, NH). R1881 and [^{3}H]R1881 were obtained from Dupont-New England Nuclear (Boston, MA). Mouse anti-actin antibody (1378 996) was obtained from Boehringer Manheim (Indianapolis, IN). Anti-human p21, p27, CDK2, protein A-agarose beads, and anti-rabbit IgG and anti-mouse IgG antibodies with HRP conjugate were purchased from Santa Cruz Biotech (Santa Cruz, CA).

2.2. Cell culture and stable transfection

LNCaP-104S (androgen dependent) and -104R1 (androgen independent) cells were the generous gifts of Drs Shutsung Liao and John Kokontis from the University of Chicago and were passaged and maintained as previously described (Kokontis et al., 1994, 1998). For LNCaP-104S cells, experiments were conducted in RPMI-1640 media supplemented with 10% FBS, 100 IU/ml penicillin, 100 μg/ml streptomycin, and 2 mM L-glutamine. For LNCaP-104R1 cells, experiments were conducted in DMEM media supplemented with 10% CSS, 50 IU/ml penicillin, and 50 μg/ml streptomycin. ALVA31 cells (Loop et al., 1993) were generously provided by Drs Stephen Loop and Richard Ostenson (Department of Veterans Affairs Medical Center, Tacoma, WA). ALVA31 cells stably expressing a human AR cDNA (ALVA-AR) were generated essentially as previously described (Dai et al., 1996). Cells stably expressing the pcDNA3 vector alone (ALVA-NEO) were also generated to serve as controls. Briefly, cells were transfected with either the expression vector alone or vector containing the human AR cDNA using the calcium phosphate method followed by glycerol shock. Following transfection, cells were incubated overnight in RPMI-1640 media supplemented with 10% FBS. Cells were then plated in 96-well plates at limiting dilution and neomycin-resistant clones were selected in 350 μg/ml G418 (Geneticin, Life Technologies). Approximately 2 weeks later, G418-resistant cells were replated and screened for AR expression by whole-cell ligand-binding assay using tritiated R1881. These cells were maintained in G418-containing RPMI media supplemented as mentioned above. All cultures were maintained at 37 °C in a humidified atmosphere of 5% CO_2.

2.3. Assay of cell proliferation

Cells were plated at an initial density of 20 000 (ALVA-NEO, ALVA-AR) or 55 000 (LNCaP-104R1) cells per well in 6-well dishes. These cells were plated at different densities to prevent confluency during the treatment period since ALVA31 cells and its sublines proliferate more rapidly than LNCaP-104R1 cells. The following day, cells were treated with either ethanol vehicle, 10 nM 1,25-$(OH)_2$ D, 10 nM R1881, or both hormones. After the appropriate treatment period, cells were washed with PBS, trypsinized, and counted using a hemacytometer. For treatment periods greater than 3 days, cell culture media were changed after 3 days of treatment and the appropriate hormone replenished. Very few ($< 1.5\%$) floating cells were observed at the time of media change as well as at the time of harvest. Experiments were performed in triplicate. The data represent mean cell number ± SEM.

2.4. Assay of cell viability

LNCaP-104R1 cells were plated at an initial density of 55 000 cells per well in 6-well dishes and treated for 2, 4, or 6 days with either ethanol vehicle or 10 nM 1,25-$(OH)_2$ D in media containing 10% charcoal stripped serum. Following the treatment period, cells (both floating and adherent) were collected, stained with trypan blue, and counted using a hemacytometer. Floating cells account for $< 1.5\%$ of total cells (no difference between control and vit D treated). Percentage dead cells is the number of floating and adherent cells stained with trypan blue divided by the total number of cells (stained and unstained) X 100%. The experiment was performed in triplicate and the data represent mean cell number ± SEM.

2.5. Coimmunoprecipitation

Twenty-four hours after plating, LNCaP-104R1 cells were treated with either ethanol vehicle or 10 nM 1,25-$(OH)_2$ D for appropriate times. Next, cells were lysed in sample buffer containing 50 mM Tris HCl (pH 8.0), 100 mM NaCl, 0.5% NP-40, 10 μg/ml aprotonin, 10 μg/ml leupeptin, 50 mM NaF, 0.1 mM sodium orthovanadate. Extracts (1 mg protein) were incubated with 1 μg rabbit polyclonal CDK2 antibody and agitated for 3 h at 4 °C. Samples were then equilibrated with lysis buffer and 25 μl packed volume of protein A-agarose beads for 2 h at 4 °C with agitation. Following three washes with lysis buffer, immunocomplexes were eluted by boiling in 20 μl Laemmli gel loading buffer. Samples were then subjected to Western blot analysis.

2.6. Western blot analysis

Twenty-four hours after plating, cells were treated with ethanol vehicle or 10 nM 1,25-$(OH)_2$ D for appropriate times and then washed, trypsinized, and lysed in sample buffer. Protein concentrations were determined by the Bio-Rad D_c Protein Assay (Bio-Rad, Hercules, CA) according to the manufacturer's instructions. 50 μg (to detect p27, p21) of cell extract proteins were subjected to standard SDS-PAGE and transferred to nitrocellulose membrane filters. Filters were processed for immunoblotting using standard procedures. Briefly, filters were incubated overnight at 4 °C in blocking solution (5% dry milk, 0.1% Tween in 1X wash buffer (20 mM Tris, 50 mM NaCl, 2.5 mM EDTA)) followed by incubation with the primary antibody for 1 h. Actin antibody (Boehinger Mannheim, Indianapolis, IN) was used at 0.5 μg/ml. p27, p21 and CDK2 antibodies were used at 1.0 μg/ml. After washing, blots were incubated with horseradish peroxidase-conjugated secondary antibody and proteins visualized using the ECL system

(Amersham, Buckinghamshire, England) following the supplier's instructions.

2.7. Reporter plasmids and chloramphenicol acetyltransferase assay

The reporter plasmid MOP VDRE-tkCAT (Zhuang et al., 1997) contains two copies of the VDRE of the mouse osteopontin (MOP) gene (Noda et al., 1990) 5′ to the thymidine kinase (tk) promoter and chloramphenicol acetyltransferase (CAT) gene of the vector PBLCAT2. The MMTV-CAT reporter plasmid contains the mouse mammary tumor virus long terminal repeat (MMTV-LTR) linked to CAT. Cells were transfected with 5.0 μg CAT reporter plasmid (MMTV-CAT or MOP VDRE-tkCAT) and 0.5 μg CMV-β-gal vectors and treated with either ethanol vehicle or R1881 at concentrations ranging from 0.01–100 nM for 48 h. Following the treatment period, cells were washed, collected, and lysed by four freeze-thaw cycles. β-galactosidase activities were measured to normalize for transfection efficiency. Cell extracts containing equivalent amounts of β-galactosidase activities were assayed for CAT activity as previously described (Dai et al., 1996).

2.8. Flow cytometric analysis

LNCaP-104R1 cells were plated at ≈20% confluency in 60 mm dishes in DMEM supplemented with 10% CSS and incubated overnight. The next day, cells were treated with 10 nM 1,25-$(OH)_2$ D or equal volume of ethanol vehicle. Cells were cultured for either 2, 4, or 6 days (with medium change and re-treatment on day 4), trypsinized, resuspended in medium, pelleted, and fixed in 70% ethanol overnight at 4 °C with agitation. Cells were then pelleted and stained with a propidium iodide cocktail (1 mg/ml RNAse A, 50 μg/ml propidium iodide in PBS). Cell cycle profiles and distributions were then determined by flow cytometric analysis of 5000 cells (2 days treatment) or 10 000 cells (4 and 6 days treatment) using the FACSCAN apparatus (Becton Dickinson, San Jose, CA).

2.9. Radioligand binding assays

A single-point whole-cell monolayer binding assay was performed as previously described (Dai et al., 1996) to assess AR levels in ALVA31 cells stably transfected with the AR cDNA. Briefly, cells were grown to near confluence and incubated for 2 h with media containing 1 nM [^{3}H]R1881 (specific activity 86.5 Ci/mmol) in the absence or presence of 100 nM unlabeled R1881 to determine total and nonspecific binding. Specific R1881 binding was calculated by subtraction of nonspecific from total binding. Radioactivity was determined by scintillation counting and protein concentration determined by the Bio-Rad D_c Protein Assay (Bio-Rad, Hercules, CA) according to the manufacturer's instructions.

2.10. Statistical analysis

Cell growth curve data were analyzed with either a repeated measures one way ANOVA test followed by either a Bonferroni's or Dunnett's multiple comparison post-test (ALVA cells) or a two tailed unpaired *t*-test (LNCaP-104R1 cells) using GraphPad Prism version 3.00 for Windows (GraphPad Software, San Diego, CA). Flow cytometric analysis of cell cycle distribution data were analyzed with an unpaired, two-tailed *t* test also using GraphPad Prism version 3.00 for Windows.

3. Results

3.1. Introduction of AR into ALVA31 cells does not confer 1,25-$(OH)_2$ vitamin D3-mediated growth inhibition

Since few models of AR-positive androgen-independent prostate cancer exist, it has been difficult to evaluate the role of AR in 1,25-$(OH)_2$ D-mediated growth inhibition in this later stage of the disease. To investigate the possible interaction of AR and VDR signaling pathways in the antiproliferative action of 1,25-$(OH)_2$ D, we introduced AR into ALVA 31 cells. ALVA 31 cells were chosen as these cells express higher levels of functional VDRs than LNCaP cells yet are only minimally growth inhibited by 1,25-$(OH)_2$ D (Zhuang et al., 1997; Zhuang and Burnstein 1998). ALVA31 cells were stably transfected with an expression vector containing the human AR cDNA to generate ALVA-AR. Clonal isolates were first screened for AR expression by Western blot and hormone binding assays. ALVA-NEO cells, which were transfected with the pcDNA3 vector alone, served as a negative control. We selected a clone hereafter termed ALVA-AR, in which AR protein was readily detected by both methods. Single point binding studies with tritiated R1881, a synthetic non-metabolizable androgen analog, showed that ALVA-AR express ≈60–80 fmol/mg protein of AR, which is about 1/4 the AR levels in LNCaP cells tested in the same experiment (≈300 fmol/mg protein AR). To determine that these cells expressed transcriptionally active AR, a reporter gene assay was performed using the androgen responsive MMTV-LTR linked to the CAT gene (Fig. 1(A)). ALVA-AR (Fig. 1(A)) but not ALVA-NEO (data not shown) exhibited dose-dependent AR transcriptional activity similar to LNCaP and other AR expressing cells (Kokontis et al., 1994, 1998; Zhao et al., 1997, 2000a). We also confirmed the presence of

functional endogenous VDR in ALVA-AR by reporter gene assay using the MOP gene VDRE linked to CAT (Fig. 1(B)). These experiments show that introduction of AR into ALVA cells did not affect VDR transcriptional activity. Since overexpression of AR in another prostate cancer cell line, PC3, can result in androgen repressible growth (Shen et al., 2000), we also examined androgen effects on ALVA-AR proliferation. R1881 (0.01–100 nM) had no significant effect on ALVA-AR or ALVA-NEO proliferation (data not shown).

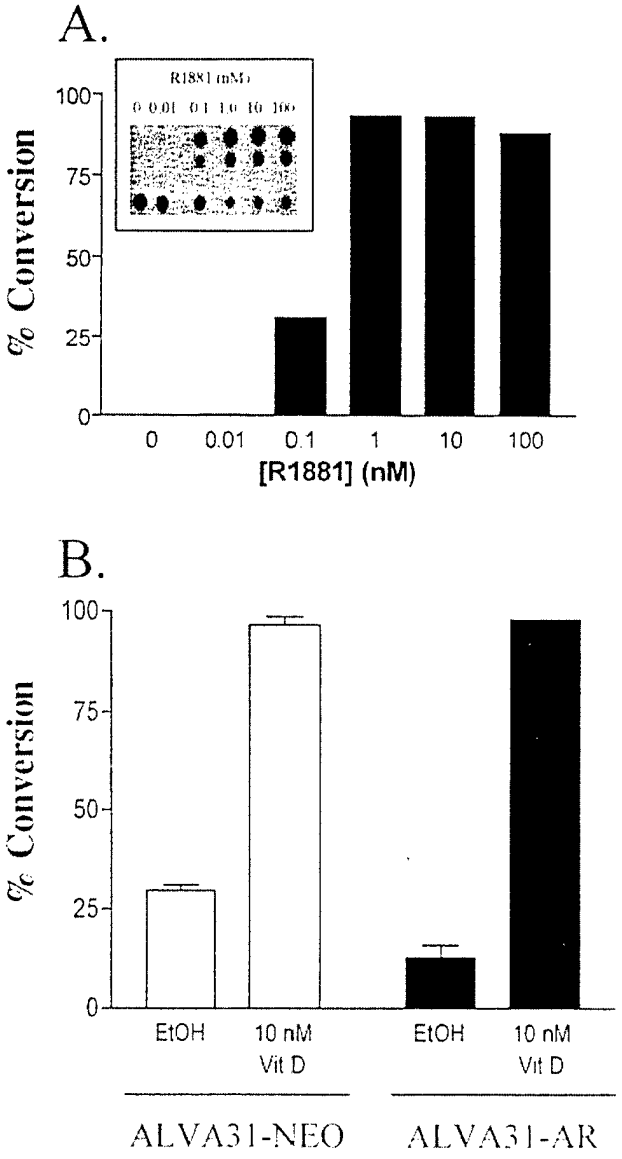

Fig. 1. ALVA-AR cells express functional AR and VDR. ALVA 31 cells stably expressing the AR cDNA (ALVA-AR) or neo vector alone (ALVA-NEO) were co-transfected with either the MMTV-CAT (panel A) or the 2X-VDRE-CAT (panel B) reporter plasmids and CMV-β-gal (containing the β-galactosidase gene) and treated with various doses of R1881 (for MMTV-CAT) or with 10 nM 1,25-$(OH)_2$ D (2X-VDRE-CAT) for 48 h. Cell lysates containing equivalent amounts of β-galactosidase activity were used for analysis of CAT activity (shown in inset of panel A). Percentage conversion is the ratio of acetylated ^{14}C-chloramphenicol to the total acetylated and non-acetylated ^{14}C-chloramphenicol measured using a phosphorimager. Panel A is representative of two experiments. Panel B is one experiment conducted in duplicate.

The studies above established that ALVA-AR express functional AR and VDR and are not growth regulated by androgen (i.e. actively cycle in media depleted of androgen). Thus, these cells are appropriate for assessing the effect of androgen/AR on 1,25-$(OH)_2$ D-mediated growth inhibition. After 3 days of 10 nM 1,25-$(OH)_2$ D treatment in the absence of androgen, both ALVA-AR and ALVA-NEO cells were minimally growth inhibited (Fig. 2 (A) and (B)) as was observed previously for the parent ALVA31 cell line (Zhuang et al., 1997; Zhuang and Burnstein 1998). The addition of 10 nM R1881 did not enhance this minimal 1,25-$(OH)_2$ D-mediated inhibition of ALVA-AR cells (Fig. 2(B)). The time course was extended to 6 days and yielded similar results (data not shown). TGF-β was used as a positive control for growth inhibition of these cells (Fig. 2(A) and (B); Knight et al., manuscript in preparation). Thus, in this model of androgen independent prostate cancer, the lack of 1,25-$(OH)_2$ D antiproliferative activity is not due to absence of AR.

3.2. Androgen independent LNCaP-104R1 cells do not require androgen for 1,25(OH)$_2$ vitamin D$_3$-mediated growth inhibition

LNCaP-104R1, an AR-expressing, androgen-independent prostate cancer cell line, was derived by repeated passaging of LNCaP cells in the absence of androgen (Kokontis et al., 1994, 1998). These cells, unlike the parental LNCaP line, proliferate rapidly in vitro in the absence of androgen and form tumors in castrated nude mice (Umekita et al., 1996). However similar to LNCaP cells, LNCaP-104R1 cells maintain AR expression and secrete PSA in response to androgen (Kokontis et al., 1994).

We tested the effects of 1,25-$(OH)_2$ D on the growth of LNCaP-104R1 cells in the absence of androgen. LNCaP-104R1 cells cultured in media supplemented with charcoal-stripped serum (androgen depleted) were $\approx$77% growth inhibited after 6 days treatment with 1,25-$(OH)_2$ D (10 nM) (Fig. 3). Growth inhibition was observed after 2 and 4 days treatments as well (Fig. 3). The extent of growth inhibition by 1,25-$(OH)_2$ D is comparable to that observed in LNCaP cells only when LNCaP cells are cultured under conditions in which the cells are actively cycling (media containing 10% serum) (Zhuang et al., 1997; Zhuang and Burnstein 1998). Since low levels of androgen could remain in the charcoal stripped serum, we tested the effect of the antiandrogen Casodex on 1,25-$(OH)_2$ D-mediated growth inhibition. Casodex had no effect confirming further the assertion that the antiproliferative effects of 1,25-$(OH)_2$ D in LNCaP-R1 cells do not require androgen

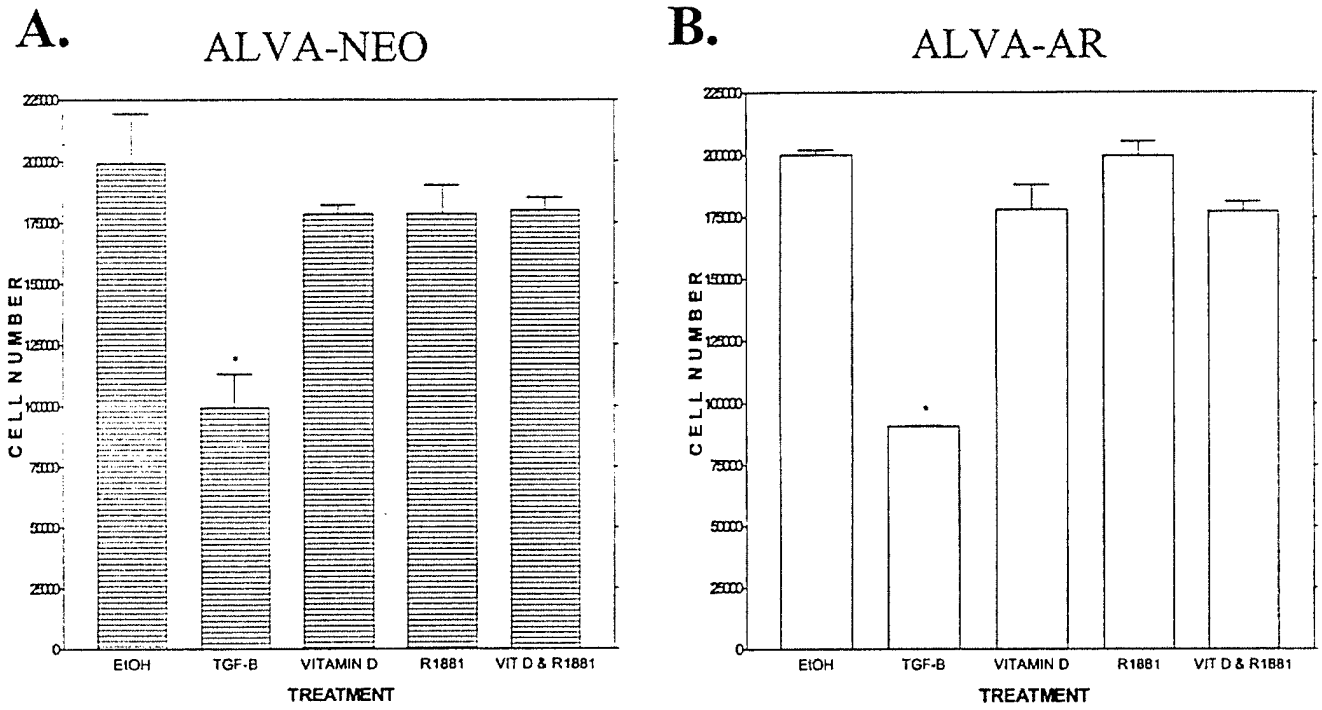

Fig. 2. Expression of functional AR in ALVA31 cells does not confer enhanced growth inhibition by vitamin D in the presence or absence of androgen. ALVA-NEO (A) and ALVA-AR (B) cells were plated at an initial density of 20 000 cells per well in six-well dishes and treated for 3 days with ethanol vehicle, 5 ng/ml TGF-β (positive control for ALVA growth inhibition), 10 nM R1881, 10 nM 1,25-$(OH)_2$ D, or both R1881 and 1,25-$(OH)_2$ D. Following the treatment period, cells were washed with PBS, trypsinized, and counted using a hemacytometer. Experiments were performed in triplicate. The data were obtained from two experiments and correspond to the mean cell number ± SEM. $^*P < 0.01$ vs. control.

action (Fig. 3). Thus, androgen-independent prostate cancer cells, at least as represented by the LNCaP-104R1 model, do not require androgen for growth inhibition by 1,25-$(OH)_2$ D.

3.3. 1,25$(OH)_2$ vitamin D_3-mediated growth inhibition of LNCaP-104R1 cells occurs through inhibition of G1 to S progression

Our previous studies showed that 1,25-$(OH)_2$ D-mediated growth inhibition of LNCaP cells correlates with accumulation of cells in the G1 phase of the cell cycle but not with 1,25-$(OH)_2$ D-mediated apoptosis (Zhuang and Burnstein 1998). We first examined the effect of 1,25-$(OH)_2$ D on cell viability. 1,25-$(OH)_2$ D treatment did not result in increased cell death as assessed by trypan blue staining of total cells (floating and adherent) (data not shown). Slightly increased cell death was observed in 6 days vehicle treated cells, most likely due to these cells reaching confluency at this time point. Regardless of treatment, the number of floating cells was always less than 1.5% of total cell number and 1,25-$(OH)_2$ D did not influence the proportion of floating cells (data not shown).

To determine whether 1,25-$(OH)_2$ D-mediated growth inhibition of LNCaP-104R1 is due to effects on cell cycle distribution, we performed flow cytometric analysis. 10 nM 1,25-$(OH)_2$ D treatment of LNCaP-104R1 cells cultured in androgen-depleted media resulted in a significantly increased percentage of cells in the G1 phase of the cell cycle as compared to the ethanol vehicle treated controls (from 51 to 65% after 2 days, from 49 to 76% after 6 days) (Fig. 4(A) and (B)).

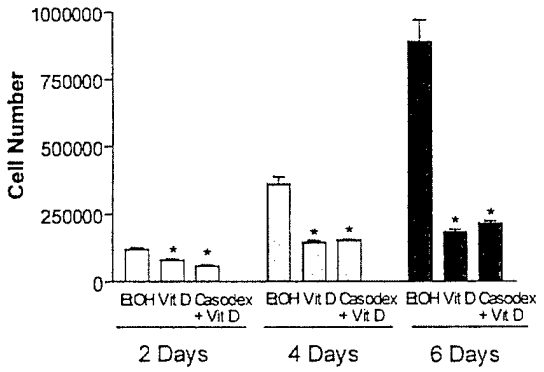

Fig. 3. Vitamin D inhibition of LNCaP-104R1 cell growth is independent of androgen action. LNCaP-R1 cells were plated at an initial density of 55 000 cells per well in six-well dishes and treated for 2, 4, or 6 days with either ethanol vehicle, 10 nM 1,25-$(OH)_2$ D or 1,25-$(OH)_2$ D plus 1 μM of the antiandrogen casodex in media containing 10% charcoal stripped serum. Following the treatment period, cells were washed, trypsinized, and counted using a hemacytometer. Experiments were performed in triplicate. Data from three experiments are shown and correspond to mean cell number ± SEM. $^*P < 0.005$ vs. control.

The percentage of 1,25-$(OH)_2$ D treated cells in the S and G2/M phases showed concomitant decreases.

3.4. 1,25$(OH)_2$ vitamin D_3 upregulates the cyclin dependent kinase inhibitor p27 in LNCaP and LNCaP-104R1 cells

The cyclin-dependent kinase inhibitors (CKIs) p21 and p27 are pivotal in the regulation of G1 to S phase transition, and play an important role in growth inhibition mediated by 1,25-$(OH)_2$ D and vitamin D analogs (Campbell et al., 1997; Zhuang and Burnstein 1998). In particular, recent data show that low levels of p27 predict more aggressive prostate cancer and poorer prognosis (Cheng et al., 2000; Cote et al., 1998; Fernandez et al., 1999; Guo et al., 1997; Yang et al., 1998). Because of the emerging role of p27 in controlling prostate cancer growth, we investigated 1,25-$(OH)_2$ D regulation of this CKI in both LNCaP and LNCaP-104R1 cells. 1,25 D treatment for 2 or 4 days results in up-regulation of p27 levels in both LNCaP (serum containing media) and in LNCaP-104R1 (charcoal-stripped serum containing media) cells but not the ALVA-NEO/AR cells (Fig. 5).

We previously showed that p21 is transiently upregulated in LNCaP cells treated with 1,25-$(OH)_2$ D (Zhuang and Burnstein, 1998). In contrast, p21 was not consistently induced by 1,25-$(OH)_2$ D in LNCaP-104R1 cells (data not shown). Also, similar to the findings in LNCaP, 1,25-$(OH)_2$ D did not regulate the expression of other G1 regulatory proteins, including CDK2 and cyclins D and E (data not shown). Together, these results further suggest that CKI induction by 1,25-$(OH)_2$ D (p21 and p27 in LNCaP, p27 in LNCaP-104R1) is important for growth inhibition.

3.5. 1,25$(OH)_2$ vitamin D_3 treatment results in increased association of p27 with cyclin dependent kinase 2

We previously showed that 1,25-$(OH)_2$ D inhibited CDK2 activity by $\sim 80\%$ in LNCaP cells (Zhuang and Burnstein 1998). Since both p21 and p27 can inhibit CDK2 activity by associating with CDK2/cyclin complexes, we determined the effect of 1,25-$(OH)_2$ D treatment on the amount of these CKIs bound to CDK2 in LNCaP and LNCaP-104R1 cell lysates. Whole cell extracts were immunoprecipitated with CDK2 antibody and the composition of the complexes was probed by immunoblotting using p27 and CDK2 antibodies. Consistent with induction of p27 levels by 1,25-$(OH)_2$ D in LNCaP and LNCaP-R1 cells (Fig. 5), we observed increased association of this CKI with CDK2 in both cell lines after 1,25-$(OH)_2$ D treatment (Fig. 6). The kinetics of this increased association correlate with the kinetics of CKI upregulation in these cells, namely p27

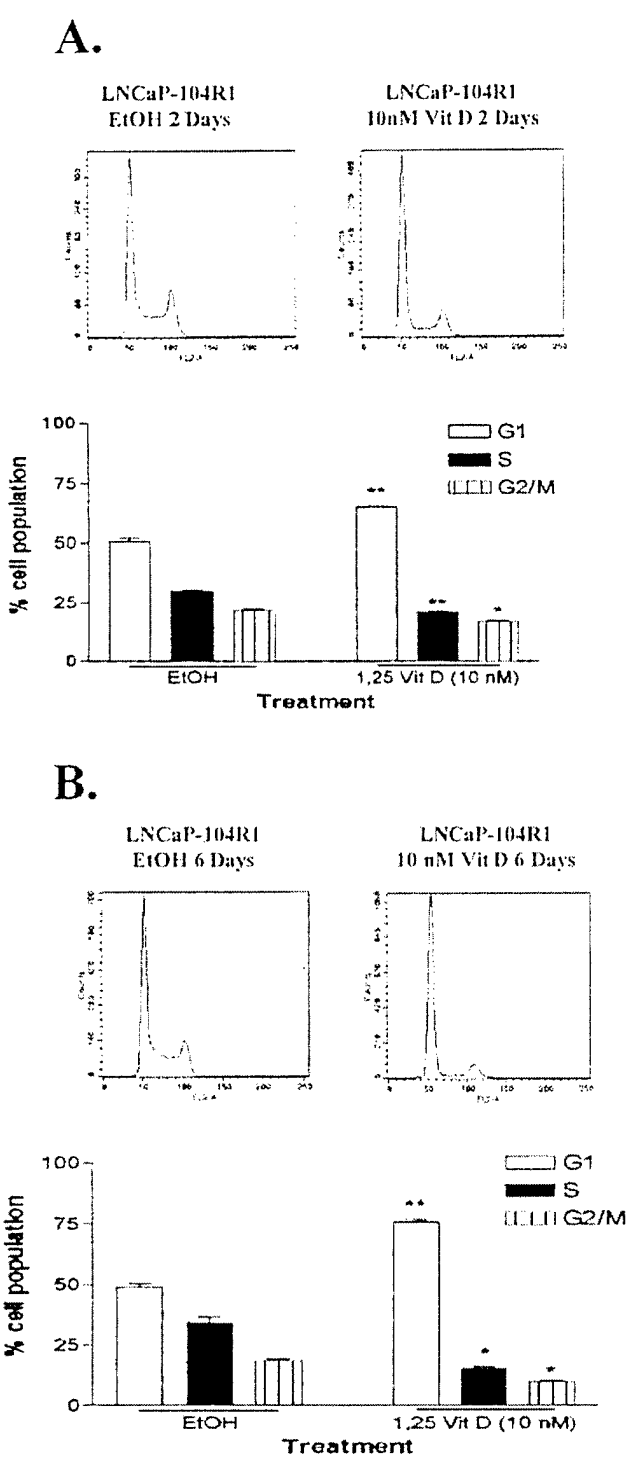

Fig. 4. Vitamin D treatment of LNCaP-104R1 cells results in accumulation of cells in the G1 phase of the cell cycle. Cells were plated in 60 mm dishes and treated with either ethanol vehicle or 10 nM 1,25-$(OH)_2$ D for 2 days (A) or 6 days (B). Cells were fixed in 70% ethanol and stained with propidium iodide. Cell cycle profiles and distributions were then determined by flow cytometric analysis of 5000 cells (2 days treatment) or 10 000 cells (6 days treatment). The experiment shown is representative of two experiments. The data shown here are mean percentage cell population ± SEM in the G1, S, or G2/M phases of the cell cycle. Note graph scale differences between untreated and treated groups. $^{*}P < 0.01$ vs. control, $^{**}P < 0.001$ vs. control.

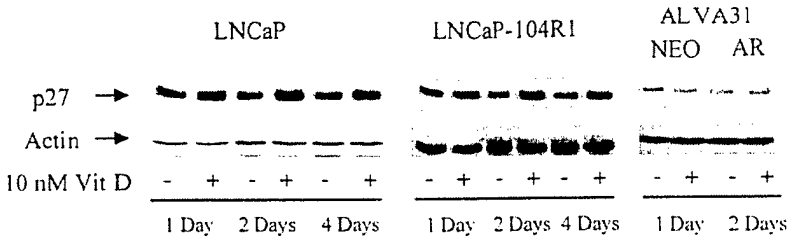

Fig. 5. Vitamin D upregulates the cyclin-dependent kinase inhibitor p27 in LNCaP and LNCaP-104R1 but not ALVA-AR cells. LNCaP, LNCaP-104R1, and ALVA-AR cells were treated with 10 nM 1,25-$(OH)_2$ D for the indicated times. 50 μg of cell extract proteins were immunoblotted with p27 antibody, and visualized by ECL. Actin was also analyzed as a loading control. The data shown here is representative of three experiments.

is induced by 1,25-$(OH)_2$ D after 2 days of treatment (Fig. 5). CDK2 levels were not altered by 1,25-$(OH)_2$ D treatment in either cell line (data not shown). Thus, this increased association of p27 with CDK2 provides a basis for G1 accumulation in response to 1,25-$(OH)_2$ D. These experiments establish further the importance of CKI regulation in the antiproliferative action of 1,25-$(OH)_2$.

4. Discussion

This study examined the potential role of androgen/AR in the antiproliferative effects of 1,25-$(OH)_2$ D in prostate cancer cells. Because most androgen independent prostate cancer cell lines lack AR and because of the difficulty assessing a possible role of AR in the antiproliferative effects of 1,25-$(OH)_2$ D in cells that depend on androgen for growth, we utilized two new, AR and VDR-expressing androgen independent prostate cancer models, ALVA-AR and LNCaP-104R1. These models allowed us to focus on some of the relevant characteristics of androgen-independent prostate cancer in relation to 1,25-$(OH)_2$ D action. First, most prostate cancer specimens maintain AR expression regardless of androgen sensitivity (reviewed in Amanatullah et al., 2000). Both ALVA-AR and LNCaP-104R1 cells express functional AR as well as VDR (Fig. 1, Kokontis et al., 1994, 1998; Zhuang et al., 1997). Second, as models of androgen independent prostate cancer, these cell lines are considered to have a more aggressive phenotype. Neither cell line requires androgen for growth (Kokontis et al., 1994, 1998; Loop et al., 1993; Umekita et al., 1996 and data not shown). ALVA31 cells, the parent cells of ALVA-AR, form tumors in castrated athymic mice more readily than the less aggressive LNCaP cells (Loop et al., 1993). In contrast to LNCaP, LNCaP-104R1 cells proliferate rapidly in media devoid of androgen and also form tumors in castrated athymic mice (Kokontis et al., 1994, 1998; Umekita et al., 1996). In addition, both cell models express lower levels of the CKIs p21 (data not shown) and p27 (Fig. 5) compared to the less aggressive LNCaP cells. These features allowed us to test the issue of androgen's role in 1,25-$(OH)_2$ D-mediated growth and cell cycle inhibition.

We found that ALVA-AR, like the parent cell line ALVA31, was relatively resistant to growth inhibition by 1,25-$(OH)_2$ D even in the presence of androgen. The lack of growth inhibition by 1,25-$(OH)_2$ D was not due to loss of VDR as ALVA-AR retained transcriptionally active VDR (Fig. 1(B)). Thus in this model, AR is not a defining factor in the antiproliferative effects of 1,25-$(OH)_2$ D. In a second model of androgen independence, LNCaP-104R1, 1,25-$(OH)_2$ D inhibited proliferation (Fig. 3). These effects did not require androgen and were not blocked by the antiandrogen casodex (Fig. 3). Since casodex did not influence this 1,25-$(OH)_2$ D-mediated growth inhibition, it is unlikely that AR had a role due to receptor activation by very low levels of androgen or as a result of ligand-independent mechanisms (Hobisch et al., 1998; Nazareth and Weigel 1996; Sadar 1999; Sadar and Gleave 2000).

Similar to the androgen dependent parent cell line, LNCaP, growth inhibition of LNCaP-R1 cells by 1,25-$(OH)_2$ D involved accumulation of cells in the G1 phase of the cell cycle. The mechanism for this inhibition of both cell lines involves 1,25-$(OH)_2$ D induction of p27 levels and increased p27 association with CDK2 (Figs. 5 and 6). p27 was not induced by 1,25-$(OH)_2$ D in ALVA31 cells (Fig. 5). Thus, p27 induction appears to

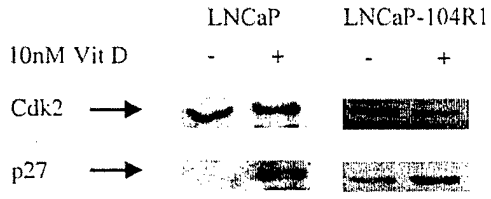

Fig. 6. Vitamin D increases the association of p27 with CDK2 in LNCaP and LNCaP-104R1 cells. Following 1,25-$(OH)_2$ D treatment, whole cell extracts were incubated with CDK2 antibody. Immunocomplexes were then obtained using protein A-agarose beads. Samples were immunoblotted with p27 and CDK2 antibody, and visualized by ECL. Blotting for CDK2 showed that equivalent amounts were present in the immunoprecipitates. The data shown here is representative of two experiments.

be a critical determinant of 1,25-$(OH)_2$ D's antiproliferative effects whereas AR signaling is not sufficient.

Consistent with the involvement of cell cycle regulatory mechanisms, 1,25-$(OH)_2$ D-mediated growth inhibition requires that cells are actively cycling. The doubling time of the androgen dependent LNCaP cells in CSS (androgen deprived) increases from 1.5 to 6 days (Zhao et al., 1997) and this correlates with the loss of sensitivity to 1,25-$(OH)_2$ D growth inhibition after 6 days of treatment. The addition of the antiandrogen Casodex also increases the doubling time of LNCaP cells (Zhao et al., 1997). Since the experimental conditions in which 1,25-$(OH)_2$ D is not effective (absence of androgen) have also been shown to substantially decrease the basal rate of cell cycling, the role of androgen in 1,25-$(OH)_2$ D mediated growth inhibition cannot be assessed in this model.

ALVA31 cells, despite containing the highest VDR content of the established prostate cancer cell lines (Miller et al., 1995; Zhuang et al., 1997), are relatively insensitive to 1,25-$(OH)_2$ D-mediated antiproliferative effects compared to LNCaP and LNCaP-R1 cells (Zhuang et al., 1997; Zhuang and Burnstein 1998 and Figs. 2 and 3). ALVA31 cells have very low levels of p21 and p27 compared to LNCaP cells, and 1,25-$(OH)_2$ D fails to upregulate these CKIs (Zhuang and Burnstein 1998, Fig. 5). However, TGF-β, which we used as a positive control for ALVA 31 (ALVA-NEO and ALVA-AR) cell growth inhibition, upregulated the CKIs p21 and p27 and resulted in G1 accumulation of ALVA 31 (Knight et al., manuscript in preparation). The deficiency in ALVA 31 cells may be within the complex pathway(s) of VDR regulation of target gene transcription or at a point downstream such that CKIs are not induced by 1,25-$(OH)_2$ D_3. However, these CKIs can be induced by other factors. Another possibility for the failure of 1,25-$(OH)_2$ D to inhibit ALVA-AR cells is insufficient levels of AR. ALVA-AR express approximately one-fourth the levels in LNCaP cells. However, we observed robust transcriptional activation by AR in these cells (Fig. 1(A)) and no difference in 1,25-$(OH)_2$ D effects on ALVA-AR compared to ALVA-NEO growth (Fig. 2) suggesting that lower levels of AR are unlikely to be the basis for the resistance of these cells to 1,25-$(OH)_2$ D-mediated growth inhibition.

Although 1,25-$(OH)_2$ D promotes G1 accumulation of both LNCaP and LNCaP-R1, p21 levels are only induced in LNCaP (Zhuang and Burnstein 1998) and not in LNCaP-R1 cells (data not shown). The basis for the lack of p21 induction by 1,25-$(OH)_2$ D in LNCaP-R1 cells is not known; however, p21 appears to play a lesser role in the antiproliferative actions of 1,25-$(OH)_2$ D. Our previous report showed that p21 induction in LNCaP cells is transient (Zhuang and Burnstein 1998). Further, p21 can also stimulate CDK4 activity by promoting assembly of CDK4/cyclin D complexes (LaBaer et al., 1997; Sherr and Roberts 1999). It is postulated that androgen's growth promoting effects in LNCaP and its androgen-independent derivative LNCaP-AI may be mediated in part by induction of p21 (Lu et al., 1999). Since 1,25-$(OH)_2$ D induces p27 levels in both LNCaP and LNCaP-R1 cells, which is reflected in increased p27 association with CDK2, it is likely that p27 has a more dominant role in 1,25-$(OH)_2$ D inhibition of cell cycle progression.

In this report, we have shown that 1,25-$(OH)_2$ D can, in the absence of androgen, inhibit the growth of LNCaP-104R1 cells. These cells resemble clinical androgen-independent cancer in that they express AR and PSA and exhibit a more aggressive phenotype. In addition, we have found that the mechanism of inhibition by 1,25-$(OH)_2$ D for both LNCaP-R1 and the parent LNCaP is G1 cell cycle accumulation involving upregulation of the CKI p27, and increased association of p27 with CDK2. This mechanism of action not only requires the cells to be cycling but also depends on intact signaling between VDR and the cell cycle regulators and therefore may limit chemotherapeutic potential of 1,25-$(OH)_2$ D. However, in the absence of this control, 1,25-$(OH)_2$ D may be useful in conjunction with other agents (Qadan et al., 2000).

Acknowledgements

We thank Drs Shutsung Liao and John Kokontis (University of Chicago) for providing the LNCaP-104R1 cells and Dr Michael McPhaul (University of Texas Southwestern) for providing the AR cDNA. This work was supported by grants from the NIEHS (Fellowship # F30 ES05910-02), Pfeiffer Research Foundation, American Institute for Cancer Research, Pharmaceutical Research and Manufacturers of America Foundation and US Department of Defense (DAMD-17-98-1-8525). This work is dedicated to the memory of Dr Gary Miller whose pioneering work on vitamin D and prostate cancer will continue to inspire researchers.

References

Amanatullah, D.F., Reutens, A.T., Zafonte, B.T., Fu, M., Mani, S., Pestell, R.G., 2000. Cell-cycle dysregulation and the molecular mechanisms of prostate cancer. Frontiers Biosci. 5, D372–D390.

Bikle, D.D., 1992. Clinical counterpoint: vitamin D: new actions, new analogs, new therapeutic potential. Endocr. Rev. 13, 765–784.

Blutt, S.E., Allegretto, E.A., Pike, J.W., Weigel, N.L., 1997a. 1,25-dihydroxyvitamin D3 and 9-*cis*-retinoic acid act synergistically to inhibit the growth of LNCaP prostate cells and cause accumulation of cells in G1. Endocrinology 138, 1491–1497.

Blutt, S.E., Allegretto, E.A., Pike, J.W., Weigel, N.L., 1997b. 1,25-dihydroxyvitamin D3 and 9-*cis*-retinoic acid act synergistically to inhibit the growth of LNCaP prostate cells and cause accumulation of cells in G1. Endocrinology 138, 1491–1497.

Campbell, M.J., Elstner, E., Holden, S., Uskokovic, M., Koeffler, H.P., 1997. Inhibition of proliferation of prostate cancer cells by a 19-nor-hexafluoride vitamin D3 analogue involves the induction of p21waf, p27kipl, and E-cadherin. J. Mol. Endocrinol. 19, 15–27.

Cheng, L., Lloyd, R.V., Weaver, A.L., Pisansky, T.M., Cheville, J.C., Ramnani, D.M., Leibovich, B.C., Blute, M.L., Zincke, H., Bostwick, D.G., 2000. The cell cycle inhibitors p21WAF1 and p27KIP1 are associated with survival in patients treated by salvage prostatectomy after radiation therapy. Clin. Cancer. Res. 6, 1896–1899.

Cote, R.J., Shi, Y., Groshen, S., Feng, A.C., Cordon-Cardo, C., Skinner, D., Lieskovosky, G., 1998. Association of p27Kip1 levels with recurrence and survival in patients with stage C prostate carcinoma. J. National Cancer Inst. 90, 916–920.

Dai, J.L., Maiorino, C.A., Gkonos, P.J., Burnstein, K.L., 1996. Androgenic up-regulation of androgen receptor cDNA expression in androgen-independent prostate cancer cells. Steroids 61, 531–539.

Esquenet, M., Swinnen, J.V., Heyns, W., Verhoeven, G., 1996. Control of LNCaP proliferation and differentiation: actions and interactions of androgens, 1α,25-dihydroxycholecalciferol, all-trans retinoic acid, 9-*cis* retinoic acid, and phenylacetate. The Prostate 28, 182–194.

Feldman, D., Glorieux, F.H., Pike, J.W. (Eds.), 1997. Vitamin D. Academic Press, San Diego.

Fernandez, P.L., Arce, Y., Farre, X., Martinez, A., Nadal, A., Rey, M.J., Peiro, N., Campo, E., Cardesa, A., 1999. Expression of p27/Kip1 is down-regulated in human prostate carcinoma progression. J. Pathol. 187, 563–566.

Glass, C.K., 1994. Differential recognition of target genes by nuclear receptor monomers, dimmers, and heterodimers. Endocr. Rev. 15, 391–407.

Guo, Y., Sklar, G.N., Borkowski, A., Kyprianou, N., 1997. Loss of the cyclin-dependent kinase inhibitor p27(Kip1) protein in human prostate cancer correlates with tumor grade. Clin. Cancer Res. 3, 2269–2274.

Hobisch, A., Eder, I.E., Putz, T., Horninger, W., Bartsch, G., Klocker, H., Culig, Z., 1998. Interleukin-6 regulates prostate-specific protein expression in prostate carcinoma cells by activation of the androgen receptor. Cancer Res. 58, 4640–4645.

Kokontis, J., Takakura, K., Hay, N., Liao, S., 1994. Increased androgen receptor activity and altered c-myc expression in prostate cancer cells after long-term androgen deprivation. Cancer Res. 54, 1566–1573.

Kokontis, J.M., Hay, N., Liao, S., 1998. Progression of LNCaP prostate tumor cells during androgen deprivation: hormone-independent growth, repression of proliferation by androgen, and role for $p27^{kip1}$ in androgen-induced cell cycle arrest. Mol. Endocr. 12, 941–953.

LaBaer, J., Garrett, M.D., Stevenson, L.F., Slingerland, J.M., Sandhu, C., Chou, H.S., Fattaey, A., Harlow, E., 1997. New functional activities for the p21 family of CDK inhibitors. Genes Dev. 11, 847–862.

Loop, S.M., Rozanski, T.A., Ostenson, R.C., 1993. Human primary prostate tumor cell line, ALVA31: a new model for studying the hormonal regulation of prostate tumor cell growth. Prostate 22, 93–108.

Lu, S., Tsai, S.Y., Tsai, M.J., 1999. Molecular mechanisms of androgen-independent growth of human prostate cancer LNCaP-AI cells. Endocrinology 140, 5054–5059.

Miller, G.J., Stapleton, G.E., Ferrara, J.A., Lucia, M.S., Pfister, S., Hedlund, T.E., Upadhya, P., 1992. The human prostatic carcinoma cell line LNCaP expresses biologically active, specific receptors for 1α,25-dihydroxyvitamin D3. Cancer Res. 52, 515–520.

Miller, G.J., Stapleton, G.E., Hedlund, T.E., Moffatt, K.A., 1995. Vitamin D receptor expression, 24-hydroxylase activity, and inhibition of growth by 1α,25-dihydroxyvitamin D3 in seven human prostatic carcinoma cell lines. Clin. Cancer Res. 1, 997–1003.

Nazareth, L.V., Weigel, N.L., 1996. Activation of the human androgen receptor through a protein kinase: a signaling pathway. J. Biol. Chem. 271, 19900–19907.

Noda, M., Vogel, R.L., Craig, A.M., Prahl, J., DeLuca, H.F., Denhardt, D.T., 1990. Identification of a DNA sequence responsible for binding of the 1,25-dihydroxyvitamin D3 receptor and 1,25-dihydroxyvitamin D3 enhancement of mouse secreted phosphoprotein 1 (SPP-1 or osteopontin) gene expression. Proceedings of the National Academy of Sciences of the United States of America 87, 9995–9999.

Pols, H.A., Birkenhager, J.C., Foekens, J.A., van Leeuwen, J.P., 1990. Vitamin D: a modulator of cell proliferation and differentiation. J. Steroid Biochem. Mol. Biol. 37, 873–876.

Qadan, L.R., Perez-Stable, C.M., Schwall, R.H., Burnstein, K.L., Ostenson, R.C., Howard, G.A., Roos, B.A., 2000. Endocrinology 141, 2567–2573.

Sadar, M.D., 1999. Androgen-independent induction of prostate-specific antigen gene expression via cross-talk between the androgen receptor and protein kinase: a signal transduction pathways. J. Biol. Chem. 274, 7777–7783.

Sadar, M.D., Gleave, M.E., 2000. Ligand-independent activation of the androgen receptor by the differentiation agent butyrate in human prostate cancer cells. Cancer Res. 60, 5825–5831.

Schwartz, G.G., Oeler, T.A., Uskokovic, M.R., Bahnson, R.R., 1994. Human prostate cancer cells: inhibition of proliferation by vitamin D analogs. Anticancer Res. 14, 1077–1081.

Shen, R., Sumitomo, M., Dai, J., Harris, A., Kaminetzky, D., Gao, M., Burnstein, K.L., Nanus, D.M., 2000. Androgen-induced growth inhibition of androgen receptor expressing androgen-independent prostate cancer cells is mediated by increased levels of neutral endopeptidase. Endocrinology 141, 1699–1704.

Sherr, C.J., Roberts, J.M., 1999. CDK inhibitors: positive and negative regulators of G1-phase progression. Genes Dev. 13, 1501–1512.

Skowronski, R.J., Peehl, D.M., Feldman, D., 1993. Vitamin D and prostate cancer: 1,25 dihydroxyvitamin D3 receptors and actions in human prostate cancer cell lines. Endocrinology 132, 1952–1960.

Tsihlias, J., Kapusta, L.R., DeBoer, G., Morava-Protzner, I., Zbieranowski, I., Bhattacharya, N., Catzavelos, G.C., Klotz, L.H., Slingerland, J.M., 1998. Loss of cyclin-dependent kinase inhibitor p27Kip1 is a novel prognostic factor in localized human prostate adenocarcinoma. Cancer Res. 58, 542–548.

Umekita, Y., Hiipakka, R.A., Kokontis, J.M., Liao, S., 1996. Human prostate tumor growth in athymic mice: inhibition by androgens and stimulation by finasteride. Proceedings of the National Academy of Sciences of the United States of America 93, 11802–11807.

Walters, M.R., 1992. Newly identified actions of the vitamin D endocrine system. Endocr. Rev. 13, 719–764.

Yang, R.M., Naitoh, J., Murphy, M., Wang, H.J., Phillipson, J., deKernion, J.B., Loda, M., Reiter, R.E., 1998. Low p27 expression predicts poor disease-free survival in patients with prostate cancer. J. Urol. 159, 941–945.

Zhao, X.-Y., Ly, L.H., Peehl, D.M., Feldman, D., 1997. 1α,25-Dihydroxyvitamin D3 actions in LNCaP human prostate cancer cells are androgen-dependent. Endocrinology 138, 3290–3298.

Zhao, X.-Y., Boyle, B., Krishnan, A.V., Navone, N.M., Peehl, D.M., Feldman, D., 1999. Two mutations identified in the androgen receptor of the new human prostate cancer cell line MDA PCA 2A. J. Urol. 162, 2192–2199.

Zhao, X.-Y., Peehl, D.M., Navone, N.M., Feldman, D., 2000a. 1α,25-Dihydroxyvitamin D_3 inhibits prostate cancer cell growth by androgen-dependent and androgen-independent mechanisms. Endocrinology 141, 2548–2556.

Zhao, X.Y., Malloy, P.J., Krishnan, A.V., Swami, S., Navone, N.M., Peehl, D.M., Feldman, D., 2000b. Glucocorticoids can promote androgen-independent growth of prostate cancer cells through a mutated androgen receptor. Nat. Med. 6, 703–706.

Zhuang, S.-H., Schwartz, G.G., Cameron, D., Burnstein, K.L., 1997. Vitamin D receptor content and transcriptional activity do not fully predict antiproliferative effects of vitamin D in human prostate cancer cell lines. Mol. Cell. Endocrinol. 126, 83–90.

Zhuang, S.-H., Burnstein, K.L., 1998. Antiproliferative effect of 1α,25-dihydroxyvitamin D3 in human prostate cancer line LNCaP involves reduction of cyclin-dependent kinase 2 activity and persistent G1 accumulation. Endocrinology 139, 1197–1207.

Cancer Epidemiol Biomarkers Prev,
under review, 2002

The Gγ/T-15 Transgenic Mouse Model of Androgen-Independent Prostate Cancer: Target Cells of Carcinogenesis and the Effect of the Vitamin D Analog EB 1089[1]

Carlos M. Perez-Stable[2], Gary G. Schwartz, Adan Farinas, Milton Finegold, Lise Binderup, Guy A. Howard, and Bernard A. Roos

Geriatric Research, Education, and Clinical Center and Research Service, VA Medical Center, Miami, Florida 33125 [C. M. P.-S., A. F., G. A. H., B. A. R.]; Departments of Medicine [C. M. P.-S., G. A. H., B. A. R.], Biochemistry and Molecular Biology [G. A. H.], and Neurology [B. A. R.] and Sylvester Comprehensive Cancer Center [C. M. P.-S., G. A. H., B. A. R.], University of Miami School of Medicine, Miami FL 33101; Department of Cancer Biology, Wake Forest University School of Medicine, Winston-Salem, NC 27157 [G. G. S.]; Texas Children's Hospital, Houston, TX 77030 (M. F.); Leo Pharmaceuticals, Ballerup, Denmark [L. B.]

Running Title: EB 1089 treatment of transgenic mice with prostate cancer

Abstract

Transgenic mouse models of prostate cancer provide unique opportunities to understand the molecular events in prostate carcinogenesis and for the preclinical testing of new therapies. We studied the GγT-15 transgenic mouse line, which contains the human fetal globin promoter linked to SV40 T antigen (Tag) and which develops androgen-independent prostate cancer. Using immunohistochemistry of normal mouse prostates before tumor formation, we showed that the target cells of carcinogenesis in GγT-15 mice are located in the basal epithelial layer. We tested the efficacy of the $1,25(OH)_2D_3$ analog, EB 1089, to chemoprevent prostate cancer in these transgenic mice. Compared to treatment with placebo, treatment with EB 1089 at three different time points before the onset of prostate tumors in mice did not prevent or delay tumor onset. However, EB 1089 significantly inhibited prostate tumor growth. At the highest dose, EB1089 inhibited prostate tumor growth by 60% ($P = 0.0003$) and the number of metastases, although this dose also caused significant hypercalcemia and weight loss. We conducted several *in vitro* experiments to explore why EB 1089 did not prevent the occurrence of the primary tumors. EB1089 significantly inhibited the growth of a Tag-expressing human prostate epithelial cell line, BPH-1, and an androgen-insensitive subline of LNCaP cells (which was not inhibited by $1,25(OH)_2D_3$). Thus, neither Tag expression nor androgen insensitivity explain the absence of chemopreventive effect. Conversely, neither $1,25(OH)_2D_3$ nor EB 1089 inhibited the growth of the normal rat prostate basal epithelial cell line, NRP-152. It is likely that EB 1089 was not effective in delaying the growth of the primary tumor in GγT-15 transgenic mice because the target cells of carcinogenesis in these mice are located in the basal epithelial layer. We conclude

that GγT-15 transgenic mice are a useful model for testing vitamin D-based therapies in androgen-insensitive prostate cancer but are not suitable for studies of vitamin D-based chemoprevention. The superiority of EB 1089 over $1,25(OH)_2D_3$ in the growth suppression of androgen-insensitive prostate cancer cells supports the use of EB 1089 in androgen-insensitive prostate cancer.

Introduction

Androgen-independent prostate cancer (AIPC)[3] is the second leading cause of cancer death in American men (1). Men with cancer that has spread beyond the prostate typically undergo androgen deprivation for palliation. However, the average duration of response to androgen deprivation is only two years, and there are no effective therapies for androgen-independent disease (2). Thus, effective treatments for AIPC are urgently needed.

In addition to their responsiveness to androgens, prostate cancer cells respond to another member of the steroid hormone superfamily, $1,25(OH)_2D_3$ (calcitriol). The therapeutic use of vitamin D metabolites is supported by epidemiological studies which first suggested that $1,25(OH)_2D_3$ maintains the differentiated phenotype of prostate cells and that reduced serum levels of $1,25(OH)_2D_3$ or its precursor, 25-hydroxyvitamin D_3, permits the progression of preclinical prostate cancer to clinical disease (3-6). Vitamin D receptor (VDR) is expressed in most prostate cancer cell lines, and high levels are necessary to mediate the antiproliferative effects *in vitro* (7). However, factors other than VDR density are also important in mediating the antiproliferative effect. For example, the androgen-dependent cell line LNCaP is more sensitive to $1,25(OH)_2D_3$ compared to the androgen-independent PC-3 and DU 145 prostate cancer cell lines, and these differences are not solely attributable to differences in VDR levels (8).

A phase II clinical trial in AIPC showed that $1,25(OH)_2D_3$ could lower serum PSA levels in some men (9). However, treatment with $1,25(OH)_2D_3$ causes significant hypercalcemia and/or hypercalciurea (10). Synthetic analogs of $1,25(OH)_2D_3$, such as EB 1089 (Seocalcitol) (11), with potent antiproliferative effects but reduced calcemic effects, can inhibit androgen-independent

PC-3 prostate cancer cells *in vitro* (12, 13). EB 1089, acting through VDR, has a similar cell growth inhibition mechanism as $1,25(OH)_2D_3$, but with longer lasting and stronger effects. In LNCaP cells, EB 1089 inhibits the growth of prostate cancer cells by inducing G1 cell cycle block *in vitro* and has been shown to inhibit tumor growth *in vivo* without producing hypercalcemia (14, 15). In addition, a recent comparison of EB 1089 and $1,25(OH)_2D_3$ treatment in the MATLyLu model of advanced AIPC showed that EB 1089 was as effective as $1,25(OH)_2D_3$ in inhibiting metastases but was significantly less calcemic (16). These results suggest that EB 1089 may offer a therapeutic option in AIPC.

In addition to its therapeutic uses, vitamin D and its analogs may be candidates for prostate cancer chemoprevention (17). The rationale for the use of vitamin D metabolites in chemoprevention is that vitamin D may maintain the differentiated phenotype of prostatic cells and delay or reverse the carcinogenic process before invasion and metastasis occur (5, 18). Testing these hypotheses in animals ideally requires models in which the cancer originates from normal prostate epithelial cells in their natural microenvironment and progresses through multiple stages, similar to human prostate cancer (19, 20). One study using the Lobound-Wistar rat model of urogenital cancer showed that treatment with the less calcemic $1,25(OH)_2D_3$ analog Ro24-5531 resulted in a limited chemoprevention effect (21).

Recently, the advent of several transgenic mouse models of prostate cancer that target the expression of SV40 Tag to specific prostate epithelial cells, have provided more suitable systems to test the chemoprevention and therapeutic potential of drugs (20, 22). The present study utilized Gγ/T-15 transgenic mice (23, 24) to test the efficacy of EB 1089 in the prevention of tumor onset and in the growth inhibition of AIPC. Unlike transgenic models utilizing prostate-specific

promoters to target Tag to the prostate epithelial cells, the Gγ/T-15 transgenic mice utilize the fetal Gγ-globin gene promoter (25). The progression of prostate cancer in 75% of the transgenic males has important similarities to the progression of prostate cancer in men, e.g., originating from high-grade PIN and progressing to advanced metastatic carcinomas. These tumors are clearly androgen-independent because castration of transgenic males before prostate tumor formation still results in the development of prostate tumors (24). Although Tag is not the cause of prostate cancer in men, the Gγ/T-15 transgenic mice serve as a model of an aggressive highly metastatic form of AIPC, which is the cause of virtually all deaths from prostate cancer in men.

Materials and Methods

Reagents. EB 1089 was synthesized by Leo Pharmaceuticals (Ballerup, Denmark). EB 1089 was used as a stock solution of 100 μg/ml in Solutol H15 (10 mg/ml), 7.7 mg/ml sodium phosphate dibasic anhydrous, 1 mg/ml sodium phosphate monobasic anhydrous, 2.8 mg/ml sodium chloride, and 10 mg/ml sodium ascorbate and stored in the dark at +4°C. $1,25(OH)_2D_3$ obtained from Biomol (Plymouth Meeting, PA) was dissolved in ethanol and stored in the dark at -20°C.

Immunohistochemistry. Our previous results showed that onset of prostate tumors in Gγ/T-15 transgenic mice occurs between 16 and 32 weeks of age (24). To identify the target cells of carcinogenesis, prostates from Gγ/T-15 transgenic mice (14-32 weeks old; n = 10) without palpable or visible tumors were removed at necropsy, fixed in 10% buffered formalin for 6 hours,

dehydrated, embedded in paraffin, and sectioned at 5 μm. Immunostaining for Tag was performed as previously described (26) using a 1/100 dilution of rabbit polyclonal antibody to Tag. The secondary antibody was a biotinylated goat anti-rabbit IgG. Specific color was developed with the Vector ABC kit (Zymed Laboratories Inc., South San Francisco, CA) and enhanced with DAB-Nickel chloride; the sections were counterstained with nuclear fast red.

Treatment of Gγ/T-15 Transgenic Males with EB 1089. We utilized the Gγ/T-15 transgenic mouse model of AIPC (23, 24) to assess the *in vivo* anti-tumor effect of EB 1089. These mice begin to develop prostate tumors by 16 weeks of age (24). At 11 weeks, 3 of 4 transgenic males expressed Tag mRNA in the prostate as determined by RPA (data not shown). For this reason, we chose 3 different treatment starting time points (14, 11, and 9 weeks) before tumor onset to test the ability of EB 1089 to chemoprevent prostate tumors. Transgenic mice (CBA x C57) were identified by DNA slot blot analysis as previously described (24). Transgenic male mice (14, 11, and 9 weeks of age) without palpable tumors were randomly divided into experimental and control groups and injected i.p. three times per week with 0.1 ml of freshly prepared EB 1089 at doses of 0.5, 2, 3, 4, 5, and 10 μg/kg body weight (BW) diluted in Solutol H15 or placebo control (Solutol H15). Mice were kept in a 12-hour day/night cycle and fed a normal rodent diet containing 0.95% calcium and 4.5 IU/g vitamin D_3 (Laboratory Rodent Diet 5001, PMI Nutrition International, Richmond, IN). Starting at 16 weeks, mice were palpated in the urogenital area 3 days per week to detect prostate tumor mass. Endpoints were 21 days after first detecting palpable prostate tumor mass or at 24 weeks of age. The percentage of mice that developed prostate tumors by 24 weeks of age and the average age when tumors were first detected by

palpation (age of onset) were determined for each EB 1089 dose group at 14, 11, and 9 weeks and compared with placebo controls. Mice without a palpable prostate tumor at the 24-week endpoint but with a visible tumor nodule upon dissection of the prostate (usually weighing 25-100 mg) were considered positive for prostate tumor formation. All animal studies were carried out with the approval of the Institutional Animal Care and Use Committee at the Miami VA Medical Center (AAALAC accredited) and conducted in accordance with the NIH Guidelines for the Care and Use of Laboratory Animals.

Prostate Tumor Weight, Serum Calcium, and Body Weight. Twenty-one days after prostate tumors were first detected by palpation, EB 1089- and placebo-treated mice were anesthetized, their blood was collected by cardiac puncture, and centrifuged, and the sera were frozen and stored at −80°C. Primary prostate tumors and visible metastases to lymph nodes, adrenal glands, or kidney were removed, and their wet weights determined. Serum calcium was measured by dry slide technology on an automated Kodak Ektachem 700XR clinical chemistry analyzer (Rochester, NY). The body weight for EB 1089- and placebo-treated mice was determined at the end of the study. Statistical differences in the wet weights of primary tumor and total metastases, serum calcium, and final body weight between EB 1089- and placebo-treated mice were determined using two-tailed Student's *t*-test.

VDR mRNA Expression by RT-PCR and RPA. RNA from mouse prostate, kidney, and Gγ/T-15 prostate tumor tissue was isolated by the LiCl-urea method (27) and treated with RNase-free DNase. The following DNA oligonucleotides synthesized by Operon Technologies (Alameda,

CA) were used for RT-PCR to detect VDR mRNA in mouse prostate and Gγ/T-15 prostate tumor RNA: forward, 5'-GAGTTCTTTTGGTTGGACA-3'; reverse, 5'-CAGCCTTCACAGGTCATA-3' (28). Conditions for RT-PCR were: 2 min at 94°C for 1 cycle; 1 min at 94°C, 1 min at 55°C, and 2 min at 72°C for 35 cycles; 7 min at 72°C for 1 cycle. The expected 209-base-pair (bp) fragment from mouse prostate was cloned into the TA vector pCRII (Invitrogen, Carlsbad, CA), and its identity was confirmed by DNA sequencing. VDR mRNA in mouse kidney, prostate, and Gγ/T-15 prostate tumor was measured by RPA with ^{32}P-labeled Sp6 polymerase-synthesized antisense RNA probe from EcoRV-digested mouse VDR/PCRII DNA, using conditions previously described (23).

VDR and AR Western Blot Analysis. Nuclear extracts from mouse (C57) prostate and kidney and from Gγ/T-15 prostate tumors were prepared according to the procedure of Dent and Latchman (29), and protein concentrations were determined with the Bio-Rad protein assay (Bio-Rad Laboratories, Hercules, CA). After separation of 10 μg protein by SDS-PAGE, proteins were transferred by electrophoresis to Immobilon-P membrane (Millipore Corp., Bedford, MA) and incubated in 5% nonfat dry milk, PBS, and 0.25% Tween-20 for 1 hour. Rabbit polyclonal antibodies specific for VDR (1/1000 dilution; C-20, Santa Cruz Biotechnology, Santa Cruz, CA) and AR (1/1000 dilution; N-20, Santa Cruz Biotechnology) were diluted in 5% nonfat dry milk, PBS, and 0.25% Tween-20 and incubated overnight at 4°C. Membranes were washed in PBS and 0.25% Tween-20 (three times, 10 min each time) and incubated with horseradish peroxidase-conjugated secondary antibody (anti-rabbit; 1/2000 dilution; Santa Cruz Biotechnology) for 1 hour, washed in PBS and 0.25% Tween-20, and analyzed by exposure to X-ray film (X-Omat,

Eastman Kodak Co., Rochester, NY) using enhanced chemiluminescence plus (ECL plus, Amersham Pharmacia Biotech, Arlington Heights, IL).

Cell Culture and Treatment with $1,25(OH)_2D_3$ and EB 1089. LNCaP-AI is an androgen-independent derivative of the human prostate cancer cell line LNCaP-FGC (30) (ATCC, Manassas, VA), which was spontaneously derived in our laboratory. These cells express AR and PSA, similar to LNCaP-FGC (data not shown). LNCaP-AI cells were maintained in RPMI 1640 (Gibco BRL) with 5% fetal bovine serum (FBS; Hyclone, Logan, UT), 100 U/ml penicillin, 100 μg/ml streptomycin, and 0.25 μg/ml amphotericin (Gibco BRL). Unlike androgen-dependent LNCaP-FGC, the LNCaP-AI cells are able to grow long-term in RPMI 1640 with 5% charcoal-stripped fetal bovine serum (Hyclone) and are referred to as LNCaP-AI/CSS. The Tag-expressing human prostate epithelial cell line BPH-1, generously provided by S. Hayward, was maintained in RPMI 1640 with 5% FBS (31). The normal rat prostate basal epithelial cell line NRP-152, generously provided by D. Danielpour, was maintained in HEPES-free DMEM/F12 (1:1, v/v; Gibco BRL) with 5% FBS, antibiotic/antimycotic, 20 ng/ml EGF, 10 ng/ml CT, 5 μg/ml insulin (Gibco BRL), and 0.1 μM Dex (Sigma, St. Louis, MO) (32).

To determine and compare prostate cell growth inhibition by $1,25(OH)_2D_3$ and EB 1089, 7.5×10^4 LNCaP-AI/CSS, 0.75×10^4 BPH-1, and 1.5×10^4 NRP-152 cells were seeded in 6-well plates in their corresponding media containing 5% FBS and allowed to attach overnight. The next day, fresh media containing $1,25(OH)_2D_3$ or EB 1089 (1 and 10 nM) or ethanol vehicle control (0.1% total volume) were added. After 3 days, the medium was changed and replenished. On the sixth day cells were removed by trypsin-EDTA (Gibco BRL), and viable cells were

counted with a Neubauer hemacytometer. In all the experiments, the control treated cells reached 80-90% confluency after 6 days of growth and were presumed to be in a log growth phase. Cell numbers in each experiment were derived from the average value of quadruplicate wells repeated three independent times and calculated as percentage of vehicle control. Statistical differences between $1,25(OH)_2D_3$- and EB 1089-treated and control cells were determined by two-tailed Student's *t*-test.

Results

Localization of Tag-Expressing Cells to the Basal Epithelial Layer of Transgenic Prostates. Although our previous results in the Gγ/T-15 transgenic mice suggest that the targeted prostate cells are androgen-independent (24), the location of the Tag-expressing target cells before tumor formation was not identified. To localize putative target cells, prostates without visible tumors were analyzed for Tag expression. Results showed areas of preneoplastic foci similar to high-grade PIN and dysplasia containing epithelial cells expressing Tag surrounded by normal-appearing prostate (Fig. 1). In these latter areas, isolated dispersed Tag-expressing cells were identified only in the basal epithelial layer. In proliferating areas, Tag-expressing cells were seen producing an elevation of the surface layer into and filling the prostatic lumen (Fig. 1C, D). These results indicate that the target cells of carcinogenesis in Gγ/T-15 are located in the basal epithelial layer.

VDR Expression in Advanced Gγ/T-15 Prostate Tumors. It has previously been shown that $1,25(OH)_2D_3$ does not inhibit the proliferation of prostate cancer cells that do not express VDR (7). Although we detected VDR mRNA in Gγ/T-15 prostate tumors by RT-PCR, we were unable to detect VDR mRNA by RPA and VDR protein by Western blot analysis (Fig. 2). As positive controls, VDR mRNA was detected in mouse kidney and VDR protein was detected in normal mouse prostate and kidney. In contrast to VDR expression, abundant amounts of AR protein were detected in advanced Gγ/T-15 prostate tumors (Fig. 2C). These results indicate that not all steroid hormone receptors are lost during prostate tumor progression in Gγ/T-15.

Can EB 1089 Prevent or Delay Prostate Tumors in Gγ/T-15 Mice? Gγ/T-15 mice express Tag mRNA in the prostate at 11 weeks (data not shown) and start developing prostate tumors by 16 weeks of age (24). We chose three different treatment starting time points (14, 11, and 9 weeks) before tumor onset to test the ability of EB 1089 to chemoprevent or delay the onset of prostate tumors in Gγ/T-15 mice. Our results showed that EB 1089 treatment (0.5, 2, 3, 4, 5, and 10 μg/kg) starting at 14 weeks did not prevent or delay tumor onset compared to placebo-treated mice (Table 1). The percentage of mice at 24 weeks that developed prostate tumors and the average age of tumor onset were not significantly different between any of the EB 1089 treatment groups compared to placebo-treated mice. Similar results were obtained when EB 1089 treatment started at 11 weeks (0.5, 2, 3, and 4 μg/kg) and at 9 weeks (2 μg/kg) (Table 1). Overall, 86% of EB 1089-treated (n = 116) compared to 94% of placebo-treated (n = 31) mice developed prostate tumors by 24 weeks of age, indicating that EB 1089 did not prevent or delay the onset of prostate tumors in the Gγ/T-15 transgenic mice.

Can EB 1089 Slow the Growth of Primary and Metastatic Prostate Tumors in Gγ/T-15 Mice? We next sought to determine whether EB 1089-treated mice in the 14, 11, and 9 week groups have smaller prostate tumors compared to placebo-treated mice. Twenty-one days after first detecting a palpable mass in the urogenital region, primary prostate tumors and metastases to lymph nodes, adrenal glands, and kidney were removed and their wet weights determined. Results showed that in the 14-week group, compared to placebo-treated mice, there was a significant 30-60% reduction in the weight of primary prostate tumors using EB 1089 doses of 4, 5, and 10 μg/kg (Fig. 3A). There was a significant decrease in the number of metastases in mice treated with 10 μg/kg EB 1089 compared to placebo controls (0.8 vs.1.9 metastases per mouse; Table 2) but no differences in the sites of metastasis (lymph nodes, adrenal, and kidney) in any of the treatment groups. There was no significant difference in the weights of metastatic prostate tumors (Fig. 3B). As expected, there was a significant increase in serum calcium and decrease in body weight with increasing EB 1089 doses (Fig. 3C, D). Because mice treated with EB 1089 lost body weight, we performed an analysis of covariance to determine whether the observed decrease in tumor weight could be accounted for by the decrease in overall body weight. ANCOVA indicated that the decrease in tumor weight was independent of the loss in body mass ($p< 0.01$).

Because of the concern that long-term treatment with high doses of EB 1089 (>4 μg/kg) could result in hypercalcemia and loss of body weight, we treated Gγ/T-15 transgenic mice in the 11- and 9-week groups with lower doses of EB 1089. The results showed that there were no significant differences in the weights of primary and metastatic prostate tumors and in the number of metastases for all EB 1089 doses in the 11-(0.5, 2, 3 and 4 μg/kg) and 9-(2 μg/kg)

week groups (Figs. 4, 5; Table 2). Overall, our results indicate that high doses of EB 1089 (4, 5, and 10 μg/kg) had a significant anti-prostate tumor effect in the 14-week group of Gγ/T-15 transgenic mice.

Tag-Expressing Prostate Cells Are Inhibited by EB 1089. Why did EB 1089 inhibit the growth of prostate tumors but not prevent or delay their occurrence? One possible explanation is that expression of Tag blocks EB 1089's antiproliferative effect. A previous report showed that when human prostate cancer cells are transformed with Tag, but not human papillomavirus, the result is a loss of growth inhibition by $1,25(OH)_2D_3$ (33). Preliminary experiments showed that mouse cell lines derived from Gγ/T-15 prostate tumors were growth inhibited by $1,25(OH)_2D_3$, despite expression of Tag (data not shown). To address this issue further, we compared the antiproliferative effects of $1,25(OH)_2D_3$ and EB 1089 utilizing the Tag-expressing human prostate epithelial cell line BPH-1 (31). Our results showed that EB 1089 significantly inhibited the growth of BPH-1 cells and was more effective than $1,25(OH)_2D_3$ (Fig. 6). Thus, these results indicate that the expression of Tag does not explain EB 1089's lack of chemoprevention effect.

EB 1089, But Not $1,25(OH)_2D_3$, Inhibits Androgen-Independent LNCaP-AI/CSS Cells. Another possibility for the inability of vitamin D compounds to chemoprevent prostate tumors in this model is that AIPC cells may be resistant to the antiproliferative effects of EB 1089, as they are to the antiproliferative effects of $1,25(OH)_2D_3$ (8). To address this possibility, we compared the antiproliferative effects of $1,25(OH)_2D_3$ and EB 1089 utilizing LNCaP-AI/CSS, an androgen-independent derivative of LNCaP-FGC grown long-term in charcoal-stripped FBS (androgen-

depleted conditions). Our results showed that EB 1089, but not $1,25(OH)_2D_3$, significantly inhibits the growth of LNCaP-AI/CSS cells (Fig. 6). Thus, we conclude that the inability of EB1089 to chemoprevent prostate tumors in these mice is not due to the androgen-insensitivity of this tumor.

Prostate Basal Epithelial Cells NRP-152 Are Insensitive to EB 1089's Antiproliferative Effects. Alternatively, it is possible that EB 1089 cannot inhibit the growth of the Tag-expressing target cells located in the basal epithelial layer (Fig. 1). To address this possibility, we utilized the normal rat prostate basal epithelial cell line NRP-152, known to express VDR (32). These cells can differentiate from a basal to a luminal prostate epithelial phenotype *in vitro* and *in vivo* (34, 35). Our results showed that neither $1,25(OH)_2D_3$ nor EB 1089 (1 and 10 nM) inhibited the growth of NRP-152 cells; in fact, a small stimulation (6-16%) of cell growth was observed (Fig. 6). Thus, these results suggest that EB 1089 was not effective in chemopreventing prostate tumors in these transgenic mice, because, like NRP-152 cells, the target cells of carcinogenesis are located in the basal epithelial layer.

Discussion

In this report, we showed that the Gγ/T-15 transgenic mouse model of AIPC expresses Tag to the basal epithelial layer of cells, distinguishing these mice from transgenic mouse models that express Tag to secretory luminal epithelial and neuroendocrine cells (36-42). We utilized the Gγ/T-15 mice to test the efficacy of the $1,25(OH)_2D_3$ analog EB 1089 against AIPC. Our results showed that EB 1089 did not prevent or delay prostate tumor incidence. However, high doses of EB 1089 (> 4 μg/kg) significantly inhibited primary prostate tumor growth, although this inhibition was accompanied by significant hyperalcemia and weight loss. Only the highest dose of EB 1089 (10 μg/kg) inhibited the number of metastases. We provide evidence suggesting that EB 1089 is ineffective in preventing or delaying primary prostate tumor onset in these mice because the target Tag-expressing epithelial cells are insensitive to the EB 1089's antiproliferative effects. Our data also suggest that low doses of EB 1089 did not inhibit prostate tumor growth because of the low expression levels of VDR.

Transgenic models of prostate cancer that employ Tag have several notable properties. Prostate-specific promoters that target Tag to androgen-dependent secretory luminal epithelial cells result in tumor progression similar to human prostate cancer — i.e., initiation as androgen-dependent and variable progression to androgen-independent disease (36-40). In contrast, targeting of Tag to mouse prostatic neuroendocrine cells results in rapid neoplastic transformation and progression to AIPC, with similarities to prostate small cell carcinoma in humans, which does not express AR (42). Although advanced prostate tumors in Gγ/T-15 mice express the neuroendocrine marker chromogranin A (24), the target cells are probably not

neuroendocrine cells because normal Tag-expressing epithelial cells are detected before neoplasia; i.e., there is a latent period before transformation (Fig.1), and AR is expressed in advanced tumors (Fig. 2).

Advanced prostate tumors in Gγ/T-15 mice are probably not basal cell carcinomas, which are uncommon in humans (43), because they express cytokeratin 8 (24 and data not shown) and AR (Fig. 2), common markers of luminal secretory epithelial cells and prostate cancer in humans (44). A prevailing view is that prostate stem cells are located in the basal epithelial layer and that they give rise to basal, neuroendocrine, and luminal epithelial cells during the process of cellular differentiation (45, 46). In addition, increasing evidence shows that more-aggressive metastatic AIPC express markers found in normal basal and neuroendocrine epithelial cells, suggesting a role in the origin of prostate cancer (47). More definitive experiments — e.g., co-localization of Tag with a basal epithelial-specific marker — will be required to confirm that the target cells of carcinogenesis in the Gγ/T-15 mice are basal epithelial cells. Future studies will determine the molecular changes that occur during the progression from the Tag-expressing target cells to high-grade PIN and early prostate tumors in the Gγ/T-15 mice.

Our data do not support the hypothesis that expression of Tag blocks EB 1089's antiproliferative effect and therefore accounts for the lack of chemopreventive effect in Gγ/T-15 mice. We demonstrated that EB 1089 significantly inhibited the proliferation of the Tag-expressing BPH-1 cell line and that EB 1089 was more effective in this regard than $1,25(OH)_2D_3$ (Fig. 6). These results suggest that EB 1089 might be useful in the treatment of benign prostatic hyperplasia (BPH). Additionally, our findings should encourage treatment of TRAMP mice (37, 39) with EB 1089 without the concern that Tag expression will block its antiproliferative effect.

The TRAMP mice develop prostate cancer from Tag-expressing normal androgen-dependent luminal epithelial cells and progresses through androgen-dependent and -independent stages of prostate tumor growth, leading to distant metastases (37, 39). Rather, our data suggest that EB 1089 had minimal effect on prostate tumor incidence in Gγ/T-15 mice because the target cells of carcinogenesis in this model were insensitive to EB 1089. Data obtained *in vitro* showed that, unlike other prostate epithelial cell types, only the rat basal epithelial cell line NRP-152 (32, 34) was insensitive to EB 1089 (Fig. 6). It is interesting that these cells have been previously shown to express VDR and respond to $1,25(OH)_2D_3$; thus the lack of response is not due to lack of the appropriate receptor (32, 48). It is not uncommon for $1,25(OH)_2D_3$ and its analogs to have different potencies in the same cell line (cf. the lack of effect of $1,25(OH)_2D_3$ in LNCaP-AI/CSS cells in which EB 1089 was strongly antiproliferative). NRP-152 cells are considered to have stem cell properties because they can differentiate into luminal epithelial cells *in vitro* and *in vivo* (34, 35). It would be interesting to determine whether EB 1089 is more effective in preventing or delaying prostate tumors in TRAMP mice, in which secretory luminal epithelial cells are more likely to be sensitive to EB 1089's antiproliferative effects.

Our results also suggest that the minimal antiproliferative effect of EB 1089 at low doses in Gγ/T-15 mice may be due to low levels of VDR protein expression (Fig. 2). The effects of $1,25(OH)_2D_3$ on growth and differentiation of prostate cancer cells are generally thought to require the presence of active VDR (7). Recent results demonstrate high variability in the expression of VDR in secretory luminal epithelial cells present in normal human prostates (49). Given the varying sensitivities to growth inhibition by $1,25(OH)_2D_3$ in prostate cancer cell lines and the variable expression of VDR in normal human prostate, such variability is likely to exist

in human prostate cancers. It is noteworthy that EB1089 was effective in suppressing the growth of androgen-insensitive prostate cancer cells in which $1,25(OH)_2D_3$ had little or no effect (e.g., LNCaP-AI/CSS and BPH-1, Fig. 6) (50). These findings support the use of EB 1089 in AIPC. A recent clinical trial indicates that very high doses of $1,25(OH)_2D_3$ can be administered orally without inducing hypercalcemia by giving the drug in pulses (51). This approach may similarly permit the administration of higher doses of EB1089, which is also administered orally.

The mechanisms of how high doses of EB 1089 inhibits the growth of primary prostate tumors in the Gγ/T-15 mice is currently unknown. However, it is reasonable to expect that these mechanisms are similar to those by which $1,25(OH)_2D_3$ inhibits tumor growth, e.g., induction of cyclin-dependent kinase inhibitor p21 and G1/G0 cell cycle arrest (7). Due to the large size of the primary prostate tumors, there were extensive areas of necrosis, making it difficult to identify histological differences. This question may be resolved in the future by treating transgenic males with EB 1089 (10 μg/kg) for a short period of time in order to obtain smaller prostate tumors and histological sections with less areas of necrosis.

A high dose of EB 1089 (10 μg/kg) was required to inhibit the number of metastases in the Gγ/T-15 mice (Table 2). This is in agreement with the anti-metastasis effect of EB 1089 in the MatLyLu model of prostate cancer (16). The differences in our results and the more striking effect on metastasis in the MatLyLu model may be attributed to the sites of tumor growth, i.e., in its natural prostate microenvironment in Gγ/T-15 mice compared to subcutaneous in MatLyLu rats. It may be easier for tumor cells to migrate from the subcutaneous microenvironment rather than invade through the prostate stroma into the vasculature.

In summary, we suggest that EB 1089 does not chemoprevent prostate tumors in Gγ/T-15 transgenic mice primarily because the target cells are insensitive to its antiproliferative effect. Low levels of VDR expression in Gγ/T-15 prostate tumors may also contribute to a lack of growth-inhibitory effect of EB 1089 at low doses. However, high doses of EB 1089 had a significant anti-prostate tumor effect in Gγ/T-15 mice. To our knowledge, this is the first report of testing the efficacy of a vitamin D analog in a transgenic mouse model of prostate cancer. These data underscore that chemoprevention and chemotherapy involve different biological processes. We conclude that the Gγ/T-15 transgenic mice provide an effective preclinical animal model system of AIPC in which to test novel therapies (52). The superiority of EB 1089 over $1,25(OH)_2D_3$ in inhibiting the growth of AIPC *in vitro* suggests that this analog may be useful clinically, particularly if the problem of hypercalcemia can be overcome.

Acknowledgments.

The authors thank the anonymous reviewers for their thoughtful suggestions; Ms. Alicia De Las Pozas for excellent technical assistance; Dr. Kerry Burnstein for critical comments; Drs. David Danielpour and Simon Hayward for prostate cell lines; and Dr. Carolyn Cray for serum calcium measurements.

References

1. Greenlee, R. T., Murray, T., and Thun, M. Cancer Statistics, 2001. CA Cancer J Clin *51:*15-36, 2001.

2. Pilat, M. J., Kamradt, J. M., and Pienta, K. J. Hormone resistance in prostate cancer. Cancer Metast. Rev. *17:* 373-381, 1999.

3. Schwartz, G. G., and Hulka, B. S. Is vitamin D deficiency a risk factor for prostate cancer? (Hypothesis) Anticancer Res. *10:* 1307-1311, 1990.

4. Hanchette, C. L., and Schwartz, G. G. Geographic patterns of prostate cancer mortality: evidence for a protective effect of ultraviolet radiation. Cancer (Phila.), *70:* 2861-2869, 1992.

5. Schwartz, G. G. Prostate cancer and vitamin D: From concept to clinic. A 10-year update. In: A.W., Norman, R. Bouillon, Thomasset M., Vitamin D Endocrine System. University of California Press, 445-452, 2000.

6. Ahonen, M. H., Tenkanen, L., Teppo, L., Hakama, M., and Tuohimaa, P. Prostate cancer risk and prediagnostic serum 25-hydroxyvitamin D levels (Finland). Cancer Causes Cont. *11:* 847-852, 2000.

7. Miller, G. J. Vitamin D and prostate cancer: biological interactions and clinical potentials. Cancer Mets Rev *17:* 353-360, 1999.

8. Zhuang, S-H, Schwartz, G. G., Cameron, D., and Burnstein, K. L. Vitamin D receptor content and transcriptional activity do not fully predict antiproliferative effects of vitamin D in human prostate cancer cell lines. Mol. Cell. Endo., *126:* 83-90, 1997.

9. Osborn, J. L., Schwartz, G. G., Smith, D. C., Bahnson, R., Day, R., and Trump, D. L. Phase II trial of oral 1,25-dihydroxyvitamin D (calcitriol) in hormone refractory prostate cancer. Urol. Oncol., *1:* 195-198, 1995.

10. Gross, C., Stamey, T., Hancock, S., and Feldman, D. Treatment of early recurrent prostate cancer with 1,25-dihydroxyvitamin D3 (calcitriol). J Urol *159:* 2035-2040, 1998.

11. Mathiasen, I. S., Colston, K. W., and Binderup, L. EB 1089, a novel vitamin D analogue, has strong antiproliferative and differentiation inducing effects on cancer cells. J. Steroid Biochem. Molec. Biol., *46:* 365-371, 1993.

12. De Vos, S., Holden, S., Heber, D., Elstner, E., Binderup, L., Uskokovic, M., Rude, B., Chen, D. L., Le, J., Cho, S. K., and Koeffler, H. P. Effects of potent vitamin D_3 analogs on clonal proliferation of human prostate cancer cell lines. Prostate *31:* 77-83, 1997.

13. Wang, X., Chen, X., Akhter, J., and Morris, D. L. The in vitro effect of vitamin D3 analogue EB-1089 on a human prostate cancer cell line (PC-3). Brit. J. Urol. 80: 260-262, 1997.

14. Skowronski, R. J., Peehl, D. M., and Feldman, D. Actions of vitamin D_3 analogs on human prostate cancer cell lines: comparison with 1,25-dihydroxyvitamin D_3. Endocrin. *136:* 20-26, 1995.

15. Blutt, S. E., Polek, T. C., Stewart, L. V., Kattan, M. W., and Weigel, N. L. A calcitriol analogue, EB 1089, inhibits the growth of LNCaP tumors in nude mice. Cancer Res. *60:* 779-782, 2000.

16. Lokeshwar, B. L., Schwartz, G. G., Selzer, M. G., Burnstein, K. L., Zhuang, S-H., Block, N. L,, Binderup, L. Inhibition of prostate cancer metastasis in vivo: a comparison of 1,25-dihydroxyvitamin D (calcitriol) and EB 1089. Cancer Epi Biom Prev *8:* 241-248, 1999.

17. Xue, L., Lipkin, M., Newmark, H., and Wang, J. Influence of dietary calcium and vitamin D on diet-induced epithelial cell hyperproliferation in mice. J. Natl. Cancer Inst. *91:* 176-181, 1999.

18. Schwartz, G. G., Wang, M. H., Zang, M., Singh, R. K., and Siegal, G. P. 1 alpha, 25-Dihydroxyvitamin D (calcitriol) inhibits the invasiveness of human prostate cancer cells. Cancer Epidemiol. Biomarkers Prev. *6:* 727-732, 1997.

19. Lucia, M. S., Bostwick, D. G., Bosland, M., Cockett, A. T., Knapp, D. W., Leav, I., Pollard, M., Rinker-Schaeffer, C., Shirai, T., and Watkins, B. A. Workgroup I: rodent models of prostate cancer. Prostate *36:* 49-55, 1998.

20. Green, J. E., Greenberg, N. M., Ashendel, C. L., Barrett, J. C., Boone, C., Getzenberg, R. H., Henkin, J., Matusik, R., Janus, T. J., and Scher, H. I. Workgroup 3: transgenic and reconstitution models of prostate cancer. Prostate *36:* 59-63, 1998.

21. Lucia, M. S., Anzano, M. A., Slayter, M. V., Anver, M. R., Green, D. M., Shrader, M. W., Logsdon, D. L., Driver, C. L., Brown, C. C., Peer, C. W., Roberts, A. B., and Sporn, M. B. Chemopreventive activity of tamoxifen, N-(4-hydroxyphenyl) retinamide, and the vitamin D analogue Ro24-5531 for androgen-promoted carcinomas of the rat seminal vesicle and prostate. Cancer Res. *55:* 5621-5627, 1995.

22. Sharma, P. and Schreiber-Agus, N. Mouse models of prostate cancer. Oncogene. *18:* 5349-5355, 1999.

23. Perez-Stable, C., Altman, N. H., Brown, J., Harbison, M. Cray, C., and Roos, B. A. Prostate, adrenocortical, and brown adipose tumors in fetal globin/T antigen transgenic mice. Lab. Invest. *74:* 363-373, 1996.

24. Perez-Stable, C., Altman, N., Mehta, P., Deftos, L., and Roos, B. A. Prostate cancer progression, metastasis, and gene expression in transgenic mice. Cancer Res. *57:* 900-906, 1997.

25. Perez-Stable, C. Distinct negative regulatory mechanisms involved in the repression of human embryonic ϵ- and fetal Gγ-globin genes in transgenic mice. J. Biol. Chem. *269:* 33109-33115, 1994.

26. Sepulveda, A. R., Finegold, M. J., Smith, B., Slagle, B. L., DeMayo, J. L., Shen, R. F., Woo, S. L., and Butel, J. S. Development of a transgenic mouse system for the analysis of stages in liver carcinogenesis using tissue-specific expression of SV40 large T-antigen controlled by regulatory elements of the human alpha-1-antitrypsin gene. Cancer Res. *49:* 6108-6117, 1989.

27. Auffray, C. and Rougeon, F. Purification of mouse immunoglobulin heavy chain messenger RNAs from total myeloma tumor DNA. Eur. J. Biochem., *107:* 303–314, 1980.

28. Kamei Y, Kawada T, Fukuwatari T, Ono T, Kato S, and Sugimoto E. Cloning and sequencing of the gene encoding the mouse vitamin D receptor. Gene *152:* 281-282, 1995.

29. Dent, C. L. and Latchman, D. S. The DNA mobility shift assay. In: Latchman, D.S., (ed.), Transcription Factors: A Practical Approach. Oxford University Press, New York, pp. 1–26, 1993.

30. Horoszewicz, J. S., Leong, S. S., Kawinski, E., Kerr, J. P., Rosenthal, H., Chu, T. M., Mirand, E. A., and Murphy, G. P. LNCaP model of human prostatic carcinoma. Cancer Res. *43:* 1809–1818, 1983.

31. Hayward, S. W., Dahiya, R., Cunha, G. R., Bartek, J., Deshpande, N., and Narayan, P. Establishment and characterization of an immortalized but non-transformed human prostate epithelial cell line: BPH-1. In Vitro Cell. Dev. Biol. *31A:* 14-24, 1995.

32. Danielpour, D., Kadomatsu, K., Anzano, M. A., Smith, J. M., and Sporn, M. B. Development and characterization of nontumorigenic and tumorigenic epithelial cell lines from rat dorsal-lateral prostate. Cancer Res. *54:* 3413-3421, 1994.

33. Gross, C., Skowronski, R. J., Plymate, S. R., Rhim, J. S., Peehl, D. M., and Feldman, D. Simian virus 40-, but not human papillomavirus-, transformation of prostate epithelial cells results in loss of growth-inhibition by 1,25-dihydroxyvitamin D3. Int. J. Oncol. *8:* 41-47, 1996.

34. Danielpour, D. Transdifferentiation of NRP-152 rat prostatic basal epithelial cells toward a luminal phenotype: regulation by glucocorticoid, insulin-like growth factor-I and transforming growth factor-beta. J. Cell Sci. *112:* 169-179, 1999.

35. Hayward, S. W., Haughney, P. C., Lopes, E. S., Danielpour, D., and Cunha, G. R. The rat prostatic epithelial cell line NRP-152 can differentiate in vivo in response to its stromal environment. Prostate *39:* 205-212, 1999.

36. Maroulakou, I. G., Anver, M., Garrett, L., and Green, J. E. Prostate and mammary adenocarcinoma in transgenic mice carrying a rat C3(1) simian virus 40 large tumor antigen fusion gene. Proc. Natl. Acad. Sci. USA *91:* 11236-11240, 1994.

37. Greenberg, N. M., DeMayo, F., Finegold, M. J., Medina, D., Tilley, W. D., Aspinall, J. O., Cunha, G. R., Donjacour, A. A., Matusik, R. J., and Rosen, J. M. Prostate cancer in a transgenic mouse. Proc. Natl. Acad. Sci. USA *92:* 3439-3443, 1995.

38. Kasper, S., Sheppard, P. C., Yan, Y., Pettigrew, N., Borowsky, A. D., Prins, G. S., Dodd, J. G., Duckworth, M. L., and Matusik, R, J. Developmental progression and androgen-dependence of prostate tumors in probasin-large T antigen transgemc mice: a model for prostate cancer. Lab. Invest. *78:* 319-333, 1998.

39. Gingrich, J. R., Barrios, R. J., Kattan, M. W., Nahm, H. S., Finegold, M. J., and Greenberg, N. M.. Androgen-independent prostate cancer progression in the TRAMP model. Cancer Res. *57:* 4687-4691, 1997.

40. Masumori, N., Thomas, T. Z., Chaurand, P., Case, T., Paul, M., Kasper, S., Caprioli, R. M., Tsukamoto, T., Shappell, S. B., and Matusik, R. J. A probasin-large T antigen transgenic mouse line develops prostate adenocarcinoma and neuroendocrine carcinoma with metastatic potential. Cancer Res. *61:* 2239-2249, 2001.

41. Skalnik, D. G., Dorfman, D. M., Williams, D. A., and Orkin, S. H. Restriction of neuroblastoma to the prostate gland in transgenic mice. Mol. Cell. Biol. *11:* 4518-4527, 1991.

42. Garabedian, E. M., Humphrey, P. A., and Gordon, J. I. A transgenic mouse model of metastatic prostate cancer originating from neuroendocrine cells. Proc. Natl. Acad. Sci.

USA *95:* 15382-15387, 1998.

43. Denholm, S. W., Webb, J. N., Howard, G. C., and Chisholm, G. D. Basaloid carcinoma of the prostate gland: histogenesis and review of the literature. Histopath. *20:* 151-155, 1992.

44. Mehta, P. P., Perez-Stable, C., Roos, B. A., and Nadji, M..Identification, characterization and differentiation of human prostate cells. In: Methods in Molecular Biology: Developmental Biology Protocols,. Eds., RS Tuan and CW Lo, Humana Press Inc., *137:* 317-335, 2000.

45. Isaacs, J. T. and Coffey, D. S. Etiology and disease process of benign prostatic hyperplasia. Prostate Suppl. *2:* 33-50, 1989.

46. Bonkhoff, H. and Remberger, K. Differentiation pathways and histogenetic aspects of normal and abnormal prostatic growth: a stem cell model. Prostate *28:* 98-106, 1996.

47. Bui, M. and Reiter, R. E. Stem cell genes in androgen-independent prostate cancer. Cancer Metast. Rev. *17:* 391-399, 1999.

48. Danielpour, D. Induction of transforming growth factor-β autocrine activity by all-*trans*-retinoic acid and 1α,25-dihydroxyvitamin D_3 in NRP-152 rat prostatic epithelial cells. J Cell Physiol *166:* 231-239, 1996.

49. Kivineva, M., Blauer, M., Syvala, H., Tammela, T., and Tuohimaa, P. Localization of 1,25-dihydroxyvitamin D3 receptor (VDR) expression in human prostate. J. Steroid Biochem. Molec. Biol. *66:* 121-127, 1998.

50. Hansen, C.M., Binderup, L., Hamberg, K.J., Carlberg, C. Vitamin D and cancer: Effects of $1,25(OH)_2D_3$ and its analogs on growth control and tumorigenesis. Front. Biosci. *6:* D820-848, 2001.

51. Beer, T.M., Munar, M., Henner, W.D. A Phase I trial of pulse calcitriol in pateints with refractory malignancies: Pulse dosing permits substantial dose escalation. Cancer *91:* 2431-2439, 2001.

52. Qadan, L. R., Perez-Stable, C. M., Anderson, C. D'Ippolito, G., Herron, A., Howard, G. A., and Roos, B. A. 2-Methoxyestradiol induces G2/M arrest and apoptosis in prostate cancer. Biochem. Biophys. Res. Comm. *285:* 1259-1266, 2001.

Footnotes

[1] Supported by a VA Merit Review Entry Program grant 98-69-01 to C. P-S, R01 CA 68565 to G.G.S., a Department of Defense grant DAMD-17-98-1-8525 to B. A. R., and the VA Medical Research Service. G. A. H. has a Senior Research Career Scientist award from the Department of Veterans Affairs.

[2] To whom correspondence should be addressed, at VAMC, GRECC (11-GRC), 1201 NW 16 St, Miami, FL 33125. Phone: (305) 324-4455x4391; Fax: (305) 324-3365; E-mail: cperez@med.miami.edu.

[3] The abbreviations used are: AIPC, androgen-independent prostate cancer; $1,25(OH)_2D_3$, 1,25-dihydroxyvitamin D_3; VDR, vitamin D receptor; PSA, prostate-specific antigen; Tag, SV40 T antigen; RPA, RNase protection assay; AR, androgen receptor; FBS, fetal bovine serum; PIN, prostate intraepithelial neoplasia.

Table 1 Prostate tumor frequency and age of onset in EB 1089- and placebo-treated Gγ/T-15 transgenic mice

Treatment	Start (weeks)[a]	No. of mice	% Prostate tumor[b]	Avg. age of onset (weeks)[c]
Placebo	14	12	100 (12/12)	19.4 (3.0)
EB 1089				
0.5		10	80 (8/10)	18.5 (3.2)
2		9	78 (7/9)	20.4 (2.2)
3		14	86 (12/14)	19.3 (2.4)
4		11	91 (10/11)	18.6 (3.1)
5		13	77 (10/13)	20.2 (3.0)
10		6	83 (5/6)	17.5 (2.0)
Placebo	11	10	90 (9/10)	18.9 (3.1)
EB 1089				
0.5		5	100 (5/5)	16.3 (2.3)
2		9	100 (9/9)	20.1 (3.1)
3		11	100 (12/12)	18.6 (3.2)
4		14	93 (13/14)	18.5 (3.3)

Placebo	9	9	89 (8/9)	18.1 (2.7)
EB 1089				
2		14	79 (11/14)	18.1 (2.9)

[a] Age of Gγ/T-15 mice when treatment began.

[b] Percent of mice at 24 weeks that developed prostate tumors.

[c] Age of mice when prostate tumors were first detected by palpation. Number in the parenthesis is standard deviation. There were no significant differences in % prostate tumor and age of onset between EB 1089- and placebo-treated mice.

Table 2 Number of metastases in EB 1089- and placebo-treated Gγ/T-15 transgenic mice

Treatment	Start (weeks)[a]	No. of mice[b]	No. of metastases[c]
Placebo	14	9	1.89 (0.6)
EB 1089			
0.5		7	2.29 (1.1)
2		5	2.40 (0.5)
3		10	1.60 (0.5)
4		8	1.50 (1.1)
5		6	2.17 (0.8)
10		5	0.80 (0.4)[d]
Placebo	11	7	1.86 (0.4)
EB 1089			
0.5		5	2.20 (1.1)
2		6	2.00 (0.6)
3		9	1.89 (0.6)
4		12	1.67 (0.9)

Placebo	9	7	2.29 (1.3)
EB 1089			
2		10	2.00 (1.2)

[a] Age of Gγ/T-15 mice when treatment began.

[b] Gγ/T-15 mice with prostate tumors treated for 21 days with placebo or EB 1089.

[c] Number of visible metastatic lesions (lymph node, adrenal, and kidney) per mouse. Number in the parenthesis is standard deviation.

[d] Significant difference $P<0.005$, two-tailed Student's *t*-test.

Figure Legends

Fig. 1. Prostatic target cells of carcinogenesis in Gγ/T-15 transgenic mice. (A) Light micrograph (H&E, x400) of preneoplastic lesion similar to high grade PIN (arrow) containing epithelial cells protruding into the lumen (L). (B) Light micrograph (nuclear fast red, x200) of Tag immunohistochemistry showing a normal appearing prostate acini containing Tag-expressing epithelial cells located in the basal epithelial layer (arrows pointing to cells containing black nucleus) next to an acini not containing Tag-expressing cells. (C) Light micrograph (nuclear fast red, x200) showing proliferating Tag-expressing cells (arrows) producing an elevation towards the surface layer into the lumen (L) of prostate gland. (D) Light micrograph (nuclear fast red, x200) showing prostate duct filled with Tag-expressing dysplastic cells (large arrow) next to a normal appearing prostate duct containing Tag-expressing epithelial cells in the basal layer (small arrows).

Fig. 2. Low level expression of VDR in Gγ/T-15 prostate tumors. (A) RT-PCR of mouse VDR mRNA was performed using total RNA from mouse prostate (Pr) and prostate tumors (PT). A 209 bp product was detected in RNA samples containing RT (+), but not without RT (-). (B) Quantitative RPA detecting mouse VDR mRNA in kidney (Ki), but not in prostate (Pr) or prostate tumors (PT). GAPDH was used as an internal RNA control. Autoradiograms were exposed to film for 7 days. The sizes of the protected fragments are 209 bp (VDR) and 135 bp (GAPDH). (C) Ten μg of nuclear protein from mouse kidney (Ki), prostate (Pr), and prostate tumor (PT) were analyzed by Western blot using antibodies specific for VDR (48 kd) and AR

(110 kd). Results showed little or no expression of VDR in prostate tumor, but abundant expression in kidney. VDR protein was detected in prostate, despite not being detected by RPA (B). In contrast, there was abundant expression of AR in prostate and prostate tumor and minimal expression in kidney. A major non-specific band reacting with the VDR antibody is represented by NS. Relatively equal amounts of proteins were loaded based on Coomassie Blue staining of membranes after ECL detection.

Fig. 3. High doses of EB 1089 inhibits primary prostate tumor growth in Gγ/T-15 transgenic mice. Transgenic males 14 weeks of age were treated with EB 1089 or placebo. Treatment period for the 14-week group is represented by the bar at the top. The open portion of the bar (14 to 16 weeks) represents the period between the start of treatment and examination of mice for tumor formation by palpation. The hatched portion of the bar (16 to 24 weeks) represents the period of tumor onsets (16 weeks) and the end point of the study (24 weeks). Average weights of primary (A) and metastatic (B) prostate tumors excised from Gγ/T-15 males treated with increasing doses of EB 1089 (0.5, 2, 3, 4, 5, and 10 μg/kg) (solid bars) compared to the weights of prostate tumors excised from placebo-treated mice (open bars). Prostate tumors were allowed to grow for 21 days after first detecting by palpation (see Materials and Methods). Significant difference in the primary (A) but not metastatic (B) prostate tumor weight was achieved using the 4, 5, and 10 μg/kg dose of EB 1089 (*, $P<0.05$; **, $P<0.005$, two-tailed Student's *t*-test). Increase in serum calcium levels (mg/dl) (C) and decrease in total body weight (grams) (D) in Gγ/T-15 mice treated with increasing doses of EB 1089 (0.5, 2, 3, 4, 5, and 10 μg/kg) compared to placebo-treated

mice. Results are expressed as means ± standard deviation (error bars). (*, $P<0.05$; **, $P<0.005$, two-tailed Student's *t*-test).

Fig. 4. Treatment of Gγ/T-15 mice with EB 1089 compared to placebo control: 11-week group. Methods are similar to the 14-week group (see Fig. 3 legend) except that treatment started at an earlier time point (11 weeks). No significant difference in the primary (A) and metastatic (B) prostate tumor weight was achieved using EB 1089 doses of 0.5, 2, 3, and 4 μg/kg (solid bars) compared to placebo controls (open bars). Increase in serum calcium levels (mg/dl) (C) and decrease in total body weight (grams) (D) in Gγ/T-15 mice treated with increasing doses of EB 1089 (0.5, 2, 3, and 4 μg/kg) compared to placebo-treated mice. Results are expressed as means ± standard deviation (error bars). (*, $P<0.05$; **, $P<0.005$, two-tailed Student's *t*-test).

Fig. 5. Treatment of Gγ/T-15 mice with EB 1089 compared to placebo control: 9-week group. Methods are similar to the 14-week group (see Fig. 3 legend) except that treatment started at an earlier time point (9 weeks). No significant difference in the primary (A), metastatic (B) prostate tumor weight, serum calcium levels (C), and total body weight (two-tailed Student's *t*-test) was achieved using EB 1089 dose 2 μg/kg (solid bars) compared to placebo controls (open bars). Results are expressed as means ± standard deviation (error bars).

Fig. 6. EB 1089 inhibits growth of androgen-independent LNCaP and Tag-expressing BPH-1, but not basal epithelial prostate NRP-152 cells. LNCaP-AI/CSS, BPH-1, and NRP-152 cells were treated for 6 days with 1 and 10 nM $1,25(OH)_2D_3$ (D) or EB 1089 (EB) and cell numbers

expressed as % of vehicle control (see Materials and Methods). EB 1089 was a better inhibitor of LNCaP-AI/CSS and BPH-1 cells compared to $1,25(OH)_2D_3$. In contrast, EB 1089 and $1,25(OH)_2D_3$ treatment resulted in a small increase in NRP-152 cell numbers. Error bars are standard deviation. Statistical differences between $1,25(OH)_2D_3$- and EB 1089-treated and control cells were determined by two-tailed Student's *t*-test (*, $P<0.05$; **, $P<0.005$). Cell numbers from each experiment were derived from the average value of quadruplicate wells repeated three independent times.

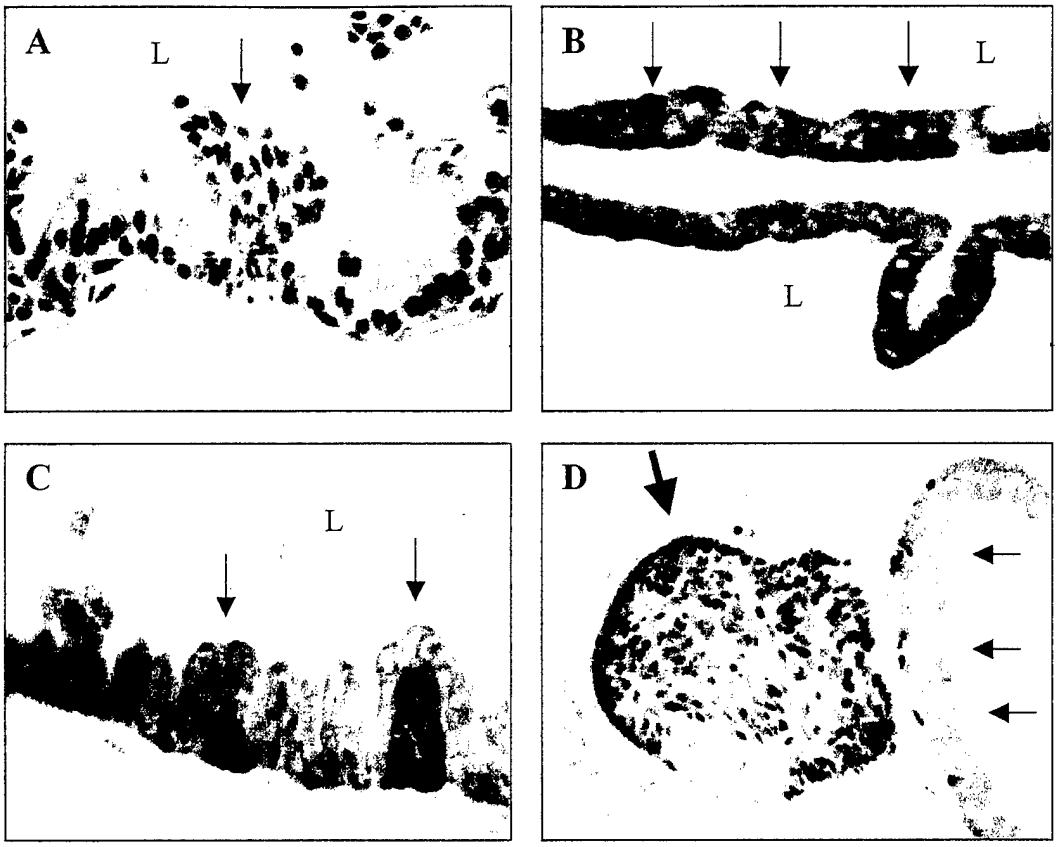
A
L
B
L
L
C
L
D

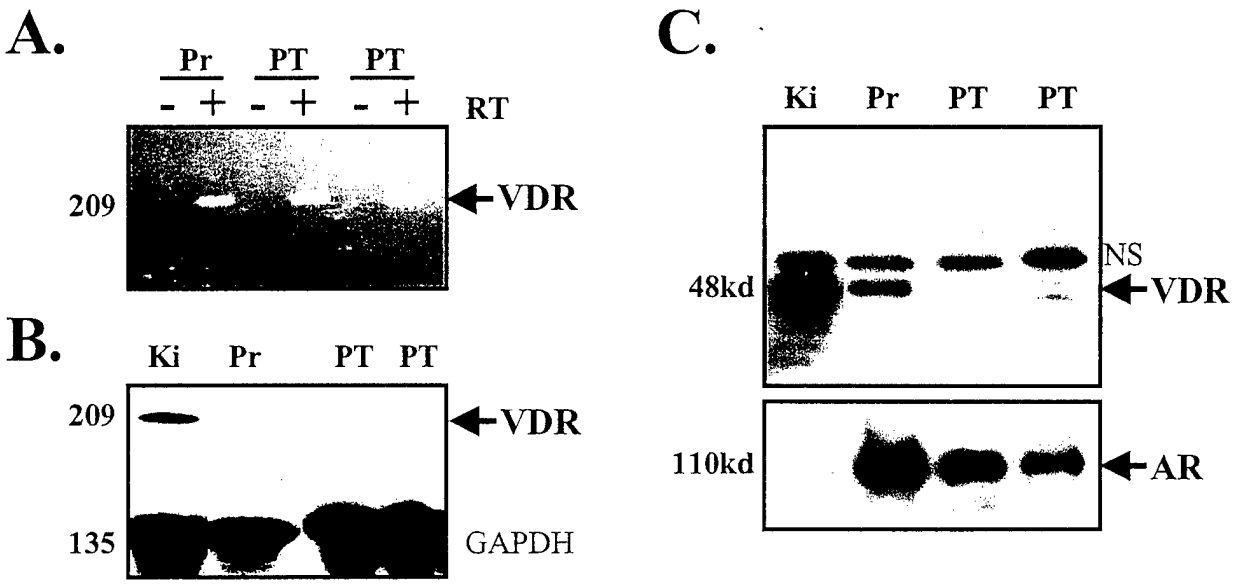
A.
Pr
PT
PT
- + - + - +
RT
209
VDR
B.
Ki
Pr
PT
PT
209
VDR
135
GAPDH
C.
Ki
Pr
PT
PT
48kd
NS
VDR
110kd
AR

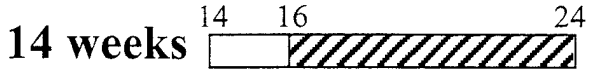
14 weeks
14
16
24

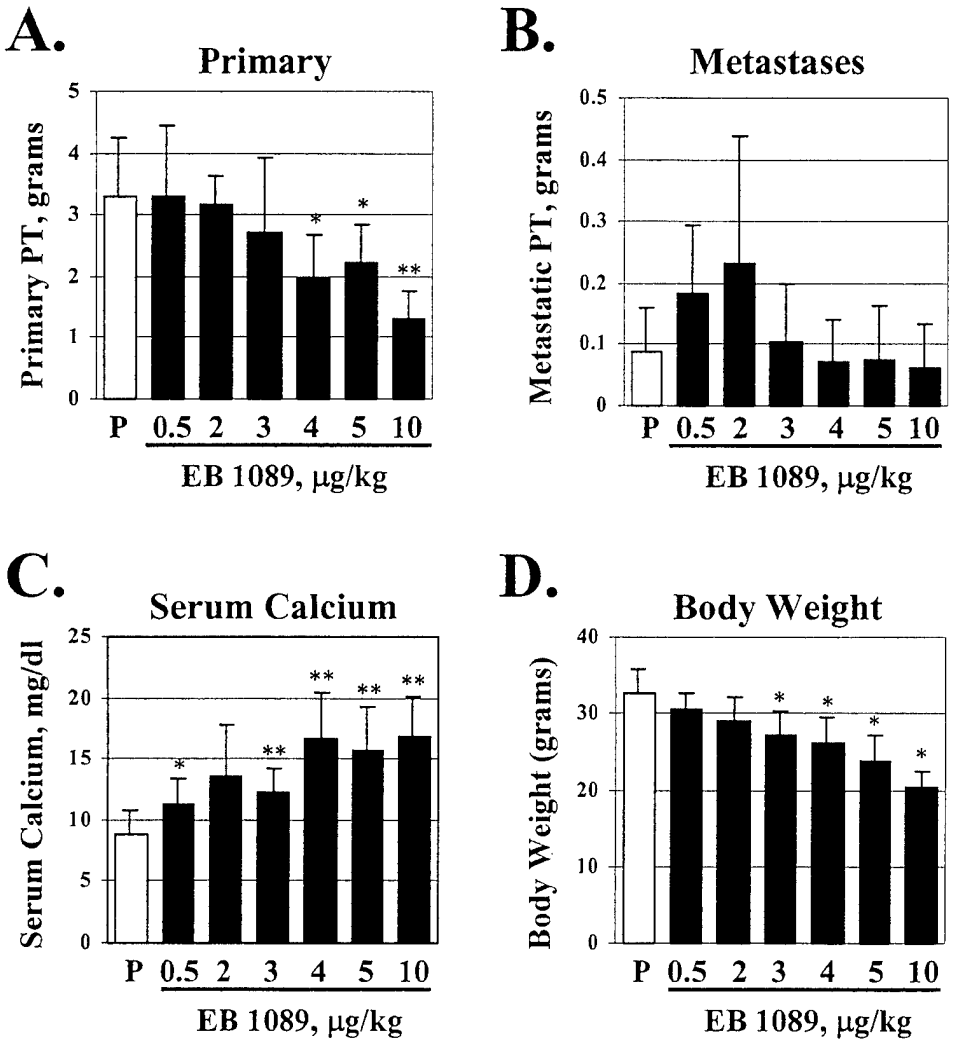
A.
Primary
Primary PT, grams
0
1
2
3
4
5
P
0.5
2
3
4
5
10
EB 1089, µg/kg
B.
Metastases
Metastatic PT, grams
0
0.1
0.2
0.3
0.4
0.5
P
0.5
2
3
4
5
10
EB 1089, µg/kg
C.
Serum Calcium
Serum Calcium, mg/dl
0
5
10
15
20
25
P
0.5
2
3
4
5
10
EB 1089, µg/kg
D.
Body Weight
Body Weight (grams)
0
10
20
30
40
P
0.5
2
3
4
5
10
EB 1089, µg/kg

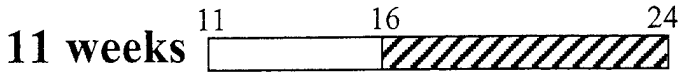
11 weeks
11
16
24

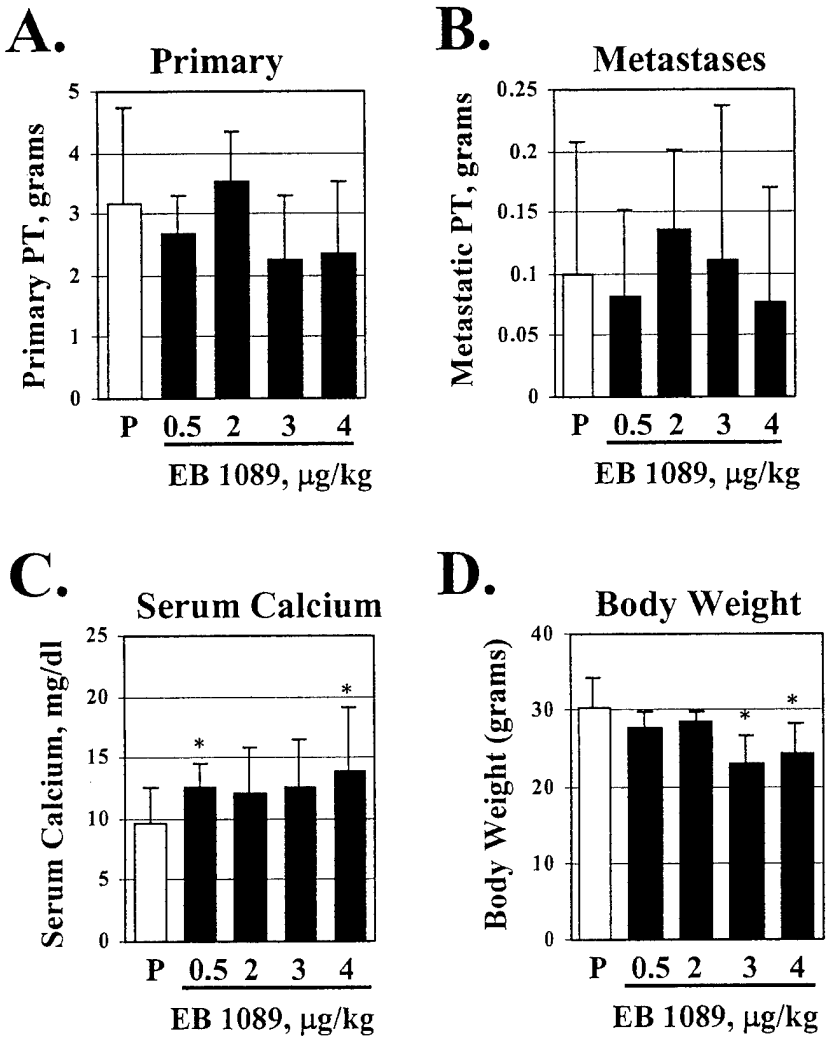
A.
Primary
Primary PT, grams
0
1
2
3
4
5
P
0.5
2
3
4
EB 1089, µg/kg
B.
Metastases
Metastatic PT, grams
0
0.05
0.1
0.15
0.2
0.25
P
0.5
2
3
4
EB 1089, µg/kg
C.
Serum Calcium
Serum Calcium, mg/dl
0
5
10
15
20
25
*
*
P
0.5
2
3
4
EB 1089, µg/kg
D.
Body Weight
Body Weight (grams)
0
10
20
30
40
*
*
P
0.5
2
3
4
EB 1089, µg/kg

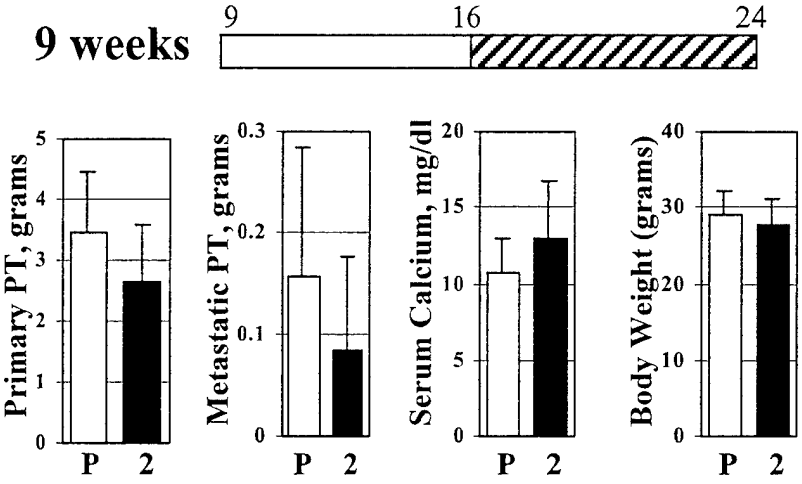
9 weeks
9
16
24
Primary PT, grams
0
1
2
3
4
5
P
2
Metastatic PT, grams
0
0.1
0.2
0.3
P
2
Serum Calcium, mg/dl
0
5
10
15
20
P
2
Body Weight (grams)
0
10
20
30
40
P
2

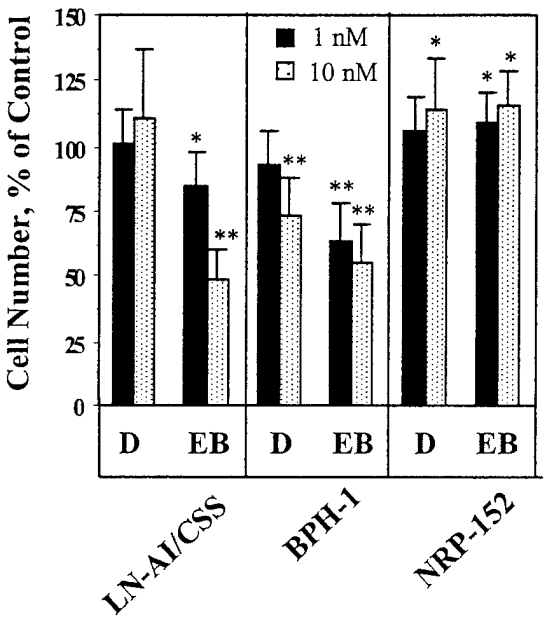
Cell Number, % of Control
150
125
100
75
50
25
0
1 nM
10 nM
*
**
D
EB
LN-AI/CSS
BPH-1
NRP-152

Program & Abstracts

Volume II (June 14-15)

10th International Congress of Endocrinology (ICE '96)

June 12-15, 1996 San Francisco, USA

Sponsored by the International Society of Endocrinology
and The Endocrine Society

Session OR53:Basic Oral Session Hormones & Cancer II

OR53-1

1,25 DIHYDROXYVITAMIN D TRANSFORMATION OF PROSTATE CARCINOMA FROM EPITHELIAL TO STROMAL MORPHOLOGY IS MEDIATED BY AN AUTOCRINE MECHANISM INVOLVING HEPATOCYTE GROWTH FACTOR (HGF) AND ITS RECEPTOR c-MET. LR Qadan*[2], R Schwall[2], GA Howard[1], BA Roos[1]. [1]GRECC, VAMC, and University of Miami School of Medicine, Miami, FL 33125; [2]Genentech, Inc., South San Francisco, CA 94080.

While in normal prostate HGF from stromal cells regulates basal epithelial cells via a paracrine mechanism, an autostimulatory loop can emerge in aggressive human prostate cancer and derived cell lines, such as PC-3. Since we recently uncovered evidence for an HGF/c-Met autocrine role in the regulation of growth-cartilage stem cells by 1,25 dihydroxyvitamin D (1,25diOHD) and since 1,25diOHD exerts important effects on the proliferation, differentiation, and apoptosis of prostate cancer cells including PC-3 cells, we have now asked whether 1,25diOHD action in PC-3 cells involves this HGF/c-Met activation. Accordingly, PC-3 cell cultures during 4-5-d treatment with 1,25diOHD (1-100 nM) were examined for cell-shape and colony morphology changes frequently associated with HGF/c-Met activation; in the presence of serum, 1,25diOHD transforms the cells from cuboidal to an elongated shape and individual colonies become scattered/disorganized. ELISA for HGF production by the PC-3 cells revealed low levels of growth factor, which increased with 1-100 nM 1,25diOHD; after 5 d 1,25diOHD increased HGF as much as 10-fold, with the half-maximal increase occurring at 2 nM. These results support the hypothesis that 1,25diOHD induces morphologic transformation via increases in HGF. This idea was strengthened when we observed that recombinant HGF (3-20 ng/ml) added to sparse PC-3 cultures caused the same cell and colony morphology changes as 1,25diOHD, although HGF's effect occurred sooner. Finally, to demonstrate that c-Met activation mediates the 1,25diOHD transformation, we showed that the PC-3 morphology changes were inhibited by the addition of increasing concentrations of Fab fragments prepared from bivalent anti-c-Met immunoglobulin. These results prove that the stem-cell-like PC-3 prostate cancer cells express an HGF/c-Met autocrine axis whose regulation mediates the morphological transformation by 1,25diOHD.

OR53-2

AN ACTH-PRODUCING SMALL CELL LUNG CANCER EXPRESSES AN ABERRANT GLUCOCORTICOID RECEPTOR (GR) TRANSCRIPT FROM A NORMAL GR GENE LL Parks*[2], MK Turney[2], WJ Kovacs[1,2], [1]Research Service, Department of Veterans Affairs Medical Center, Nashville, Tennessee 37212 and Division of Endocrinology[2], Vanderbilt University School of Medicine, Nashville, Tennessee 37232.

Adrenocorticotropin (ACTH) secretion from non-pituitary tumors such as small cell lung carcinomas is generally not suppressible by exogenous glucocorticoids. We postulated that defects in the glucocorticoid receptor (GR) signaling system might be responsible for this apparent glucocorticoid resistance. In a cell line (DMS-79) derived from one such ectopic ACTH-producing tumor we have found evidence for expression of a truncated, nonfunctional form of GR in which the sequences encoded by exons 8 and 9 are replaced by sequence unmatched in the DNA databases. We sought to identify the origin of the novel GR mRNA sequence and to determine whether the truncated DMS-79 GR results from a structural alteration of the GR gene (e.g., deletion of exons 8 and 9). When DMS-79 cell DNA was examined by Southern blot analysis no major structural alteration of the GR gene was discernible. Southern blotting of cosmid clones of the normal GR gene (the gift of Dr. S. Detera-Wadleigh, NIH) revealed that the novel sequence in DMS-79 cell GR mRNA is derived from intron G, between exons 7 and 8. No splice donor or acceptor site mutations were found in PCR-amplified DMS-79 DNA from the intron G-exon 8, exon 8-intron H, and intron H-exon 9α boundaries. Further sequencing indicated that the aberrant GR transcript appears to use a consensus polyadenylation site found 3650 base pairs into the normal intron G. The protein encoded by this mRNA would lack the steroid-binding domain. We conclude that abnormal GR pre-mRNA processing rather than a GR gene mutation may confer the phenotype of glucocorticoid resistance on these tumor cells.

OR53-3

NOVEL TUMOR-SPECIFIC EXPRESSION OF ESTROGEN RECEPTOR mRNA SPLICED VARIANTS IN HUMAN PITUITARY ADENOMAS. S S Chaidarun* and JM Alexander. Neuroendocrine Unit, Department of Medicine, Massachusetts General Hospital and Harvard Medical School, Boston, MA 02114

The well-documented mitogenic and hormone regulatory effects of estrogen on pituitary cells are mediated via its nuclear receptor (ER), a cellular homolog of *v-erbA* oncogene encoded by eight exons. ER isoforms generated by alternative exon splicing, designated Δ2ER to Δ7ER, have been recently identified in breast cancer and have been postulated to have important pathogenetic and clinical implications in its tumorigenesis and/or development of hormone resistance. Δ2ER encodes a severely truncated ER protein and retains only the A/B domain of the hormone-independent transcription activation (TAF-1) region. Δ3ER and Δ4ER are joined in-frame and lack the second zinc finger DNA binding and the hinge region, respectively. Δ5ER, a constitutively active ER isoform, causes a frame shift and lacks most of the ligand binding region while the in-frame Δ7ER lacks only the carboxy-terminal portion of the ligand binding domain. Because pituitary tumors, particularly prolactinomas, are known to be estrogen dependent, we investigated ER alternate splice variant mRNA expression in 40 human pituitary tumors using RT-PCR analysis. ER splice variants were quantitated relative to normal ER expression in each tumor sample. 8/11 prolactinomas expressed multiple splice variants lacking a single exon (Δ2ER, Δ4ER, Δ5ER and Δ7ER) at levels ranging from 24-90% relative to normal ER mRNA. 6/11 prolactinomas also expressed Δ3ER, however mRNA expression only ranged from 5-10% relative to normal ER. 3/7 gonadotroph tumors expressed Δ2ER, Δ5ER and Δ7ER, at levels ranging from 20-167% relative to normal ER. Δ6ER was not detected in any tumor studied. Variant and normal ER were not found in all three clinically nonfunctioning tumors which showed negative immunoreactivity for all pituitary hormones or their subunits (null cell tumors), or in 10 ACTH-secreting tumors from patients with Cushing's disease. Of 9 GH-secreting tumors examined, low levels of both normal and ER variants (Δ4ER, Δ5ER and Δ7ER) were restricted to tumors that also exhibited scattered PRL immunoreactivity. We conclude that alternatively spliced ER variants except Δ6ER are prevalent in prolactinomas and gonadotroph tumors. Coexpression of multiple ER variants along with normal ER in human pituitary tumors suggests interactions between normal ER and its variants in estrogen-sensitive pituitary neoplastic cell types. Future functional studies will be required to determine whether these interactions play a pathogenetic role in pituitary hormone regulation or cell proliferation in human pituitary tumors.

OR53-4

BINDING CHARACTERISTICS OF NOVEL NONSTEROIDAL ANTIESTROGENS TO THE RAT UTERINE ESTROGEN RECEPTOR. C. Martel*, L. Provencher, X. Li, A. St-Pierre, G. Leblanc, S. Gauthier, Y. Mérand and F. Labrie. Laboratory of Molecular Endocrinology, CHUL Research Center, Québec, G1V 4G2, Canada.

Tamoxifen (TAM), the only antiestrogen currently available for the endocrine therapy of breast cancer behaves as a mixed agonist/antagonist of estrogen action, thus limiting its therapeutic potential. We report the binding characteristics of a novel series of nonsteroidal antiestrogens to the rat uterine estrogen receptor. As measured by competition studies, the affinity of EM-652, the active metabolite of the prodrug EM-800, for the estrogen receptor is 7 to 11 times higher than that of 17β-estradiol (E_2), ICI 182780, and hydroxy-Tamoxifen (OH-TAM), the active metabolite of Tamoxifen. EM-652 is 20 times more potent than ICI 164384 and Droloxifene while it is 400 times more potent than Toremifene in displacing [^{3}H]E_2 from the rat uterine estrogen receptor. On the other hand, the prodrugs EM-800 and Tamoxifen have respectively 150-fold and 410-fold less affinity for the estrogen receptor than the pure antiestrogen EM-652. No significant binding of EM-652, EM-800, TAM or OH-TAM was observed to the rat uterine progesterone receptor at concentrations up to 10 000 nM except for TAM that caused a 50% displacement of labeled R5020 at 4000 nM. No significant binding of EM-652 or EM-800 was observed on the rat ventral prostate androgen receptor or the rat uterine progesterone receptor. The present data demonstrate the high affinity and specificity of the new antiestrogen, EM-652, for the rat uterine estrogen receptor. The antiestrogen EM-652 thus becomes the compound having the highest known affinity for the estrogen receptor. Due to its unique potency and its pure antiestrogenic activity already demonstrated in many systems, this antiestrogen could well offer an important advance for the endocrine therapy of breast cancer, uterine cancer, and other estrogen-sensitive diseases in women.

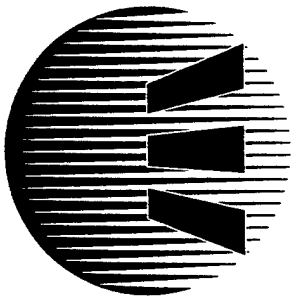

THE ENDOCRINE SOCIETY

Program & Abstracts

79th Annual Meeting

June 11-14, 1997 Minneapolis, Minnesota

P3-393

Reproductive Function in rats with Chronic Nephrosis. M Menjivar*[1](SPON:C Gual), G Ortiz[1], F Vilchis[1], and J Pedraza-Chaverri[2]. [1]Dept of Reproductive Biology, Instituto Nacional de la Nutrición Salvador Zubirán; Dept of Biology, Facultad de Química, National University of Mexico, Mexico City, MEXICO.

The Nephrotic Syndrome (NS) of rat and human is characterized by alterations in the metabolism of plasma proteins. Likewise, there is evidence that nephrotic animals also develop a marked endocrine dysfunction. In previous reports we have described the hormonal changes that occur during the acute phase of the illness. Here, we examine the reproductive function of male rats with chronic NS. Reproductive function was evaluated by assessing hormonal levels, weight of accessory sex organs and fertility. Circulating LH, FSH, Prl, P_4, T and E_2 levels, were measured by specific RIAs, while fertility was estimated by the rate of pregnancy induction. Biochemical measurements were achieved by standard methods. Experimental chronic nephrosis was induced by the administration of 7.5, 5, and 5 mg/100g b.w. of puromycin aminonucleoside (PAN) on days 0, 21 and 35 respectively. Samples were collected on days 7, 14, 28, 56, 84 and 112 (n=7 each date). The results show that all nephrotic rats exhibited persistent proteinuria. Serum gonadotropin levels decreased significantly only during the first month, Prl remained unchanged, P_4 decreased on days 28 and 56, whereas T and E_2 decreased during all dates evaluated (mean of all dates, T was N=0.81±0.16 ng/ml vs C=3.76±0.46 ng/ml, P<0.005; E_2 was N=3.15±0.51 pg/ml vs C=13.59±2.44 pg/ml, P<0.005). The weight of the prostate and seminal vesicle decreased only during the first two weeks, becoming normal thereafter. Interestingly, the capacity of fertilization of nephrotic males was entirely abolished on day 7 (0%), whereas on day 14, 16% were able to mate successfully and later on, most of them recovered their normal reproductive function. The results from this study demonstrate that rats with induced chronic nephrosis, develop chronic hypogonadism which impairs transiently the reproductive capacity.

Supported by PAPIIT (N°IN201596) National University of Mexico, Mexico City, MEXICO.

P3-395

CONSTITUTIVE ACTIVATION OF STIMULATING GTP-BINDING PROTEIN (Gs) INCREASES TUMORIGENICITY AND METASTATIC POTENTIAL OF PC-3M PROSTATE CANCER CELLS. Girish Shah[1,2], E. Wang[3], J. Chien[2], C. Pantazis[3] and M. J. Noble[1]. Departments of Surgery[1], Physiology[2] and Pathology[3], The University of Kansas Medical Center Kansas City, KS 66160

An abnormal stimulation of cAMP signaling cascade has been implicated in various human carcinomas. Since the agents activating adenylate cyclase signaling pathways have been shown to increase *in vitro* proliferation and invasiveness of prostate cancer cells, present studies examined the role of cAMP cascade in tumorigenicity and invasiveness of PC-3M cells. PC-3M prostate cancer cells were stably transfected with either carrier plasmid, plasmid containing Gs-wt cDNA and containing constitutively active form of Gs (Gs-a). The cells expressing Gs-wt and Gs-a displayed higher content of Gs protein and displayed 14-fold and 85-fold greater concentrations of baseline cAMP levels as compared to vehicle controls. The cells expressing (carrier plasmid [v], Gs-wt and Gs-a) were then tested for 1) cell migration and penetration of basement matrix in an *in vitro* invasion assay; and 2) their ability to form tumors and metastasis in nude mice.

PC-3M cells expressing Gs-a displayed approximately 15-fold increase in their ability to migrate and penetrate basement membrane as compared to those expressing either carrier plasmid or Gs-wt. PC-3M cells expressing Gs-a also displayed significantly greater tumorigenicity and metastasis forming ability when orthotopically implanted in nude mice. All mice receiving PC-3M cells produced primary tumors within five weeks after implantation. However, none of them displayed metastasis. The cells expressing Gs-a displayed a significantly faster tumor growth as assessed by prostate weight (greater than 20-fold [illegible] PC-3M cells). Further, four of the six displ[illegible]ed nodes, blood vessels, mesentery and intestir in PC-3M cells reduced their ability to form suggest that constitutive activation of cAMP accelerate tumorigenicity of prostate cancer c concentrations of cAMP agonists such as pro peptide and calcitonin in the prostate, cAMP androgen-independent progression of prostat

BASIC: Hormones & Prostate Cancer

P3-394

DIFFERENTIAL GENE EXPRESSION IN ANDROGEN-DEPENDENT AND ANDROGEN-INDEPENDENT PROSTATE CANCER. LJ Blok*, GTG Chang, M Steenbeek, WM van Weerden#, GJ van Steenbrugge# and AO Brinkmann. Depts. of Endocrinology & Reproduction and Urology#, Erasmus University, P.O.Box 1738, 3000DR Rotterdam, The Netherlands.

The transition from androgen-dependent to androgen-independent prostate cancer growth marks the progression of the disease to a non-treatable form. From the LNCaP cell line, developed from a metastatic lesion of a human prostatic carcinoma by Horoszewicz in 1980, two closely related sublines are available: LNCaP-FGC, which is androgen-dependent for its growth, and LNCaP-LNO, which is androgen-independent. These cell lines provided us with an ideal model to study gene expression related to autonomous cell growth under carefully controlled conditions. Both cell lines were cultured for 6 days in RPMI 1640 supplemented with 7.5% charcoal stripped fetal calf serum, in the presence or absence of androgens (0.1nM and 10nM R1881). Using differential display PCR on mRNA from LNCaP-FGC and LNCaP-LNO cells we identified 3 cDNA transcripts. The first novel gene, **clone 19**, was isolated as a highly expressed clone in LNCaP-FGC, and could hardly be detected in LNCaP-LNO cells. Furthermore, expression was mainly found in androgen-dependent and not in androgen-independent human prostatic carcinoma xenografts. The sequence which has been analyzed so far encodes for an open reading frame of approximately 430 amino acids, which contains a putative EF-hand-type Ca^{2+}-binding domain (these domains are often found as multiple copies in a variety of different genes). The second novel gene, **clone 79**, is expressed at a higher level in LNCaP-FGC as compared to LNCaP-LNO. Furthermore, the expression of this clone is down-regulated by androgens in both cell lines. The expression level of clone 79 was found to be extremely high in 4 out of 5 breast cancer cell lines: this in contrast to normal breast tissue in which no expression was found. Partial sequence analysis revealed that this gene contains a putative DNA binding domain (zinc cluster region) which shares homology to similar domains in the GATA transcription factor family. **Clone 8** represents a known gene: the β1-subunit of Na^+/K^+-ATPase. Clone 8 was isolated because androgen-induced down-regulation was very pronounced in LNCaP-FGC cells. Furthermore, down-regulation of β1-subunit mRNA expression by androgens was found to result in a functional down-regulation of Na^+/K^+-ATPase activity in the LNCaP-FGC cell line.

P3-396

HEPATOCYTE GROWTH FACTOR SENSITIZES PROSTATE CANCER CELLS TO ANTIPROLIFERATIVE ACTION OF VITAMIN D. LR Qadan[1], R Schwall[2], GA Howard[1], and BA Roos[1]. [1]GRECC, VAMC, and Univ. of Miami Sch. of Med., Miami, FL 33125; [2]Genentech, Inc., South San Francisco, CA 94080.

Hepatocyte growth factor (HGF) and its receptor c-met are among the many growth factors and receptors produced in normal and neoplastic prostate cells. We previously reported HGF and c-met expression in PC-3, an androgen-independent prostate cancer cell line. We showed that HGF mediates, at least partially, the morphogenic changes induced by vitamin D in that cell line. Preliminary studies suggested that vitamin D also had some antiproliferative activity in prostate cancer cells. Inhibition of proliferation by vitamin D in androgen-independent cell lines (PC-3 and ALVA-31) was minimal compared to the dramatic inhibition seen in an androgen-dependent prostate cancer cell line (LNCaP). Moreover, the LNCaP cells contained an endogenously high baseline level of HGF compared to the androgen-independent cell lines, leading us to speculate that HGF elaboration might contribute to the vitamin D sensitivity of the cancer cells. To test this possibility we compared the effects of HGF and vitamin D on cell proliferation in these 3 cell lines, which have similar levels of vitamin D receptor but differ in basal sensitivity to vitamin D. Accordingly, cell cultures were treated for 6 days with 1,25 dihydroxyvitamin D (10 nM) and HGF (10 ng/ml) alone and in combination; at the end of the incubation cell counts were made. In LNCaP cells the combination therapy had no additional inhibitory response beyond the large effect of vitamin D alone (D alone, 30% of control; HGF + D, 22%). However, the combination therapy enhanced vitamin D antiproliferative activity in both PC-3 and ALVA-31 cells — in the latter, to an extent even beyond the maximal inhibition in LNCaP cells (PC-3: D alone, 81% of control; HGF + D, 68%; ALVA-31: D alone, 45%; HGF + D, 16%). These results open the way to a novel adjuvant approach to vitamin D therapy of androgen-independent prostate cancer — namely, the activation of c-met oncogene via long-lived ligands or activating divalent antibodies to c-met before or during treatment with vitamin D.

The Jackson Laboratory

presents

Modeling Human Prostate Cancer in Mice

October 18-21, 2001

All Events are at the Main Laboratory Building, 600 Main Street, Bar Harbor, Maine unless otherwise noted.

Thursday October 18, 2001

4:30 - 7:00 p.m.	Shuttle Vans from downtown Bar Harbor to the Lab.
4:00 - 7:00 p.m.	Registration and Reception
7:00 - 9:00 p.m.	**Opening Session One:**
7:00 p.m.	**Opening remarks from the Organizers** Cory Abate-Shen, Ph.D., UMDNJ-Robert Wood Medical School Norman Greenberg, Ph.D., Baylor College of Medicine Robert Matusik, Ph.D., Vanderbilt University Medical Center
7:15 p.m.	**John T. Isaacs, Ph.D.**, Johns Hopkins Medical Institutions *"What have Mouse Models Taught Us About the Androgen Axis in Normal Versus Malignant Prostatic Tissue?"*
8:00 p.m.	**Michael Shen, Ph.D.**, UMDNJ-Robert Wood Johnson Medical School *"Molecular Genetics of Mouse Prostate Development"*
8:30 p.m.	**Jerry Cunha, Ph.D.**, University of California, San Francisco *"A new tissue recombinant model of hormonal carcinogenesis of mouse prostate"*
9:00 - 9:30 p.m.	Shuttle Vans to downtown Bar Harbor

THE G□/T-15 TRANSGENIC MOUSE MODEL OF ANDROGEN-INDEPENDENT PROSTATE CANCER: TARGET CELLS OF CARCINOGENESIS AND THE EFFECT OF THE VITAMIN D ANALOG EB 1089

Perez-Stable C [1], Schwartz G [2], Farinas A [1], Finegold M [3], Binderup L [4], Howard G [1], Roos B [1]
[1] GRECC/Miami VA Medical Center, SCCC, and University of Miami School of Medicine, Miami, FL; [2] Wake Forest University School of Medicine, Winston-Salem, NC; [3] Texas Children's Hospital, Houston, TX; [4] Leo Pharmaceuticals, Ballerup, Denmark

Transgenic mouse models of prostate cancer provides unique opportunities to understand the molecular events in prostate carcinogenesis and for the preclinical testing of new therapies. We studied the G□T-15 transgenic mouse line, which contains the human fetal globin promoter linked to SV40 T antigen (Tag), and which develops androgen-independent prostate cancer (AIPC). Immunohistochemistry of normal prostates before tumor formation showed that the target cells of carcinogenesis in G□T-15 are located in the basal epithelial layer. However, prostate tumors in G_/T-15 mice are not basal cell carcinomas, which is rare in humans, because they express cytokeratin 8 and androgen receptor, common markers of luminal secretory epithelial cells and prostate cancer in humans. A current view is that prostate basal epithelial cells give rise to luminal epithelial cells. In addition, there is increasing evidence that metastatic AIPC express markers found in normal basal epithelial cells. These results suggest a role for basal epithelial cells in the origin of prostate cancer.

The therapeutic use of vitamin D (1,25D) and its synthetic analogs is supported by studies which suggest that 1,25D maintains the differentiated phenotype of prostate cells and that reduced serum levels of 1,25D permits the progression of preclinical prostate cancer to clinical disease We tested the efficacy of the 1,25D analog, EB 1089, to chemoprevent prostate cancer in the G_/T-15 mice. Compared to placebo-treated mice, mice treated with EB 1089 at three different time points before the onset of prostate tumors did not prevent or delay the onset of tumors. However, the highest dose of EB1089 inhibited prostate tumor growth by 40% (P=0.001), although this dose also caused significant hypercalcemia and weight loss.

We conducted several in vitro experiments to explore why EB 1089 did not prevent tumor occurrence. EB1089 significantly inhibited the growth of a Tag-expressing human prostate epithelial cell line, BPH-1, and an androgen-insensitive subline of LNCaP cells (which was not inhibited by 1,25D). Thus, neither Tag expression nor androgen-insensitivity explain the lack of chemopreventive action. Conversely, neither 1,25D nor EB 1089 inhibited the growth of the normal rat prostate basal epithelial cell line, NRP-152. This suggests that EB 1089 was not effective in delaying tumor onset in our transgenic mice because the target cells of carcinogenesis in G□T-15 transgenic mice are located in the basal epithelial layer. We conclude that G□T-15 transgenic mice are a useful model for testing vitamin D-based therapies in androgen-insensitive prostate cancer but are not suitable for studies of vitamin D-based chemoprevention. The superiority of EB 1089 over 1,25D in the growth suppression of androgen-insensitive prostate cancer cells supports the use of EB 1089 in androgen-insensitive prostate cancer.

Personnel supported by research award

Curtis Anderson

Kerry L. Burnstein, Ph.D.

Mary Ann Hart

Carol Maiorino

Blanca N. Rodriguez

Bernard A. Roos, M.D.